Contents

Antimicrobial functionalization of textile materials with hydrophobins and Ag/ZnO composite nanopowders

IULIANA DUMITRESCU
OVIDIU GEORGE IORDACHE

ANA MARIA MOCIOIU
GHEORGHE NICULA

REZUMAT – ABSTRACT

Funcționalizarea antimicrobiană a materialelor textile cu hidrofobine și nanopulberi compozite de Ag/ZnO

Scopul cercetării îl constituie realizarea de textile antimicrobiene din fire de bumbac și poliester, prin funcționalizarea cu hidrofobine și nanopulberi compozite de Ag/ZnO. Soluția coloidală de nanoparticule de Ag depuse pe nanoparticule de ZnO a fost obținută prin sinteză chimică. Prin formarea de straturi proteice de hidrofobine, se urmărește o mai bună uniformizare și fixare a nanoparticulelor de AgNp/ZnONp pe materialele textile, datorită formării de legături ionice cu grupe funcționale, punți oxo, legături Van der Waals sau integrării în structura conformațională a proteinelor. Materialele tratate au fost analizate atât din punct de vedere fizico-mecanic, cât și al eficienței antimicrobiene. Rezultatele au demonstrat că metoda folosită permite depunerea unui strat subțire de hidrofobine, la care AgNp/ZnONp aderă puternic. Caracteristicile fizico-mecanice sunt modificate nesemnificativ față de materialul inițial, netratat, păstrând confortul în procesul de purtare. Testele antimicrobiene au indicat o eficiență crescută a materialelor împotriva microorganismelor analizate.

Cuvinte-cheie: hidrofobine, Ag/ZnO, funcționalizare antimicrobiană, textile

Antimicrobial functionalization of textile materials with hydrophobins and Ag/ZnO composite nanopowders

The purpose of the research was to achieve antimicrobial textiles made of cotton and polyester yarns by functionalization with hydrophobins and pigments of Ag/ZnO composite nanopowders. The colloidal suspensions consisting in Ag nanoparticles deposited on ZnO nanoparticles were obtained by chemical synthesis. By forming protein layers of hydrophobins, a better uniformity and fixation of AgNp/ZnONp on textile materials was aimed due to the formation of ionic bonds with functional groups, of oxo bridges, bonding through Van der Waals forces or integration in the proteins conformational structure. The treated materials were analyzed in terms of physical-mechanical and antimicrobial effectiveness. The results demonstrated that the used method allows the deposition of a uniform hydrophobins layer to which AgNp/ZnONp adhere strongly. The physical-mechanical characteristics insignificantly modify to the initial, untreated material, preserving wear comfort. Bioassays showed high efficiency against tested microorganisms.

Key-words: hydrophobins, Ag/ZnO, antimicrobial functionalization, textiles

Textile materials can be exposed to contamination with micro-organisms during production, usage or storage, particularly if the goods are left for a long time in favorable conditions for microbial growth. Many different finishes applied on textiles such as anti-static, thickeners, lubricants, as well as grease, sweat and dead skin from the human body provide a great source of nourishment for microbes, making textiles susceptible to microbial attack. Contamination with micro-organisms can lead to quality loss of the material itself (staining, fading and lowering tensile strength) and can affect user's comfort (smell, itching, and skin irritation). Moreover, since microbes are absorbed by textiles there is a high risk of human contamination and infection. Different finishing agents have been used to improve the anti-microbial resistance of textiles, such as silver, ZnO, TiO$_2$. The main disadvantages of these compounds consist in their low adherence and non-uniformity on the material surface. One method to avoid these drawbacks is the use of hydrophobins. Class I and class II hydrophobins are small proteins containing around 100–150 amino acids and eight cysteine units [1] that form intramolecular disulphide bridges [2]. Due to their self-assembling property at hydrophilic-hydrophobic interfaces into amphipathic membranes [3] they can be used to prevent microbial cell adhesion [4], to attach different molecules (e.g. cells, proteins, antibodies, enzymes) to hydrophobic surfaces, to improve the water resistance of hydrophilic substrates. The property of hydrophobins to coat any type of surface with a 10 nm thin film was used in the textile field to preserve the physical characteristics and especially the comfort degree [5]; to modify the surface wettability [6]; to fix metal oxides (ZnO, TiO$_2$). The aim of this research was to develop protective antimicrobial textiles coatings with hydrophobins and Ag/ZnO composite nanopowders. The antimicrobial functionalization of the textiles will assure the protection of the materials from decay or degradation, control of staining caused by microbial growth and elimination of smells created by microbes.

EXPERIMENTAL PART

Materials and chemicals

As textile support for the deposition of hydrophobins layers and subsequently AgNp/ZnONp solutions, a 3/2 twill fabric made of 57.5% cotton in weft and 42.5% polyester in warp was used. The samples are identified using numerical codes, respectively *1, 2* and *3*.

Ag/ZnONp suspensions prepared by "in situ" chemical reduction of Ag^+ ions were acquired from ICPE, their characteristics being shown in table 1.

Hydrophobins, H*Protein A (HA) and H*Protein B (HB), His6-tagged, from class I, were kindly provided by BASF-SE, Ludwigshafen, Germany. HA is a fusion protein (yaaD-A. nidulans hydrophobin DewA-His6) with a molecular weight of about 47 kDa and HB (truncated yaaD-A. nidulans hydrophobin DewA-His6) has a molecular weight of about 19 kDa [7].

Method of preparing hydrophobins solutions

The hydrophobins solutions were prepared according to the producer specification, namely, by dissolving protein (3.25 g hydrophobin HA with an active content of 61%, respectively 5 g hydrophobin HB with an active content of 40%) in 1 000 mL of de-ionized water. The solutions were stirred with a magnetic stirrer for 45 minutes at room temperature, after which were filtered and diluted with 3 000 mL Na-phosphate buffer (*p*H 6.5 – 7) to achieve hydrophobine final concentration of 0.05 wt.%.

Method of treating textile materials with hydrophobins and AgNp/ZnO Np

The fabric was immersed into 4 L of hydrophobin solution (material: solution ratio of 1:8.88) and the temperature was raised to 80°C and kept for 4 hours. Then 8 g of sodium dodecylsulphate (SDS) (93%, Consors) were added in the hydrophobin bath and the solution was heated to 100°C for 10 minutes to form an insoluble, stable hydrophobin beta-sheet on the textiles surface. Next, the material was washed with distilled water and left to dry at room temperature. Due to the very slight increase of fabrics weight, the fabric was re-immersed into a fresh hydrophobin solution and maintained at 25°C for 24 hours. The purpose was to obtain a thicker layer of hydrophobins which could include a higher amount of nanoparticles.

The fabrics previously covered with hydrophobins were immersed in Ag/ZnONp suspensions and ultrasonicated for 0.5 hours, washed with distilled water and dried at room temperature.

Analyses

Physical and mechanical analysis of fabrics treated with hydrophobins HA and HB and Ag/ZnONp were performed according to the ISO standards. The morphology of fabrics was analyzed by scanning electron microscopy (SEM, Quanta 200-FEI Netherland). The elemental composition was assessed by SEM/EDAX. The antibacterial efficiency was tested according to ASTM E2149-01 and ISO 20743:2007 standard against Pseudomonas aeruginosa (ATCC 9027), Staphylococcus aureus (ATCC 6538) and Escherichia coli (ATCC 8739). The effect of treatment on Aspergillus niger colony was visualized on SEM: the untreated and treated fabrics were inoculated with a fungal suspension of Aspergillus niger, fresh culture, grown on Czapek-Dox nutritive media. After the 2 days incubation at 28°C, the samples were visualized by SEM.

RESULTS AND DISCUSSIONS

Physical and mechanical characterization of fabrics treated with hydrophobins and AgNp/ZnONp

The characteristics of fabrics, both untreated and treated with hydrophobins HA and HB are presented in table 2.

The deposition of a thick layer (26 μm) hydrophobins on fabrics is demonstrated by the growth of mass, thickness, yarn diameter, yarn density and air/water permeability of materials, especially for hydrophobin A after the second treatment. The amphipathic character of hydrophobins allows them to be deposited on hydrophobic (polyester) and hydrophilic (cotton) materials. The amount of hydrophobin HA deposited on the polyester (warp) yarns is more than double than on cotton (weft) yarns indicating the presence of

Table 1

Sample code	AgNp/ZnONp suspension description	N_p average diameter, nm	Standard deviation, nm	Poly-dispersity index	Zeta potential, ζ, mV	Suspension *p*H value	Absorbance, a.u.				
							Wavelength, nm				
1	5 wt% ZnONp, 75 ppm AgNp	42.0	2.8	0.122	−41.25	9.41	0.299	0.189	0.233	0.177	0.237
							686	453	424	376	343
2	5 wt% ZnONp, 750 ppm AgNp	78.3	6.7	0.103	−52.43	9.83	0.280	0.112	0.196	0.154	0.216
							687	446	421	377	341
3	5 wt% ZnONp, 1 500 ppm AgNp	93.4	8.9	0.050	−64.28	9.45	0.339	0.144	0.231	0.133	0.219
							685	452	423	373	344

PHYSICAL AND OPTICAL CHARACTERISTICS OF AG/ZnO COMPOSITE NANOPOWDERS SUSPENSIONS

Table 2

PHYSICAL AND MECHANICAL CHARACTERISTICS OF FABRICS TREATED WITH HYDROPHOBIN HA AND HB						
Analysis		**Values**				
Sample		*Untreated fabric*	*Fabric treated with HA*		*Fabric treated with HB*		**Standard**
			First treatment	*Second treatment*	*First treatment*	*Second treatment*	
Mass, g/m²		155	158.4	164	157	163	SR EN 12127/2003
Thickness, mm		0.407	0.40	0.426	0.391	0.426	SR EN ISO 5084/2001
Yarn diameter, µm	warp	166	-	178.5	-	177	SR 13152/93
	weft	190	-	197	-	202	
Density, No. of yarns/10 cm	warp	350	350	350	351	350	SR EN ISO 1049-2/2000
	weft	280	288	290	289	289	
Air permeability, l/m²/s; 100 Pa		137	115	120.3	126	125	SR EN ISO 9237/1999
Water vapour permeability, %, 3 hours		36.8	35.2	41.09	37.5	43.7	SR 9005-1979
Tensile strength, N	warp	1054	1039	1046	1048	1043	SR EN ISO 13934-1-2002
	weft	501	500	494	496	456	
Break elongation, %	warp	33.3	34.7	36.3	35.2	35.5	SR EN ISO 13934-1-2002
	weft	12.35	12.32	12.27	12.10	11.55	
Thermal resistance, R_{ct}, mpK/W		0.9044	0.8888	0.9466	0.8688	0.9466	SR EN 31092; ISO 11092/1997
Thermal conductivity, mW/MK		0.45	0.45	0.45	0.45	0.45	
Creasing recovery face/back – angle, degrees	warp: face back	171 95	139 125	142 126	127 149	139 126	SR EN 22313/1997
	weft: face back	74 81	66 77	61 75	91 65	73 86	
Surface resistivity, × 10^{10} Ω		26.2	20.1	1.88	17.6	2.17	SR EN 1149-1/2006
Volume resistivity, × 10^7 Ω		603	346	9.41	392	13.5	

more hydrophobic groups on its structure. These hydrophobic groups cover the surface of polyester warp, the hydrophilic part being oriented to the air interface, where they attracts water molecules from the atmosphere, contributing to the material hydro-philization. In the case of HB, as the value of yarn diameter show, the amount is almost equal on both types of yarns, indicating a fine balance between hydrophobic and hydrophilic groups. Even, the amount of cotton is larger than polyester, the layer of HB on fabric surface is too low to offer a hydrophobic character to the material. As it is shown in the table 2, water vapour permeability is much higher for the material coated with HB (18.75%) than for HA (11.64%) demonstrating that the hydrophilization is the predominant effect. After the deposition of the second layer of hydrophobins, the thermal resistance value increases with 4.66% in both cases, confirming the formation of a thick layer of hydrophobins. Stronger decrease of thermal resistance after the first treatment, higher for hydrophobin HB compared to hydrophobin HA, confirms once more the hydrophilic character of HB. Surface resistivity and volume resis-tivity are decreased with one order of magnitude for both hydrophobins, after the second treatment, prob-ably due to polar functional groups, which led to electric conductivity increase. Tensile strength and elongation are not significantly affected by the applied treatments.

Physical-mechanical characteristics of materials treated initially with hydrophobins HA and HB, and afterwards with AgNp/ZnONp solutions are present-ed in table 3 and table 4 respectively, where sample code is formed by AgNp/ZnONp suspension code and hydrophobin type.

The results presented in table 3 indicate the modifi-cations in acceptable limits of physical-chemical properties due to deposition of ZnONp doped with AgNp on fabrics treated with hydrophobin HA. Thus, the mass of the fabrics has a minor decrease of 1.2–2.5%, and the thickness increase with 4.76%, due to nanoparticles deposition, and, probably, due

Table 3

PHYSICAL AND MECHANICAL CHARACTERISTICS OF FABRICS TREATED WITH HYDROPHOBIN HA AND AgNp/ZnONp					
Analysis		**Values**			**Standard**
Sample code		**HA (control)**	**1HA**	**2HA**	**3HA**	
Mass, g/m^2		164	160	162	162	SR EN 12127/2003
Thickness, mm		0.426	0.44	0.44	0.44	SR EN ISO 5084/2001
Yarn diameter, μm	warp	178.5	169.5	175.5	173.5	SR 13152/93
	weft	197	198.0	202.5	203.5	
Density, no. fibers/10 cm	warp	350	350	351	353	SR EN ISO 1049-2/2000
	weft	290	286	288	290	
Air permeability, l/m^2/s; 100 Pa		120.3	117.6	115	106.8	SR EN ISO 9237/1999
Water vapour permeability, %, 3 hours		41.09	39.6	40.2	40.6	SR 9005-1979
Surface resistivity, ×10^{10} Ω		1.88	538	413	216	SR EN1149-1/2006
Volume resistivity, ×10^7 Ω		9.41	216	340	173	

Table 4

PHYSICAL AND MECHANICAL CHARACTERISTICS OF FABRICS TREATED WITH HYDROPHOBIN HB AND AgNp/ZnONp					
Analysis		**Values**			**Standard**
Sample code		**HA (control)**	**1HA**	**2HA**	**3HA**	
Mass, g/m^2; Δ%		163	158/3	160/1.8	162/0.6	SR EN 12127/2003
Thickness, mm		0.426	0.44	0.44	0.43	SR EN ISO 5084/2001
Yarn diameter, μm	warp	177	173.5	171.0	175.5	SR 13152/93
	weft	202	204.0	201.5	202.0	
Density, no. yarns/10 cm	warp	350	350	351	350	SR EN ISO 1049-2/2000
	weft	289	283	288	290	
Air permeability, l/m^2/s; 100 Pa		125	123.7	124	120.2	SR EN ISO 9237/1999
Water vapour permeability, %, 3 hours		43.7	42.8	37.7	43.3	SR 9005-1979
Surface resistivity, ×10^{10} Ω		2.17	32.7	18.6	15.3	SR EN1149-1/2006
Volume resistivity, ×10^7 Ω		1.35	15.6	30	29	

to a contraction of the fabric as seen from increasing density of warp polyester fibers. Noteworthy is the increase of yarn diameter of weft cotton fibers simultaneously with increase of AgNp concentration, unlike polyester fibers, whose diameter decreases. It can be advanced the hypothesis that cotton fibers, wrapped in hydrophobin HA, are oriented with nonpolar, hydrophobic groups towards the exterior, and with polar, hydrophilic groups towards the surface of the fibers. Instead, on the polyester fibers, in case of HA, the nonpolar groups are oriented towards the surface of the fibers and the polar groups towards the exterior. Consequently, Ag/ZnO nanoparticles, having a polar character, are attracted by polar groups of hydrophobin HA existent on cotton, in larger quantity than on polyester fibers. Also, chemical interactions are possible, forming of oxo bridges and Van der Waals bonds between hydrophobin functional groups and ZnO. With the increase of AgNp concentration air permeability decreases in insignificant proportion for the first two concentrations (2.24%, respectively 2.44%) and slightly higher (11.2%) for the fabric treated with the solution containing 1 500 ppm AgNp showing a higher deposition of nanoparticles on the fabric. Water vapor permeability of materials treated with hydrophobin HA and AgNp/ZnONp decreases compared to the one of fabrics treated only with hydrophobins. Comparing only the fabrics treated with hydrophobin HA and AgNp/ZnONp it is observable an increase in water vapor permeability as the concentration of AgNp/ZnONp increases, which shows, on one hand, that with the increase of nanoparticles concentration takes place an increasing in AgNp/ZnONp deposition on the fabric, and on the other hand, AgNp/ZnONp are hydrophilic and retain a larger amount of water vapors from the atmosphere. Surface resistivity increases by two orders of magnitude in samples treated with

AgNp/ZnONp than those treated with hydrophobins, the largest increase occurring in the sample treated with the lowest concentration of nanoparticles. Studies by Jose and Khadar [8] on the behavior of a mixture of ZnO and Ag (5–30%) nanoparticles suggest that this increase in resistance is determined by the presence of Ag particles at the edge of the particles. Due to charge difference from zinc ions, silver ions, have the tendency to accumulate at the interface of zinc particles, creating an electrostatic barrier against the movement of electrons and increasing the resistance of ZnO system doped with Ag [9]. As the AgNp concentration increases there is a half decrease of surface resistivity, probably due to reduced distance between silver inclusions, which means that a greater number of AgNp provide an easier dispersion of electrostatic charges on the surface of the fabric.

As with fabrics treated with hydrophobin HA, the mass of fabrics treated with hydrophobin HB and dispersions of AgNp/ZnONp decreases by 0.6–3% while the thickness grows insignificant. Comparing only the values obtained in case of samples 1HB, 2HB and 3HB, it is visible a parallel increase in mass and density on weft with increasing quantity of AgNp/ZnONp showing a deposition of a greater quantity of nanoparticles with increasing concentration of the solutions. Although air permeability doesn't have a linear variation with increasing AgNp/ZnONp concentration, the lowest value is recorded for the material treated with the highest concentration of nanoparticles, demonstrating once more that treatment with a high concentration leads to the deposition of a greater amount of nanoparticles on the fabric.

The hypothesis is confirmed by the lowest value of air permeability together with the highest value of water vapor permeability. The deposition of a higher quantity of AgNp/ZnONp on the surface of the fabric and between fibers, involves, on one hand, passing a smaller amount of air through the fabric, and on the other hand, the absorption of a higher quantity of water vapors from the atmosphere. Comparatively with fabrics treated with hydrophobin HA, the ones treated with hydrophobin HB and AgNp/ZnONp show a significant drop in volume and surface resistivity, with increasing concentration of AgNp/ZnONp. This requires a higher deposition of nanoparticles on the fabrics treated with hydrophobin HB than those treated with hydrophobin HA. The SEM images of the fabrics treated with hydrophobins and AgNp/ZnONp are presented in figures 1–5.

From SEM images, it is visible that the hydrophobins deposited on polyester/cotton fabric at 80°C in presence of SDS, differently cover the fibers depending on their polarity and structure. Thus, hydrophobin HA covers polyester fibers as flakes, with various sizes, and cotton fibers as parallel, relatively thick rodlets. This confirms literature data according to which the hydrophobic part of hydrophobins layers has the shape of parallel fibrils with amyloidal structure.

a   *b*   *c*
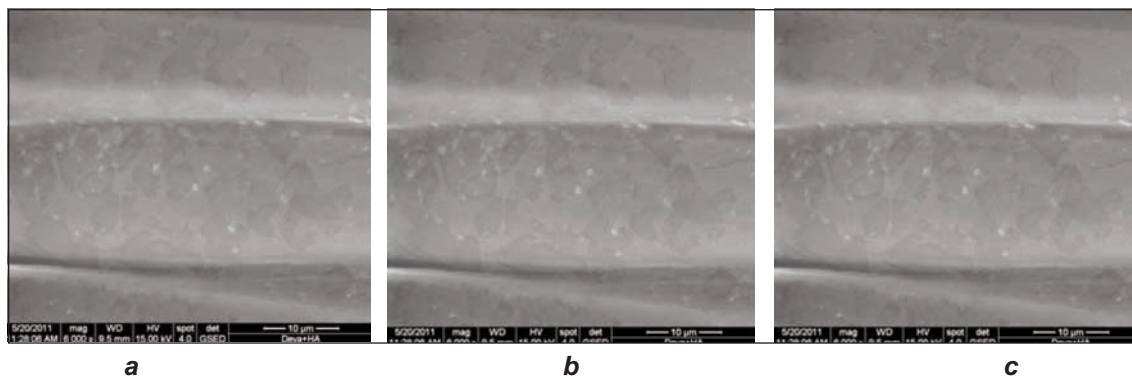
Fig. 1. SEM images of fabrics treated with hydrophobin HA:
a – polyester fibers; *b* – cotton fibers; *c* – detail of hydrophobin HA fibrils on glass slide

a   *b*   *c*
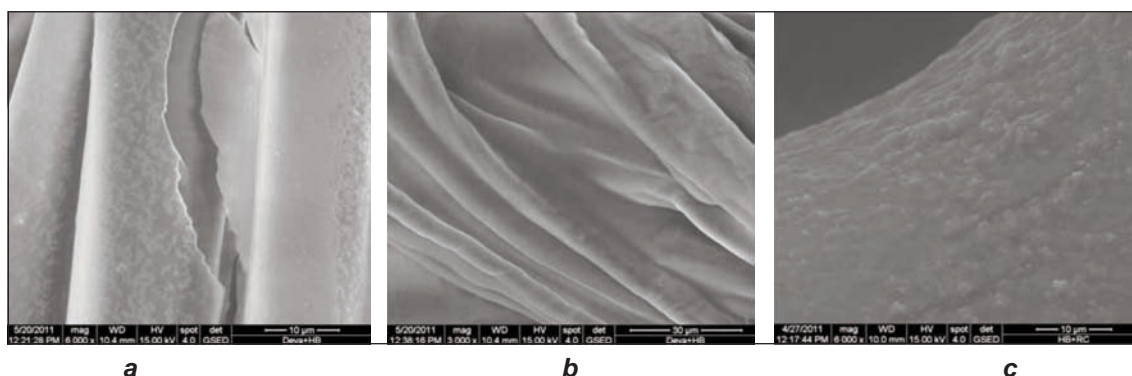
Fig. 2. SEM images of fabrics treated with hydrophobin HB:
a – polyester fibers; *b* – cotton fibers; *c* – detail of hydrophobin HB on glass slide
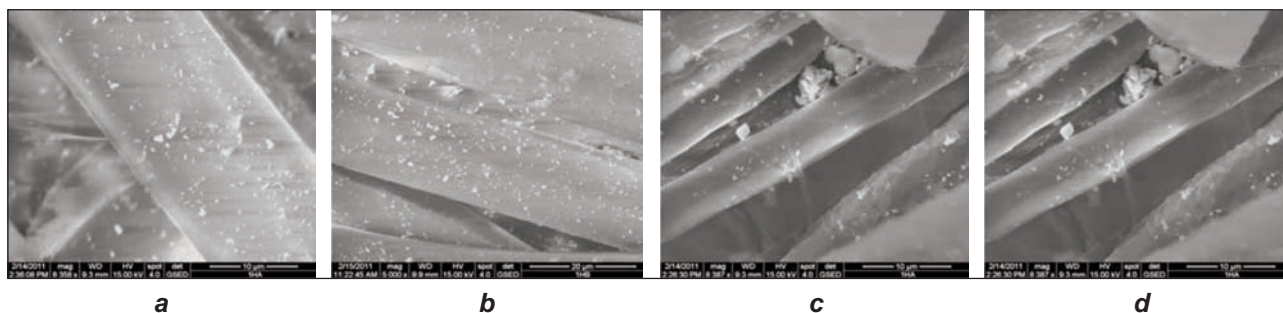
Fig. 3. SEM images of cotton/polyester fabric treated with AgNp/ZnONp solution containing
5 wt.% ZnONp and 75 ppm AgNp:
a – polyester fibers/HA/AgNp/ZnONp; *b* – polyester fibers/HB/AgNp/ZnONp;
c – cotton fibers/HA/AgNp/ZnONp; *d* – cotton fibers/HB/AgNp/ZnONp
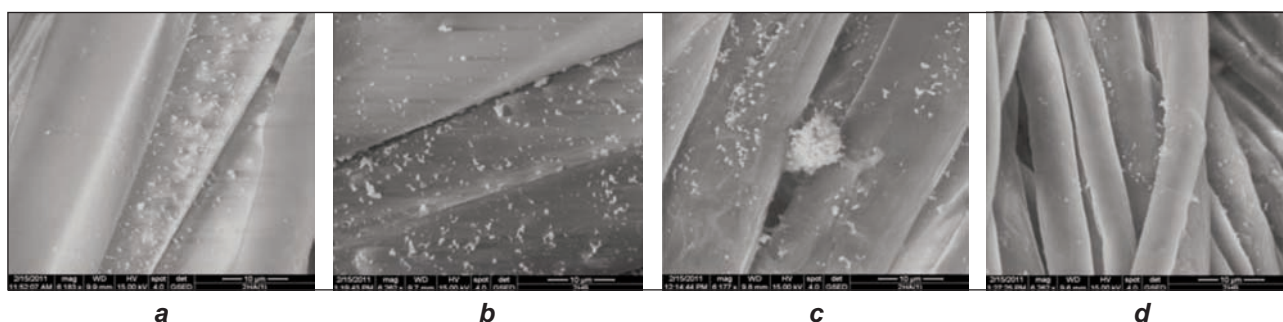
Fig. 4. SEM images of cotton/polyester fabric treated with AgNp/ZnONp solution containing
5 wt.% ZnONp and 750 ppm AgNp:
a – polyester fibers/HA/AgNp/ZnONp; *b* – polyester fibers/HB/AgNp/ZnONp;
c – cotton fibers/HA/AgNp/ZnONp; *d* – cotton fibers/HB/AgNp/ZnONp
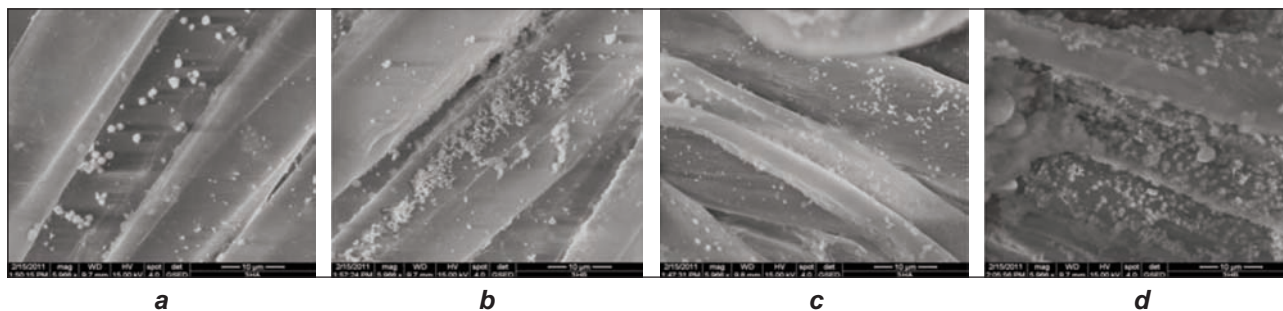
Fig. 5. SEM images of cotton/polyester fabric treated with AgNp/ZnONp solution containing
5 wt.% ZnONp and 1 500 ppm AgNp:
a – polyester fibers/HA/AgNp/ZnONp; *b* – polyester fibers/HB/AgNp/ZnONp;
c – cotton fibers/HA/AgNp/ZnONp; *d* – cotton fibers/HB/AgNp/ZnONp

Instead, hydrophobin HB covers the polyester fibers as thin layers on which surface it is distinguishable a multitude of small multi-fibril clusters, and on cotton fibers as a thick layer, of amyloidal fibrils. On the glass slide, after an incubation time of 24 hours, at room temperature, hydrophobin HA forms amyloidal structures, and hydrophobin HB forms a thick layer with many bumps.

Figures 3–5 show a large deposition of AgNp/ZnONp on both cotton and polyester fibers, deposition that is even greater as the AgNp/ZnONp concentration is higher. If at low concentrations, the deposition is relatively uniform, as the concentration increases, the nanoparticles tend to stick together, thus forming clusters due to Van der Waals attraction forces. Also, it is clearly visible the deposition of a greater number of nanoparticles on fabrics treated with hydrophobin HB than those treated with hydrophobin HA. The presence of ZnO, Ag and hydrophobins on the fabrics is highlighted by SEM/EDAX spectra (fig. 6).

Peaks located at 1.03 KeV and 8.62 KeV (9.59 KeV) can be attributed to Zn [10] – [12] and those located at 2.98 KeV and 3.14 KeV to silver [13]. The sulphur specific peaks (around 2.40 KeV) found on the treated fabrics, can be attributed to the existence of cysteinic components of the hydrophobins. The presence of hydrophobins on fabrics is demonstrated by C, N and O peaks.
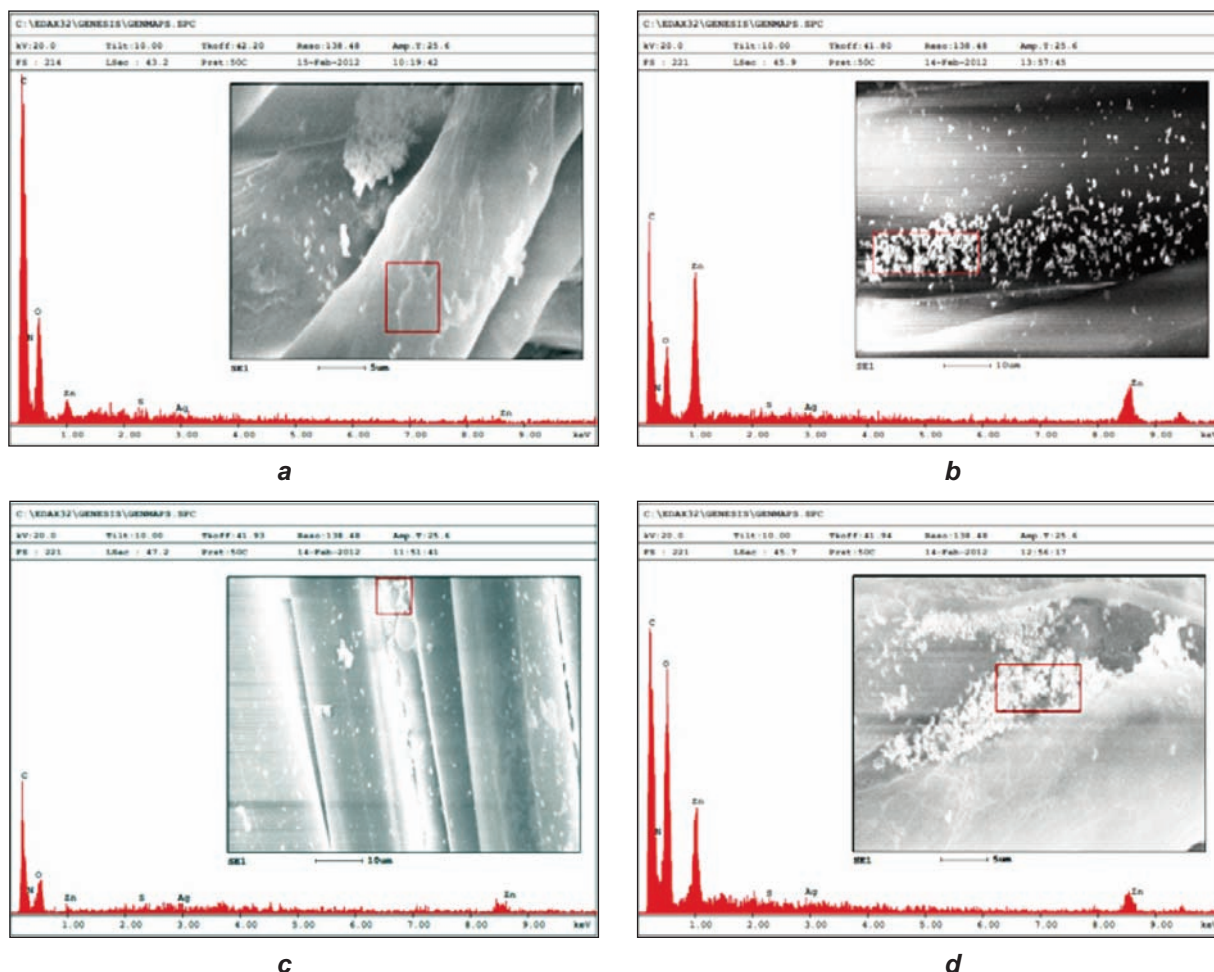
Fig. 6. SEM/EDAX Spectra of fabrics treated with hydrophobins and AgNp/ZnONp:
a – 2HA cotton fibers; *b* – 2 HA polyester fibers;
c – 3HA polyester fibers; *d* – 3 HB cotton fibers

Evaluation of antimicrobial efficiency of fabrics coated with hydrophobins and AgNp/ZnONp solutions

The results of antibacterial tests performed according to ASTM E2149-01 are presented in table 5, where *R* is the rate of reduction. Reduction is considered excellent if *R* > 99.9%, good if *R* is between 99% and 99.9%, weak if *R* is between 0% and 99%.

The results from table 5 show that the fabrics treated with hydrophobins and AgNp/ZnONp inhibit 100% of Pseudomona aeruginosa, Staphyloccocus aureus and Escherichia coli colony development.

As it is seen in table 6, both methods yielded very good rates of reduction, with a small advantage when was used ASTM E2149-01 method, the poorest value being a rate of reduction of 84%. Fabrics treated only with hydrophobin HA and hydrophobin HB were tested only by method ISO 20743:2007. It is known that native hydrophobins lack antimicrobial character, only fusion hydrophobins do so, which are used in antimicrobial coatings for anti-biofilm formation [14]. The fabrics present a very small percentage of reduction (6% for HA and 10% for HB), which may be due to a small degree of retention of microbial cells

by the hydrophobin layer. Fabrics treated with AgNp/ZnONp suspensions have a reduction rate of 100%, for all three AgNp concentrations.

Assessment of interaction between fungal strain and fabrics using scanning electron microscopy

Figure 7 presents SEM images showing interaction between Aspergillus niger and control/treated fabrics. The interaction between Aspergillus niger sporal cells and the treated material led to loss of cellular volume and the collapsing of cell wall. SEM images revealed that the majority of sporal cells underwent a dramatic change from healthy round shape to shrunken forms. The images of cells from the untreated fabric clearly display the changes suffered. In case of hyphae, the aspect turned from round-flat to a more flat looking shape. We believe that upon interaction of the cells with AgNp/ZnONp complexes, the ZnONp alter cell respiration process. The primary cause of the anti-microbial function of ZnONp might be from the disruption of cell membrane activity.

Mechanisms of reaction have been proposed, as membrane damage caused by direct or electrostatic interaction between ZnONp and cell surfaces, cellular internalization of ZnONp and the production

Table 5

	ANTIBACTERIAL EFFICIENCY AGAINST PSEUDOMONAS AERUGINOSA (ATCC 9027), STAPHYLOCOCCUS AUREUS (ATCC 6538) AND ESCHERICHIA COLI (ATCC 8739) OF FABRICS TREATED WITH HYDROPHOBINS AND AgNp/ZnONp ACCORDING TO ASTM E2149-01											
Sample code	Antibacterial efficiency											
	Pseudomonas aeruginosa (ATCC 9027)				*Staphylococcus aureus* (ATCC 6538)				*Escherichia coli* (ATCC 8739)			
	T_0, CFU/mL	T_{24}, CFU/mL	R, %	Log. red	T_0, CFU/mL	T_{24}, CFU/mL	R, %	Log. red	T_0, CFU/mL	T_{24}, CFU/mL	R, %	Log. red
1HA	0.3×10^5	0	100	4.47	0.13×10^5	0	100	4.11	0.13×10^5	0	100	4.11
2HA	0.3×10^5	0	100	4.47	0.12×10^5	0	100	4.08	0.3×10^5	0	100	4.47
3HA	0.3×10^5	0	100	4.47	0.14×10^5	0	100	4.14	0.14×10^5	0	100	4.14
1HB	0.3×10^5	0	100	4.47	0.7×10^4	0	100	4.84	0.3×10^5	0	100	4.47
2HB	0.3×10^5	0	100	4.47	0.1×10^5	0	100	4	0.1×10^5	0	100	4
3HB	0.3×10^5	0	100	4.47	0.1×10^5	0	100	4	0.1×10^5	0	100	4
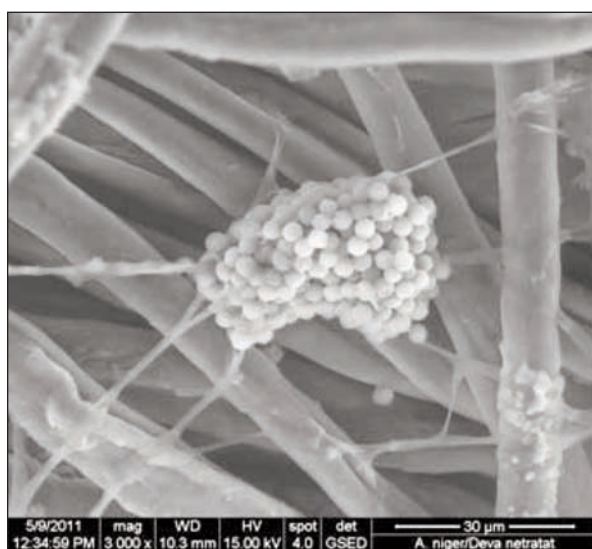
a
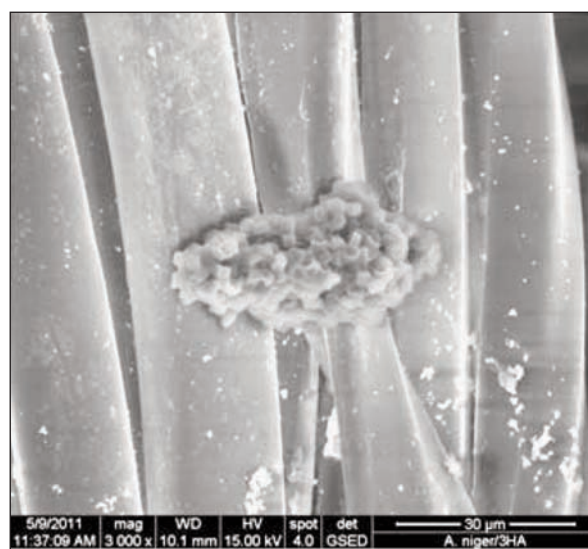
b
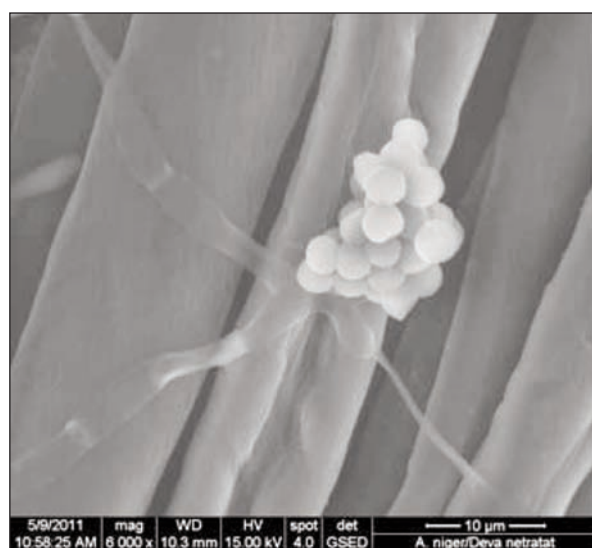
c
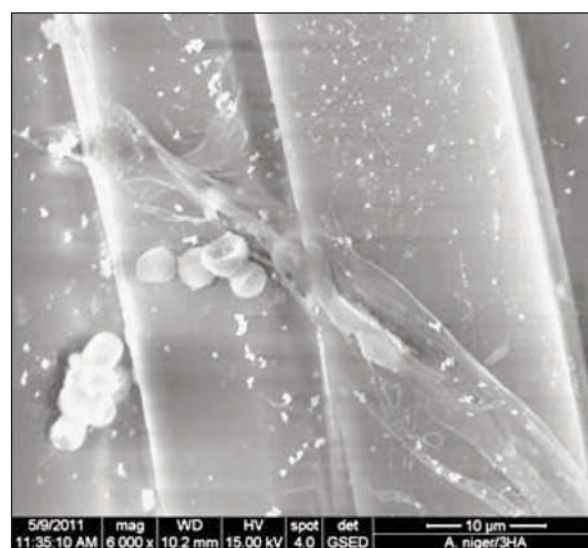
d

Fig. 7. Interaction between Aspergillus niger and the control/treated fabrics:
a and *c* – untreated fabrics; *b* and *d* – 3 HA

Table 6

ANTIFUNGAL EFFICIENCY AGAINST CANDIDA ALBICANS STRAIN OF FABRICS TREATED WITH HYDROPHOBINS AND AgNp/ZnONp ACCORDING TO ASTM E2149-01 AND ISO 20743:2007								
Sample code	Results, according to:							
	ASTM E 2149-01	ISO 20743:2007	ASTM E 2149-01	ISO 20743:2007	ASTM E 2149-01	ISO 20743:2007	ASTM E 2149-01	ISO 20743:2007
	T_0, CFU/mL		T_{24}, CFU/mL		R, %		Log. red	
Control (untreated material)	N/A	N/A	N/A	1×10^4	N/A	N/A	N/A	N/A
HA (control)	N/A	N/A	N/A	9.4×10^3	N/A	6	N/A	0.03
HB (control)	N/A	N/A	N/A	9×10^3	N/A	10	N/A	0.05
Material treated with solution 1	N/A	N/A	N/A	0	N/A	100	N/A	4
Material treated with solution 2	N/A	N/A	N/A	0	N/A	100	N/A	4
Material treated with solution 3	N/A	N/A	N/A	0	N/A	100	N/A	4
1HA	0.1×10^5	N/A	0	0	100	100	4	4
2HA	0.2×10^5	N/A	0	0	100	100	4.30	4
3HA	0.3×10^5	N/A	0	0	100	100	4.47	4
1HB	0.2×10^5	N/A	0	4.8×10^2	100	95.2	4.30	1.32
2HB	0.3×10^5	N/A	0	2×10^1	100	99.8	4.47	2.7
3HB	0.2×10^5	N/A	0	2×10^1	100	99.8	4.30	2.7

of active oxygen species, such as H2O2 [15]. The AgNp themselves present a highly reactive potential, with high antimicrobial efficiency [16].

The AgNp can disrupt the transport systems, including ion efflux, which leads to interrupting cellular processes, such as respiration and metabolism specific reactions [17]. Sulfur-containing proteins from the cell wall are likely to be preferential sites for AgNp binding.

CONCLUSIONS

The used method allows the obtaining of uniform layers of hydrophobins and AgNp/ZnONp on cotton/polyester fabrics. Hydrophobins films allow a better fixation of AgNp/ZnONp on the surface of the fabrics due to the formation of ionic bonds with functional groups, of oxo bridges (–O–), bonding through Van der Waals forces or of integration in protein conformational structure. As the concentration of AgNp increases, the number of nanoparticles that are deposited on the fabric increases as well. Physical-mechanical properties of the materials treated in this way do not change significantly. The increase of surface electrical resistivity suggests the accumulation of AgNp at the edges of ZnONp where an electrostatic barrier is created. This barrier decreases as the concentration of AgNp increases. Bioassays have shown great effectiveness against the tested microorganisms.

BIBLIOGRAPHY

[1] Wessels, J. G. H. *Developmental regulation of fungal cell wall formation*. In: Annual Rewiev of Phytopathology, 1994, vol. 32, pp. 413–37

[2] Wösten, H. A., Vocht, M. L. *Hydrophobins: The fungal coat unravelled*. In: Biochimica and Biophysica Acta, 2000, vol. 1 469, pp. 79–86

[3] Wösten, H. A. B., Asgeirsdóttir, S. A., Krook, J. H., Drenth, J. H., Wessels, J. G. *The fungal hydrophobin Sc3p self-assembles at the surface of aerial hyphae as a protein membrane constituting the hydrophobic rodlet layer*. In: European Journal of Cell Biology, 1994, vol. 63, issue 1, p. 122–9

[4] Subkowski, T., Weickert, U. *Coated stents and process for coating with protein*. WIPO Patent Applications WO/2011/121009

[5] Bauermann, L. P., del Campo, A., Bill, J., Aldinger, F. *Heterogeneous nucleation of ZnO using gelatin as the organic matrix*. In: Chemistry of Materials, 2006, vol. 18, pp. 2 016–20

[6] Opwis, K., Gutmann, J. S. *Surface modification of textile materials with hydrophobins*. In: Textile Research Journal, 2011, vol. 81, issue 15, pp. 1 594–602

[7] Wohlleben, W., Subkowski, T., Bollschweiler, C., von Vacano, B., Liu, Y., Schrepp, W. et al. *Recombinantly produced hydrophobins from fungal analogues as highly surface-active performance proteins*. In: European Biophysics Journal, 2010, vol. 39, issue 3, pp. 457–680

[8] Jose, J., Khadar, M. A. *Role of grain boundaries on the electrical properties of ZnO–Ag nanocomposites: an impedance spectroscopic study*. In: Acta Mater, 2001, vol. 49, pp. 729–735

[9] Kuo, S. T., Tuan, W. H., Shieh, J., Wang, S. F. *Effect of Ag on the microstructure and electrical properties of ZnO.* In: Journal of the European Ceramic Society, 2007, vol. 27, pp. 4 521–2

[10] Büsgen, T., Hilgendorff, M., Irsen, S., Wilhelm, F., Rogalev, A., Goll, D. et al. *Colloidal cobalt-doped ZnO nanorods: synthesis, structural and magnetic properties*. In: Journal of Physical Chemistry, 2008, vol. 112, pp. 2 412–17

[11] Qi, H., Alexson, D. A., Glembocki, O. J., Prokes, S. M. *Synthesis and oxidation of silver nano-particles*. Proceedings of SPIE 2011, 7947: 79470Y-1-11

[12] Lazić, V., Vodnik, V., Nedeljković, J., Šaponjić, Z., Jovančić, P., Radetić, M. *Antibacterial and colorimetric evaluation of cotton fabrics dyed with direct dyes and loaded with Ag nanoparticles*. In: Industria Textilă, 2013, vol. 64, issue 2, pp. 89–97

[13] Chuang, H. Y., Chen, D. H. *Fabrication and photocatalytic activities in visible and UV light regions of Ag@TiO_2 and NiAg@TiO_2 nanoparticles*. In: Nanotechnology, 2009, vol. 20, issue 10, p. 105 704

[14] Rieder, A., Schwartz, T., Obst, U., Bollschweiler, C., Gutt, B., Zoller, J. et al. *Hydrophobins – using hydrophobins to prevent microbial biofilm growth on mineral surfaces*. In: Geotechnologien Science Report, 2010, vol. 16, pp. 3–18

[15] Stoimenov, P. K., Klinger, R. L., Marchin, G. L., Klabunde, K. J. *Metal oxide nanoparticles as bactericidal agents*. Langmuir, 2002, vol. 18, pp. 6 679–86

[16] Khoddami, A., Shokohi, S. S., Sebdani, Z. M. *A facile method for anti-bacterial finishing of cotton fabrics using silver nanoparticles.* In: Industria Textilă, 2012, vol. 63, issue 1, pp. 20–26

[17] Min, J. S., Kim, K. S., Kim, S. W., Jung, J. H., Lamsal, K., Kim, S. B. et al. *Effects of colloidal silver nanoparticles on sclerotium-forming phytopathogenic fungi.* In: Plant Pathology Journal, 2012, vol. 25, issue 4, pp. 376–380

Authors:

Cerc. şt. gr. III dr. ing. IULIANA DUMITRESCU
Asist. cerc. şt. drd. ing. OVIDIU GEORGE IORDACHE
Cerc. şt. gr. III dr. ing. ANA MARIA MOCIOIU
Cerc. şt. gr. III drd. ing. GHEORGHE NICULA
Institutul Naţional de Cercetare-Dezvoltare pentru Textile şi Pielărie
Str. Lucreţiu Pătrăşcanu nr. 16, 030508 Bucureşti
e-mail: iuliana.dumitrescu@gmail.com;
certex@ns.certex.ro

Corresponding author:

OVIDIU-GEORGE IORDACHE
e-mail: iordacheovidiu.g@gmail.com

DOCUMENTARE

Noi tehnologii

PROCES ECOLOGIC DE FINISARE A BLUGILOR

Furnizorul tehnologiei de finisare a suprafeţei blugilor, *Jeanologia*, din Paterna/Spania, a expus noul laser *3E Twin Jeanologia,* pentru prima dată, la *Munich Fabric Start*, desfăşurat în februarie 2013, la Munchen, Germania.

Tehnologia cu laser de finisare a textilelor este concepută pe baza celor trei principii "Ecologie, Eficienţă şi Etică" (3E). Acest lucru permite ca, în procesul de finisare a blugilor, să se realizeze atât o scurtare a timpului, cât şi o economisire a energiei, apei şi produselor chimice.

3E Twin Jeanologia este utilizat în producţia blugilor, la scară industrială, datorită faptului că noul laser este echipat cu doi rezonatori laser, permiţând finisarea simultană a celor două părţi ale pantalonilor.

Astfel, este posibilă o producţie de 100–200 de perechi de blugi pe oră, spre deosebire de 10 perechi pe oră în cazul sablării manuale sau de numai 60 de perechi pe oră în cazul tehnicilor de sablare utilizate până în prezent.

Melliand International, martie 2013, p. 12

Yarn diameter in elasticized knitted structures

ALENKA PAVKO-CUDEN   URSKA STANKOVIĆ ELESINI

REZUMAT – ABSTRACT

Diametrul firelor din structurile tricotate elasticizate

Diametrul este un parametru de bază al firelor, care depinde atât de densitatea liniară, cât şi de structura acestora şi de compoziţia materialului. În prezent, în materialele tricotate, adesea, sunt încorporate fire foarte flexibile, cu miez de elastan. Acestea nu sunt omogene, ceea ce afectează uniformitatea diametrului firului. De obicei, structurile tricotate realizate din fire convenţionale sunt poroase, în timp ce tricotarea cu fire elasticizate are ca rezultat o structură compactă, cu efect de compresiune a firelor în cadrul buclei tricotate. Scopul studiului îl constituie compararea diametrelor firelor elasticizate, realizate prin diverse procese, cu diametrele firelor tradiţionale fără elastan, toate aceste fire fiind realizate din fibre identice, cu densitate liniară identică şi torsiune comparabilă. Modificarea diametrului firului, după relaxarea în stare umedă, a fost observată în cazul tuturor firelor testate. Rezultatele au arătat că diametrele firelor, determinate prin măsurători sau calculate din valorile parametrilor structurii fibrei sau a firului, au crescut în timpul relaxării în stare umedă. Diametrul firului în punctele de interţesere orizontale ale buclei, calculate pe baza parametrilor structurilor tricotate, a scăzut în timpul relaxării în stare umedă.

Cuvinte-cheie: diametrul firelor, grosimea firelor, structură tricotată, tricot glat, relaxare, elastan, analiza imaginilor

Yarn diameter in elasticized knitted structures

Yarn diameter is a basic yarn parameter dependent on yarn linear density, yarn structure and its material composition. Nowadays, highly extensible yarns with elastane core are often incorporated in knitted fabrics. They are non-homogeneus which affects the uniformity of the yarn diameter. Knitted structures made from conventional yarns are usually porous while knitting with elasticized yarns results in a compact structure with yarn compression within the knitted loop. The objective of this research was to compare yarn diameters of elasticized yarns produced by various processes and yarn diameters of conventional yarns without elastane, all made from identical fibers with the identical linear density and comparable twist. The change of the yarn diameter after wet relaxation was observed for all investigated yarns. The results showed that yarn diameters, determined either by measurements or calculated from the fiber or yarn structure parameters, increased during wet relaxation. The yarn diameter within the loop horizontal interlocking points calculated from the knitted structure parameters decreased during wet relaxation.

Key-words: yarn diameter, yarn thickness, knitted structure, single jersey, relaxation, elastane, image analysis

Nowadays, elastane threads are often incorporated in knitted fabrics to improve their elastic recovery. Highly extensible yarns with elastane core are at least two-component and two-layered, as a result they are therefore non-homogeneus, which affects the uniformity of the yarn diameter. Knitting with elasticized yarns results in compact structure because of the yarn extension during loop formation, fabric relaxation after knitting and during wet processes and yarn compression within the knitted structure which reflects in the yarn cross-section change.

The shrinkage of knitted fabrics made from highly elastic yarns with the elastane core after the wet relaxation is significantly higher than the shrinkage of the knitted fabric made from yarns without the elastane core. A very compact elasticized knitted structure can be defined as a supercompact structure [1] where the yarn compression in the interlocking region of the loops can be forcast. The yarn diameter within the structure varies with the tightness of knitting [2]. As the tightness of the knitted structure changes during relaxation, the change of the yarn diameter within knitted structure during relaxation can be anticipated.

Yarn diameter is a knitted fabric parameter which is difficult to determine as the yarn is not a solid body of uniform and known density; its porosity may amount to 30–70%. The yarn core is dense while the yarn sheath consists of free ends of the fibers that protrude from the yarn surface [3], [4]. Low twist of the knitting yarns results in a variable real yarn diameter within the knitted structure [2].

There are many methods for measuring yarn diameter and yarn compression. These methods have undergone considerable change and development over the years. However, none of them have been accepted as a standard method. A typical classification of the methods is as follows:

- measuring yarn diameter via mass and length;
- measuring yarn diameter using optical methods;
- measuring yarn diameter by employing mechanical methods [5].

The first two methods involve measuring yarn diameter free from any forces, i.e. free from lateral forces in a non-compressed state. There is usually only a

small longitudinal force (tension) on the yarn to keep it straight [4]. Measuring yarn diameter by microscopic observation and optical-projection method involves subjective determination of the yarn boundaries in the unloaded state, which is a weak point of these methods.

Measuring yarn diameter via mechanical measuring head involves inserting the yarn between suitable elements, one of which is fixed while the other can be displaced freely. Mechanical methods of measuring yarn diameter include direct compression of the yarn. Considering the fact that the yarn is compressed during weaving and knitting, mechanical methods enable experimental results that may exhibit the real geometry of the flat textile structure [5], [6].

Many researchers have investigated yarn geometrical parameters and measured yarn diameter by various methods [7] – [26] which indicates the importance of this parameter for the design and planning of textile structures. The analysis into the state of current reseach revealed that it has been mostly conventional yarns without elastane core which have been included in studies of the yarn diameter.

The research objective was to compare yarn diameters of elasticized yarns produced by various processes and yarn diameters of conventional yarns without elastane, all made from identical fibers with the identical linear density and comparable twist. The change of the yarn diameter after wet relaxation was observed for all investigated yarns. In the investigation, various methods of yarn diameter measurement were applied and evaluated.

THEORETICAL, EFFECTIVE AND MAXIMAL YARN DIAMETER

Yarn lengths from which knitted loops are formed, are characterized by their thickness. Yarn thickness is a basic yarn parameter dependent on yarn linear density, structure and material composition. Yarn thickness is equal to yarn diameter, if the circular cross-section of the yarn is assumed. During the knitting process, yarn thickness changes depend on loading and longitudinal extension. Yarn thickness in a loose condition differs from yarn thickness in a strongly compressed state. In the first case, yarn thickness is equal to yarn effective diameter d_e, equation (1), and in the second case, it is equal to yarn theoretical diameter d_t, equations (1) and (3). Yarn theoretical diameter d_t is a diameter of the yarn with no air pockets between the indvidual fibers. In real knitted fabric, yarn theoretical diameter d_t is only exhibited by individual sections of the knitting yarn placed over the knitting elements during the knitting process. In real knitted fabric, yarn effective diameter d_e exceeds theoretical diameter d_t [27], [28] due to the yarn voluminosity.

It holds [27], [28]:

$$d_e = k_D \cdot \sqrt{T_t} \qquad (1)$$

and

$$k_D = \frac{2}{\sqrt{\pi \cdot \gamma}} \qquad (2)$$

where:
d_e is yarn effective diameter, mm;
k_D – experimentally defined coefficient of yarn diameter, tex$^{-1/2}$ mm [28];
T_t – yarn linear density, tex;
γ – yarn density for effective yarn diameter d_e, kgm^{-3}.

For theoretical yarn diameter d_t, density of the fiber material composing the yarn can be introduced where γ_F is fiber density. It holds [28]:

$$k_D = \frac{2}{\sqrt{\pi \cdot \gamma_F}} \qquad (3)$$

For higly voluminous yarns with a low yarn density γ and multifilament yarns with low twist, yarn maximal diameter d_{max} can be defined. It exceeds yarn effective diameter d_e, caluculated by equation (1) [28]. In real knitted fabric, yarn maximal diameter d_{max} comes into effect in a very open knitted structure where the yarn can expand within the knitted structure during relaxation after the knitting process and wet processes.

In theory, yarn minimal diameter d_{min} equals theoretical diameter d_t when a round cross-section of the yarn is assumed. In real knitted fabric, yarn minimal diameter d_{min} may be less than yarn theoretical diameter d_t if the yarn cross-section is not circular [28]. This may come into effect in interlocking points of the loop if the yarn is compressed. Therefore, it can be assumed that $d_{min} \leq d_t$ in the interlocking points of a very compact, i.e. supercompact knitted structure [1].

EXPERIMENTAL PART

Samples preparation

Ring-spun yarns used for the knitted samples preparation were designed and made to order with planned parameters for the research purposes from viscose (CV) and poliacrylonitryle (PAN) fibers. From each raw material, elasticized yarns with the same linear density were made: mouliné twisted yarn (composed of an elastomeric core-spun yarn and a yarn without elastane, both ring-spun), core-twisted yarn (elastane filament yarn, core-twisted with two ring-spun yarns) and core-spun yarn (a yarn with an elastane core and staple fiber sheath covering). For comparison, ring-spun yarns without elastane with equal linear density as elasticized yarns were also produced. The knitted samples were produced on the electronic flat weft knitting machine UNIVERSAL MC 720, gauge E8. All samples were knitted with an equal yarn input tension, equal knitted fabric take-off and at identical environment conditions. From each yarn, the samples were knitted in two densities. First, all samples were statically dry relaxed, i.e. placed unloaded to the standard environment for 72 hours.

After the dry relaxation, a half portion of each sample was additionally dynamically wet relaxed. The process comprised laundering at 30°C, short spinning, 40 minutes drying, four cycles of short rinsing and 40-minute tumble drying (all delicate laundry programme), and placing wet relaxed samples flat to the standard environment for at least 24 hours after the drying was finished.

Due to their structure, high extensibility and high elastic recovery of the elastane core yarns, significant changes of the elastane core yarn thickness were expected after the dynamic wet relaxationof knitted fabrics. Therefore, yarns were relaxed simultaneously with the knitted fabrics in order to calculate the parameters of the dry and wet relaxed knitted structure and examine the yarn diameter change after wet relaxation. The dry relaxed yarns were placed unloaded to the standard environment for 72 hours. To avoid the ruffling of yarns in the laundering machine drum during rotation, the yarns were dynamically wet relaxed with a 2 hours soaking of the threads in the water at 30°C with occasional stirring. Afterwards, they were dried simultaneously with the investigated knitted fabrics in a tumble dryer at the delicate programme. SEM pictures of yarn samples are presented in table 1.

Based on the review of experimental methods [5], [7] – [26], investigations were carried out into the diameter of the elasticized yarns compared to conventional yarns without elastane. It was not possible to determine the yarn diameter at the loop interlocking points within the real knitted fabric by the image analysis due to the high compactness of the elasticized knitted fabric tested. Instead, the yarn diameter at the interlocking points was calculated from the loop width. In addition, various methods were selected to experimentally and mathematically determine the yarn diameter.

Yarn diameter determination

Maximal yarn diameter d_{max} measured by image analysis

A maximal yarn diameter d_{max} of the dry relaxed and wet relaxed samples was measured. It was determined by an optical method, a derivative of the Fletcher & Roberts method [8] – [11]. The dry and wet relaxed yarn samples were prepared from the yarn skein. A length of 50 cm was cut from the yarn skein without untwisting the yarn. The upper end of the yarn was glued to the A6 size cardboard using a glue gun. The cardboard with the glued yarn pieces was mounted in a vertical clamp. The lower end of the yarn was loaded with a preload of 0.3 cN [18] to remove the crimp, and glued to cardboard using the glue gun. On each cardboard, 10 yarns were glued. The prepared yarn samples were optically scanned with a resolution of 1 200 dpi. For each sample, a hundred yarn cutouts were prepared in Photoshop. The cutout size was 0.5 × 0.5 cm. The maximal width of the yarn was limited by the Photoshop guidebar

tool. The maximal yarn diameter was measured as a distance between the guidebars. The number of measurements for each yarn sample of yarn was one-hundred. The results of the maximal yarn diameter measurements are given in table 1 and figure 1.

Yarn diameter d_S measured by image analysis based on Sadikov method

Yarn diameter d_S was measured by the modified Sadikov method [18]. Yarn samples glued on cardboard, previously prepared for the maximal yarn diameter determination were used. 30 mm long yarn sections were scanned with a resolution of 1 200 dpi. Then, they were printed on paper at 20 × magnification and cut. The cut out samples were weighed. The average yarn diameter was calculated from the surface of the yarn sample and the yarn sample length. The results of the yarn diameter measurements by image analysis based on Sadikov method are given in table 2 and figure 2.

Minimal yarn diameter d_{min} – calculated theoretical yarn diameter

The minimal yarn diameter d_{min} was calculated for each dry and wet relaxed yarn sample from the material composition and the measured yarn linear density using the equations (1) and (2) [27], [28]. The yarn material composition is given in table 1. For the calculation of the yarn theoretical diameter, the
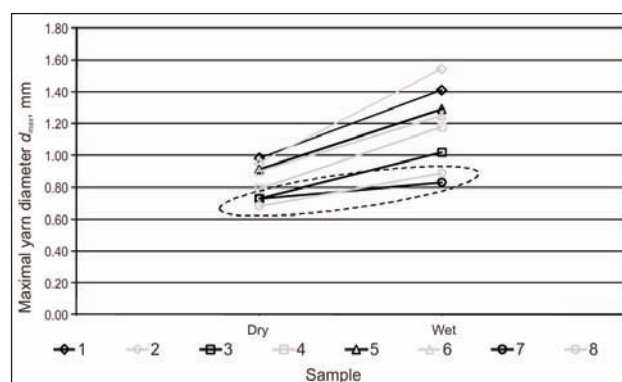
Fig. 1. Measured maximal yarn diameter d_{max} of the dry and wet relaxed yarns
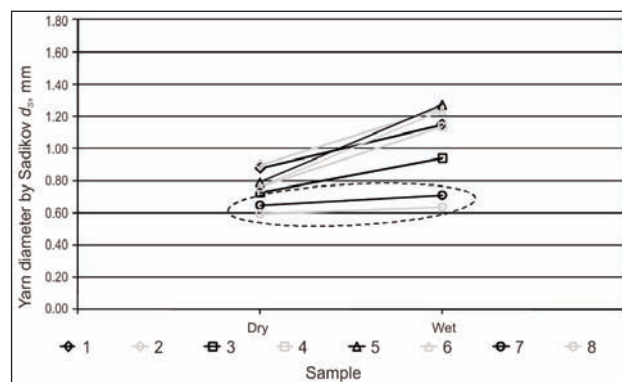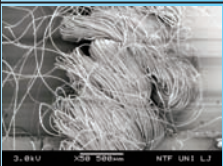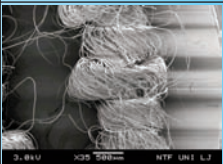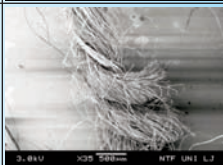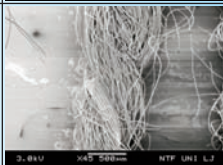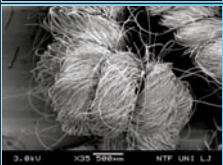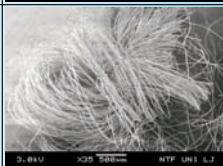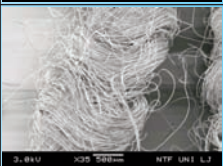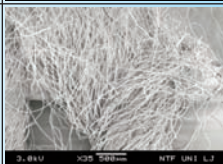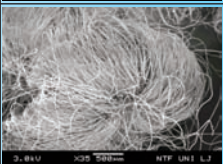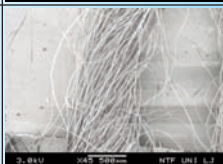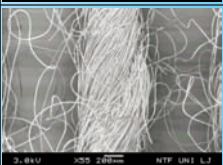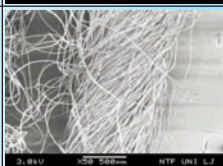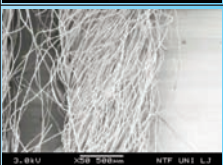
Fig. 2. Yarn diameter measured by Sadikov method d_S of the dry and wet relaxed yarns

Table 1

Yarn sample	Material composition, %	Nominal linear density, tex	Twist, m^{-1}	Breaking tenacity, $cNtex^{-1}$	Breaking extension, %	Uster value, %	No. of thin places	No. of thick places	No. of nobs	SEM photo dry relaxed yarn	SEM photo wet relaxed yarn
1	97.8% CV 2.2% EL	100	500 S	20.2	19.3	7.4	0	0	0		
2	97.8% PAN 2.2% EL	100	500 S	21.5	26.9	7.3	0	2	1		
3	97.8% CV 2.2% EL	102	500 S	20.3	19.1	7.5	0	0	0		
4	97.8% PAN 2.2% EL	102	500 S	21.2	26.5	7.4	0	0	0		
5	97.8% CV 2.2% EL	100	281 Z	18.4	17.7	8.5	0	0	1		
6	97.8% PAN 2.2% EL	100	278 Z	19.6	23.8	9.1	0	0	0		
7	100% CV	100	221 Z	21.9	17.7	8.4	0	1	0		
8	100% PAN	100	221 Z	19.7	23.0	9.1	0	1	0		

Table title: **YARN CHARACTERISTICS**

density of elastane – Lycra, viscose (Danufil) – CV and polyacrylonitrile (Leacril) – PAN fibers was considered as follows: γ_{CV} = 1 510 gdm^{-3}, γ_{PAN} = 1 180 gdm^{-3} and γ_{LYCRA} = 1 210 gdm^{-3}. The values of the measured yarn linear density and the calculated minimal diameter for each yarn sample are given in table 3 and figure 3. Yarn diameter within loop horizontal interlocking points d_H smaller than minimal yarn diameter d_{min} – which indicates the super-compact knitted structure [1].

Average yarn diameter d

Average yarn diameter d [7] – [11], [28] was calculated using equation (4) below:

$$d = \frac{d_{max} + d_{min}}{2} \qquad (4)$$

Table 2

MEASURED MAXIMAL YARN DIAMETER d_{max} AND YARN DIAMETER MEASURED
BY SADIKOV METHOD d_S OF THE DRY AND WET RELAXED YARNS

Yarn sample		Maximal yarn diameter, d_{max}			Yarn diameter mesured by Sadikov method, d_S		
		$\overline{x}$, mm	s, mm	CV, %	$\overline{x}$, mm	s, mm	CV, %
1	dry	0.98	0.08	7.87	0.88	0.10	11.15
	wet	1.41	0.11	7.79	1.15	0.11	9.18
2	dry	0.95	0.07	7.73	0.90	0.06	6.46
	wet	1.54	0.12	7.76	1.25	0.10	7.68
3	dry	0.73	0.05	7.28	0.72	0.13	17.35
	wet	1.02	0.07	6.96	0.94	0.08	8.34
4	dry	0.79	0.06	7.69	0.76	0.05	6.21
	wet	1.18	0.09	7.52	1.13	0.08	7.16
5	dry	0.91	0.07	7.26	0.79	0.07	8.60
	wet	1.29	0.10	7.59	1.27	0.20	15.79
6	dry	0.90	0.07	8.24	0.76	0.11	13.96
	wet	1.25	0.08	6.67	1.23	0.10	8.41
7	dry	0.73	0.06	7.98	0.65	0.04	5.67
	wet	0.83	0.06	7.17	0.71	0.06	8.51
8	dry	0.69	0.05	7.82	0.60	0.07	11.69
	wet	0.89	0.07	7.41	0.63	0.06	9.15

Table 3

CALCULATED MINIMAL YARN DIAMETER d_{min}, AVERAGE YARN DIAMETER d
AND YARN DIAMETER WITHIN LOOP HORIZONTAL INTELOCKING POINTS d_H
OF THE DRY AND WET RELAXED YARNS

| Yarn sample		Yarn linear density, T_t, tex	Minimal yarn diameter, d_{min}, mm	Average yarn diameter, d, mm	Yarn diameter within loop intelocking points, d_H, mm	
					close structure	open structure
1	dry	123.5	0.32	0.65	0.50	0.52
	wet	251.9	0.46	0.94	0.39	0.48
2	dry	114.1	0.35	0.65	0.52	0.57
	wet	202.2	0.46	1.00	0.43	0.48
3	dry	119.9	0.32	0.53	0.51	0.58
	wet	242.3	0.45	0.74	0.41	0.47
4	dry	105.6	0.34	0.57	0.53	0.54
	wet	178.2	0.44	0.81	0.43	0.47
5	dry	124.3	0.32	0.62	0.48	0.54
	wet	242.1	0.45	0.87	0.38	0.44
6	dry	113.7	0.35	0.63	0.53	0.61
	wet	225.5	0.49	0.87	0.43	0.50
7	dry	99.6	0.29	0.51	0.56	0.74
	wet	107.1	0.30	0.57	0.67	0.82
8	dry	95.1	0.32	0.51	0.54	0.66
	wet	95.8	0.32	0.61	0.54	0.65
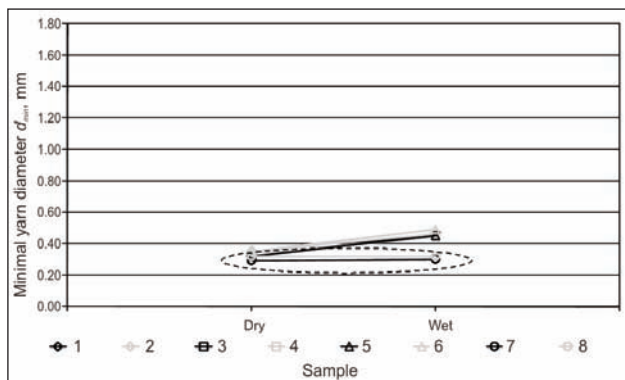
Fig. 3. Calculated minimal yarn diameter d_{min} of the dry and wet relaxed yarns

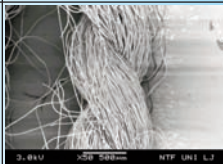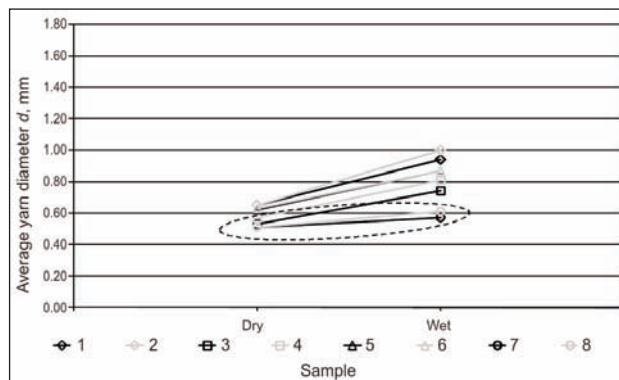Fig. 4. Calculated average yarn diameter d of the dry and wet relaxed yarns

where:

d is the average yarn diameter, mm;

d_{max} – the maximal yarn diameter, mm;

d_{min} – the minimal yarn diameter, mm.

The values of the calculated average yarn diameter are given in table 3 and figure 4.

Yarn diameter within the loop horizontal interlocking points

The yarns in the loop of the normal to supercompact knitted structure joint in the contact region, therefore $A = 4\ d_H$. Consequently, the yarn diameter within the loop horizontal interlocking points can be calculated from the measured width of loop A [1]. The values of the calculated yarn diameter within the loop horizontal interlocking points d_H are given in table 3 and figure 5.

RESULTS AND DISCUSSIONS

In table 2 and figure 1 show that the maximal yarn diameter d_{max} of the wet relaxed yarns is greater than the maximal yarn diameter d_{max} of the dry relaxed yarns. This is due to the yarn shrinking during wet processes. Differences between mean values of the yarn diameters of individual dry and wet relaxed yarns are significantly greater for the elasticized yarns which exhibit greater shrinkage compared to non-elasticized yarns. The maximal yarn diameter d_{max} of the elasticized yarns increased by 39.7% to 62.1% during wet relaxation. For non-elasticized yarns, the increase was 13.7% (CV yarn) or 30.9% (PAN yarn). Wet relaxed mouliné yarns (samples 1 and 2) and core-spun yarns (samples 5 and 6) exhibit the greatest maximal diameter d_{max}, while the conventional yarns without elastane core (samples 7 and 8) exhibit the lowest maximal diameter d_{max}. Mouliné twisted yarns are composed of an elastomeric core-spun yarn and a yarn without elastane, both ring-spun. Core-spun yarn is a yarn with an elastane core and staple fiber sheath covering. During wet relaxation, crimps are formed in these yarns due to the ununiform relaxation shrinking of the elastane core and fiber assembly in the sheath, which influences
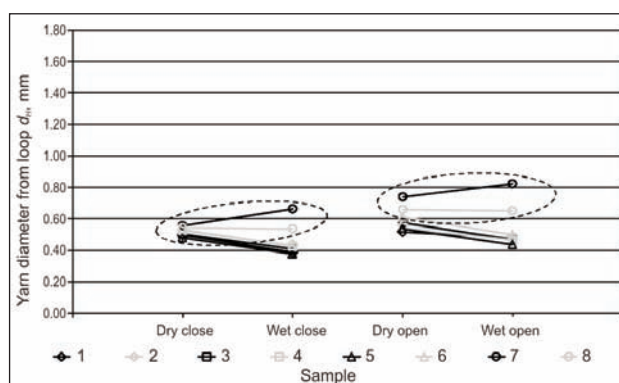
Fig. 5. Calculated yarn diameter within loop horizontal interlocking points d_H of the dry and wet relaxed yarns

the substantial increase of the maximal yarn diameter (fig. 1).

Yarn diameter measured by Sadikov method d_S is presented in table 2 and figure 2. It exhibits higher values for the wet relaxed yarns than for the dry relaxed yarns. Yarn diameter values are the lowest for the conventional yarns without elastane. The yarn diameter increase during wet relaxation is 29.8% to 61.7% for the elasticized yarns, while it is 10% for viscose conventional yarn and 6.2% for polyacrylonitrile conventional yarn. Core-spun yarns (samples 5 and 6) exhibit the largest increase, while conventional yarns without elastane (samples 7 and 8) exhibit the lowest increase.

Minimal yarn diameter d_{min} (table 3, fig. 3) increased during wet relaxation due to yarn shrinkage and resulted in a consequent increase in the yarn linear density. Therefore, the calculated average yarn diameter d increased during wet relaxation as well.

The average yarn diameter d (table 3, fig. 4) calculated from the maximal yarn diameter d_{max} and the minimal yarn diameter d_{min}, and the average yarn diameter measured by the Sadikov method d_S (table 2, fig. 2) differ significantly. Yarn diameter of the elasticized yarns measured by the Sadikov method d_S (samples 1 – 6) is significantly higher than the calculated average diameter of the yarn d. The measured average diameter d_S of the conventional yarns

without elastane (samples *7* and *8*) also exceeds the average calculated yarn diameter *d*, although the differences are smaller.

Comparison of the yarn diameters, measured and calculated by different methods, shows that the yarn diameter within the interlocking points shown in table 3 and figure 5, (which equals the quarter of the loop width, i.e. $d_H = A/4$) is smaller than the minimal yarn diameter d_{min} for all close wet relaxed samples made from elasticized yarns. It can be assumed that the yarn cross-section within the interlocking points is not circular. The fibers composing the yarn are re-arranged around the elastane core during wet relaxation so that the yarn is flattened in the interlocking points.

Yarn diameter determined either by measurements or calculated from the fiber and yarn structure parameters, increases during wet relaxation in all cases. It is lower for the conventional yarns without elastane than for the elasticized yarns. However, yarn diameter within the loop horizontal interlocking points calculated from the knitted structure parameters decreases during wet relaxation. The loop dimensions, especially loop width and height change. Furthermore, the yarn diameter also changes within the loop interlocking points due to yarn compressibility. The calculated yarn diameter within the loop horizontal interlocking points d_H is substantially lower for the elasticized yarns than for the conventional yarns without elastane.

CONCLUSIONS

Various optical and mathematical methods were applied in order to determine the yarn diameter, both experimentally and mathematically. It was not possible to determine the yarn diameter within the real knitted structure by the image analysis due to the high compactness of the tested elasticized knitted fabric. Since highly elasticized yarns extend significantly at low stress and the relation between load-extension is not linear, mechanical methods were not selected for this research either.

Yarn diameter determined either by measurements or calculated from the fiber and yarn structure parameters, increased during wet relaxation. The yarn diameter within the loop horizontal interlocking points calculated from the knitted structure parameters decreased during wet relaxation. This is explained by the loop dimensions changing as well as the changes in yarn compressibility. The calculated yarn diameter within the loop horizontal interlocking points is substantially lower for the elasticized yarns than for the conventional yarns without elastane.

Comparison of the yarn diameters measured and calculated by different methods showed that the yarn diameter within the interlocking points is smaller than the minimal yarn diameter for all close wet relaxed samples made from elasticized yarns. It can be assumed that the yarn cross-section within the interlocking points is not circular. The fibers composing the yarn are re-arranged around the elastane core during wet relaxation so that the yarn is flattened in the interlocking points.

BIBLIOGRAPHY

[1] Pavko-Cuden, A. *Parameters of compact single weft knitted structure*. Part 2: *Loop modules and Munden constants – compact and supercompact structure*. In: Tekstilec, 2010, vol. 53, no. 10/12, pp. 259–272

[2] Grosberg, P. *The geometry of knitted fabrics.* Hearle, V. J. W. S., Grosberg, P., Backer, S. *Structural mechanics of fibers*. Part 1 – *Yarns and fabrics.* New York, London, Sidney, Toronto: John Wiley & Sons, 1969, pp. 411–450

[3] Grosberg, P. *Shape and structure in textiles*. In: Journal of the Textile Institute, 1966, vol. 57, pp. T383–T394

[4] Bukhonka, N. *Experimental studies of the dimensional properties of single tuck stitches*. In: Industria Textilă, 2011, vol. 62, no. 1, pp. 14–18

[5] Mahmoudi, M. R., Oxenham, W. *A new electro-mechanical method for measuring yarn thickness*. In: Autex Research Journal, 2002, vol. 2, no. 1, pp. 28–37

[6] Onions, W. J., Oxtoby, E., Townend, P. P. *Factors affecting the thickness and compressibility of worsted-spun yarn.* In: Journal of the Textile Institute, 1968, vol. 59, pp. 293–319

[7] Barella, A. *Law of critical yarn diameter and twist*. In: Textile Research Journal, 1950, vol. 20, pp. 249–258

[8] Fletcher, H. M., Roberts, S. H. *The geometry of plain and rib knit cotton fabrics and its relation to shrinkage in laundering.* In: Textile Research Journal, 1952, vol. 22, pp. 84–88

[9] Fletcher, H. M., Roberts, S. H. *The geometry of knit fabrics made of staple rayon and nylon and its relationship to shrinkage in laundering*. In: Textile Research Journal, 1952, vol. 22, pp. 466–471

[10] Fletcher, H. M., Roberts, S. H. *Distortion in knit fabrics and its relation to shrinkage in laundering.* In: Textile Research Journal, 1953, vol. 23, pp. 37–42

[11] Fletcher, H. M., Roberts, S. H. *Relationship of the geometry of plain knit cotton fabric to its dimensional change and elastic properties.* In: Textile Research Journal, 1954, vol. 24, pp. 729–737

[12] Fletcher, H. M., Roberts, S. H. *Elastic properties of plain and double knit cotton fabrics.* In: Textile Research Journal, 1965, vol. 35, pp. 497–503

[13] Fletcher, H. M., Roberts, S. H. *Dimensional stability and elastic properties of plain knit wool fabrics with and without Wurlan finish.* In: Textile Research Journal, 1965, vol. 35, pp. 993–999

[14] Postle, R., Munden, D. L. *Analysis of the dry-relaxed knitted-loop configuration.* Part 1. *Two-dimensional analysis*. Journal of the Textile Institute, 1967, vol. 58, pp. T329–T351

[15] Lord, P. R., Mohamed, H. M., Ajgaonkar, D. B. *The performance of open-end, twistless and ring yarns in weft knitted fabrics.* In: Textile Research Journal, 1974, vol. 44, pp. 405–414

[16] Sirang, Y., Dinfon, G., Begery, H. M. *A study of hairness and diameter of open-end yarn processed through single- and double-cylinder carding machines and its comparison with ring yarn.* In: Textile Research Journal, 1982, vol. 52, pp. 274–279

[17] Lasic, V., Vrljicak, Z., Srdjak, M. *Effects of the features of the knitting machine and yarns on the structure of knit goods.* In: Tekstil, 1984, vol. 33, pp. 611–621

[18] *Laboratory practice in the study of textile materials.* Edited by A. Kobljakov. Moskva, Izdanie Mir, 1989

[19] Cybulska, M. *Assessing yarn structure with image analysis methods.* In: Textile Research Journal, 1999, vol. 69, pp. 369–373

[20] Demiroz, A., Dias, T. *A study of the graphical representation of plain-knitted structures.* Part 2. *Experimental studies and computer generation of plain-knitted structures.* In: Journal of the Textile Institute, 2000, vol. 91, pp. 481–492

[21] Nagy, V., Vas, L. M., Nagy, P., Lazar, A., Devenyi, L. *Comparative testing of spun yarns manufactured from polyester fibers of different cross sections.* Proceedings of the IN-TECH-ED Conference. Budapest, Hungarian Society of Textile Technology and Science, 2002, pp. 61–66

[22] Basu, A., Doraiswamy, I., Gotipamul, R. L. *Measurement of yarn diameter and twist by image analysisl.* In: Journal of the Textile Institute, 2003, vol. 94, no. 1–2, pp. 37–48

[23] Bueno, M., Renner, M., Nicoletti, N. *Influence of fiber morphology and yarn spinning process on the 3D loop shape of weft knitted fabrics in terms of roughness and thickness.* In: Textile Research Journal, 2004, vol. 74, pp. 297–304

[24] Carvalho, V., Soares, F. O., Belsley, M. *A comparative study between yarn diameter and yarn mass variation measurement systems using capacitive and optical sensors.* In: Indian Journal of Fibre & Textile Research, 2008, vol. 33, June, pp. 119–125

[25] Carvalho, V., Cardoso, P. J., Belsley, M. S., Vasconcelos, R. M., Soares, F. O. *Yarn diameter mesurements using coherent optical signal processing.* In: IEEE Sensors Journal, 2008, vol. 8, no. 11, pp. 1 785–1 793

[26] Rameshkumar, C., Regasamy, R. S., Anbumani, N. *Studies on polyester/waste silk core-spun yarns and fabrics.* In: Journal of Industrial Textiles, 2009, vol. 38, pp. 191–203

[27] Dalidovic, A. S. *Osnovi teorii vjazanija.* In: Legakaja industrija, Moskva, 1970, pp. 144

[28] *Laboratory practice in knitting technology.* Edited by L. Kudriavin. Moskva : Mir Publishers, 1985, pp. 81–82

Author:

Assoc. prof. dr. ALENKA PAVKO-CUDEN
Assoc. prof. dr. URSKA STANKOVIĆ ELESINI
University of Ljubljana
Faculty of Natural Sciences and Engineering
Department of Textiles, Snezniska 5, 1000-Ljubljana, Slovenia
e-mail: alenka.cuden@ntf.uni-lj.si

DOCUMENTARE

Tesătorie

O NOUĂ MAŞINĂ DE ŢESUT

În cadrul Expoziţiei internaţionale pentru industria maselor plastice şi cauciucului *Chinaplas*, care s-a desfăşurat în perioada 20-23 mai 2013, la Guangzhou – China, producătorul liniilor de fabrica-ţie a ambalajelor ţesute din plastic, **Starlinger & Co. GmbH**, din Viena – Austria, a prezentat o nouă maşină circulară de ţesut, cu 8 suveici, RX 8.0.

RX 8.0 a fost proiectată, în principal, pentru produ-cerea benzilor textile din polipropilenă (PP) şi poli-etilenă de înaltă densitate (HDPE), destinate aplica-ţiilor în condiţii grele de lucru, cum ar fi: containere flexibile vrac intermediare, foi de cort, geotextile şi agrotextile.

Bazată pe conceptul de realizare a maşinii de ţesut modelele *Starlinger SL* şi *Alpha*, noua maşină de ţesut este rentabilă şi uşor de întreţinut.

Utilizarea noilor materiale reduce tensiunea şi frecarea pe suprafaţa benzilor şi măreşte timpul de viaţă a pieselor supuse uzurii, menţinând la niveluri scăzute atât cheltuielile cu piese de schimb, cât şi cele legate de întreţinere.

Melliand International, mai 2013, p. 74

Image measuring method for fiber length measurements

HONGYAN WU   FUMEI WANG

REZUMAT – ABSTRACT

Metodă de măsurare a lungimii fibrelor pe bază de imagini

În lucrare este prezentată o nouă metodă pentru determinarea lungimii fibrelor, utilizând imaginile a două fibrograme complete, realizate în acelaşi timp. Pe baza noii metodologii, au fost efectuate experimente pentru stabilirea perfor-manţei metodei de măsurare pe bază de imagini. Rezultatele măsurătorilor demonstrează că această metodă prezintă o bună fiabilitate, repetabilitate şi compatibilitate cu AFIS şi HVI.

Cuvinte-cheie: AFIS, fibrogramă, lungimea fibrei, HVI, imagine alb-negru

Image measuring method for fiber length measurements

This paper presents a new method for measuring fiber length using image method which can obtain two whole fibrograms by one time. The methodology was introduced and experiments were performed to investigate availability of Image measuring method. The results show image measuring method has good trueness and repeatability and good agreement with AFIS and HVI.

Key-words: AFIS, fibrogram, fiber length, HVI, gray image

Length is one of the most important parameters of fibers because it has effects on yarn strength, yarn hairiness, the properties of fabrics and on the efficiency of the yarn spinning process [1], [2], [3]. There are several testing methods for fiber length measurements. The conventional method [4] is the array method which gives a weight frequency-length distribution and always serves as a benchmark to which other methods are compared [5]. This method is, however, slow and tedious and depends on operator skill for reliability and accuracy [6], [7].

Now, the two popular instruments, namely high volume instrument (HVI) and advanced fiber information system (AFIS), are fully automatic machines. HVI is the official USDA method [8]. However, it cannot obtain the entire fibrogram, because its holding length is about 4.06 mm and the start of the scan set point at 3.8 to 5.1 mm from the held point [9]. AFIS is mainly used by modern textile mills for evaluating the individual fiber properties in order to optimize their downstream processing [8]. However, there may be some questions in AFIS measurements, for example fiber break, straightening, separation, alignment and only 9–33 % of fibers are counted in the measurement unit [10].

Recently, various image analyses have been used for fiber length measurement. Fischer [11] and Y. Ikiz [9] showed image processing method to measure single fiber length, respectively. This method could test single fiber length accurately, but individualizing fibers is questionable. Weilin Xu [12] introduced a new method for cotton length measurement that involved combing fibers into a test beard, cutting the beard into a number of segments of a given interval, and counting the snippets in each segment by image processing. The method seems time-consuming and tedious.

This paper presents a new fiber length measurement method, namely Image measuring method. This new method can scan the two sides of the dual-beard from the holding line synchronously to generate two entire fibrograms. In this paper, the methodology was demonstrated and experiments were performed to examine Image measuring method.

METHODOLOGY USED

Image measuring method consisted of four parts: sampling, obtaining gray image, extracting fibro-grams and calculating fiber length, as showed in figure 1. Firstly, the dual-beard was produced through sampling. Secondly, the dual-beard was put on a scanner to produce a digital gray image. Thirdly, the fibrograms were extracted based on the image of the beard. Finally, mean length by weight, coefficient
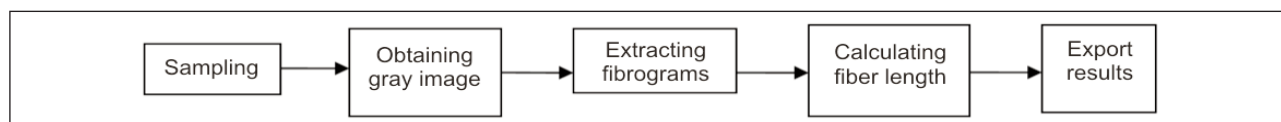
Fig. 1. The measurement flowchart of image measuring method

of variation, modal length and quality length was calculated.

Sampling

First, 0.2 to 0.3 g sample was selected randomly from tested fibers, then opened and mixed by hands, and removed trash particles with a pair of tweezers. Second, the sample was drawn three times by a fiber draw-off device to prepare a sliver in which fibers are parallel, straight and uniform nearly. Third, the sliver was clamped randomly along the fiber longitudinal axis by a clamper, and then loose fibers on the open end of the clamper were removed. Lastly, clamp the sliver with another clamper at the holding line of the first clamper, release the first clamper and remove all loose fibers on the open end of the second one. The dual-beard with 20 mg to 40 mg and 5 cm was obtained, as shown in figure 2.

The two sides of the dual-beard are approximately symmetrical and fibers in the beards are well straightened and parallel, which allow two entire fibrograms (fig. 4) scans apart from the holding line simultaneously.

Obtaining gray image

The dual-beard sample was scanned by a scanner to a digital gray image. A grayscale digital image is an image in which the value of each pixel is a single intensity value, that is, it contains only the luminance information without color information. Often, the grayscale intensity is stored as an 8-bit integer giving 256 (from 0 to 255) possible different shades of gray from black at the weakest intensity to white at the strongest.
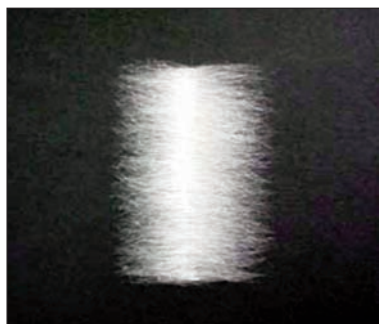
Fig. 2. Dual-beard sample
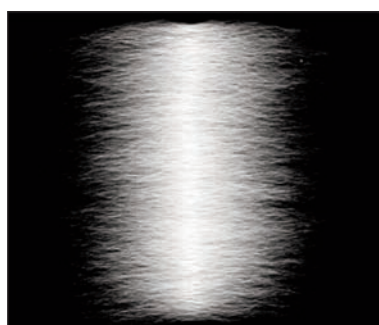
Fig. 3. Digital gray image of the dual-beard

The dual-beard was put on the glass tray of the scanner. The properties of the scanner were set as follows: scan type was gray scale; resolution was 1 000 dpi (0.0254 mm per pixel). A beard image, with high 2 257 pixels and width 2 339 pixels, was shown in figure 3.

Extracting the fibrograms

As shown in figure 3, the higher gray value is, the more quantity of fibers is. Hence, the decline of gray values along the horizontal direction indicated the gradually descent of fibers quantity. The progressive accumulate gray values of every column vertical with fiber long direction was calculated by computer software. The origin of the coordinates is set at the location of the holding line where the progressive accumulate gray value is set 1. So, at the ith column, the relative quantity of fiber equaled the value that the gray values at this column divided by the gray values at the holding line, and the protruding distance to zero point equaled $i \times 0.0254$ mm. The fibrogram is the beard curve that shows the quantity of fibers at each protruding distance from the holding line, as shown in figure 4. The abscissa and ordinate values are protruding distance and relative quantity of fiber, respectively.

Calculating fiber length

To calculate fiber length, the equations [13] have been extracted directly from the fibrogram by author. According to the equations, the computer software was developed for calculating fiber length: mean length by weight, modal length, quality length and the coefficient of variation.

EXPERIMENTAL VERIFICATION

Trueness of image measuring method

Samples used

Six groups of kapok fibers marked as 1# ~ 6#, two groups of cotton samples marked as 7# and 8# and one group of polyester fibers with same cut lengths marked as 9# were tested, which contained a broad range of length-distribution properties.
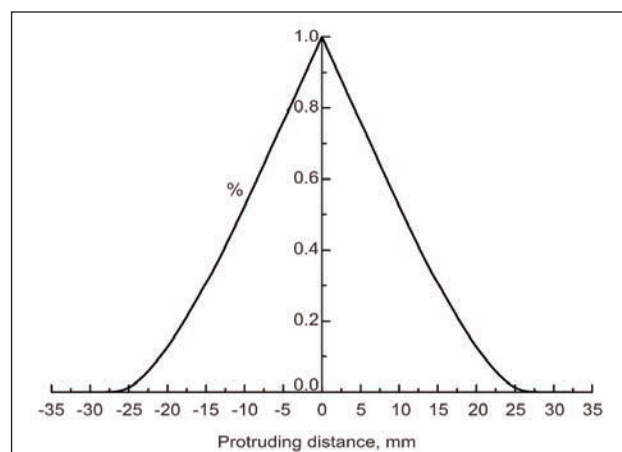
Fig. 4. The fibrograms
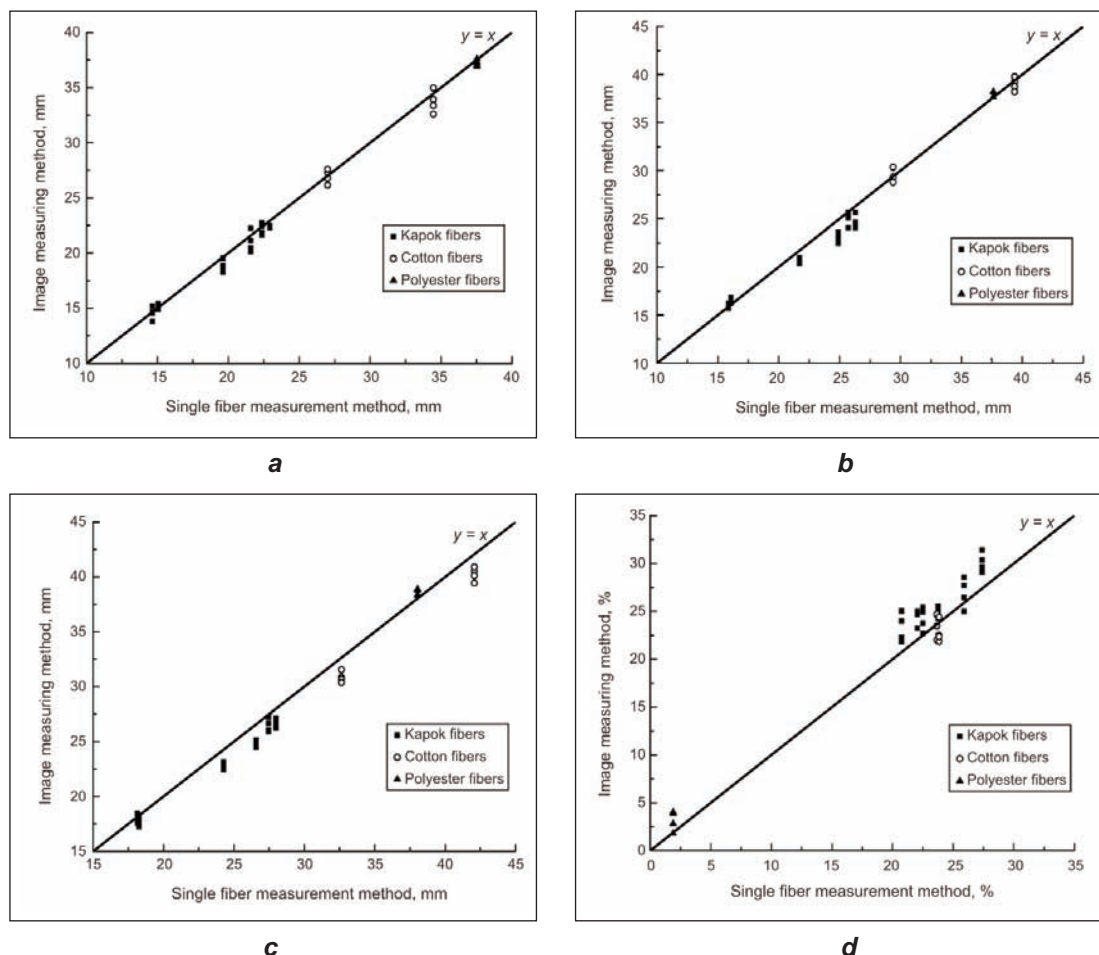
Fig. 5. The results of the two test methods:
a – mean length by weight; *b* – modal length; *c* – quality length; *d* – coefficient of variation

Methods used

For every sample, four measurements were performed by image measuring method. The results of one measurement were the average of length indexes at the both ends of the dual-beard.

Single fiber measurement method is the most accurate method for fiber length test, so it was selected to examine trueness of Image measuring method. The procedure of single fiber measurement method was as follows: pick up single fiber with tweezers, drag it on velvet board to straight it and measure it with a scale reading one decimal. And then the fiber length distribution by number was obtained, which was converted to the fiber length distribution by weight based on the assumption that the fibers were uniform in cross section. Thus fiber length characteristics by weight can be calculated. For every sample, 900 ~ 1 000 individual fibers were tested by single fiber measurement method, except for polyester fibers where 100 individual fibers were measured.

Results and discussions

The results of the two methods are showed in figure 5. In figure 5 the line *y* = *x* is the perfect correlation line of the two methods; an abscissa point corresponds to four ordinate points which are four measurement results of one sample by Image measuring method.

Figure 5 shows, for mean length by weight, modal length, quality length and coefficient of variation, Image measuring method agrees well with single fiber measurement method. However, due to random error, data of Image measuring method fluctuate slightly with the ideal line. In order to examine the trueness of Image measuring method, the mean value of four measurements of every sample by Image measuring method were calculated. Then the biases of Image measuring method were calculated in table 1, which were equal to the results of Image measuring method minus the results of single fiber measurement method.

From table 1, it is observed that biases of Image measuring method are small. The average biases of mean length, modal length and quality length are all less than 1 mm. In order to test significance of bias, T-test was applied. Under significance level α = 0.01, it can be obtained equation (1):

$$t_{1-\alpha/2}(n-1) = t_{1-0.005}(8) = 3.3554 \qquad (1)$$

In table 1, T-test statistics all are less than 3.3554, so biases of image measuring method are not significant. It shows that the trueness of Image measuring method is high.

Besides, from table 1, it is observed that the average biases of mean length, modal length and quality length

Table 1

BIASES OF IMAGE MEASURING METHOD				
Sample	Mean length, mm	Modal length, mm	Quality length, mm	Coefficient of variation, %
1#	–0.09	0.21	–0.32	2.74
2#	0.07	0.39	–0.08	0.56
3#	–0.90	–1.04	–1.43	1.03
4#	–0.60	–1.99	–1.81	1.68
5#	–0.21	–0.72	–0.99	2.40
6#	–0.54	–1.31	–1.22	2.53
7#	–0.05	0.04	–1.80	0.04
8#	–0.75	–0.40	–1.95	–1.08
9#	–0.31	0.32	0.65	1.98
Average bias	–0.38	–0.50	–0.99	1.32
Standard deviation	0.337	0.827	0.898	1.287
T-test statistics	3.3398	1.8125	3.3182	3.0760

Table 2

VARIANCE OF THREE METHODS					
Method		Mean length, mm^2	Modal length, mm^2	Quality length, mm^2	Coefficient of variation, %
Image measuring method	S_1^2	0.093	0.291	0.166	1.413
AFIS	S_2^2	0.020	1.742	-	0.828
HVI	S_3^2	0.116	-	-	-

are negative, that shows the results of Image measuring method are slightly shorter than single fiber measurement method. This was due to that the straight degree of the fibers in single fiber measurement method was slightly higher than which in Image measuring method, because of fibers dragged on velvet board by tweezers in single fiber measurement method.

Repeatability of Image measuring method

Sample used

The 7# cotton fiber was tested.

Methods used

The sample was tested five times by Image measuring method, HVI and AFIS, respectively.

Results and discussions

Variance of five measurements by the three methods were caculated in table 2. F-test was applied to test variance of the three methods. Under significance level α = 0.05, for mean length, it can be obtained equations (2):

$$S_1^2 / S_2^2 = 4.73$$

$$S_3^2 / S_1^2 = 1.25 \qquad (2)$$

$$S_3^2 / S_2^2 = 5.80$$

which are all less than:

$$F_{(1-0.025)}(4.4) = 9.60 \qquad (3)$$

So, for mean length, repeatability of the three methods was in the same level. Similarly, for modal length and coefficient of variation, repeatability of Image measuring method and AFIS was in the same level. Because AFIS and HVI do not provide quality length,

variance of quality length of the three methods cannot be compared, whereas it is obvious variance of quality length by Image measuring method is small. So repeatability of Image measuring method is good.

Compared to other measurement methods

Besides 7# and 8# cotton samples, three groups of cotton fiber, marked as 10#, 11# and 12#, were tested by image measuring method, HVI and AFIS, respectively. The results of the three methods are showed in figure 6.

Figure 6a shows mean length of Image measuring method are very close to AFIS's which are slightly higher than HVI's. The square of correlation coefficient was R^2 = 0.9901 between image measuring mehtod and AFIS, and was R^2 = 0.9901 between Image measuring method and HVI. So, the mean length obtained from Image measuring method has good agreement with AFIS's and HVI's. The small difference of the three methods may be due to random error and different measuring principles.

In figure 6b, quality length, upper quartile length (UQL) and upper half mean length (UHML) are compared. Quality length is defined as the weight-weighted average length of fibers whose length exceeds the modal length; upper quartile length (UQL) is the value of length for which 75% of all the observed values are lower, and 25% higher; upper half mean length (UHML) is the average length of the longest one-half of the fibers when they are divided on a weight basis. Though, the three length indices have different meaning, they present weight average length of fibers with longer length. From figure 6b, it is obvious that the quality length of Image measuring method is same with UQL from AFIS which is slightly greater than UHML from HVI and the three methods has high consistency.

Figure 3c shows modal length of Image measuring method are so close to AFIS's. Figure 3d shows coefficient of variation of Image measuring method is agreed well with AFIS's and R^2 of the two methods is 0.8316. HVI do not provide modal length and coefficient of variation.
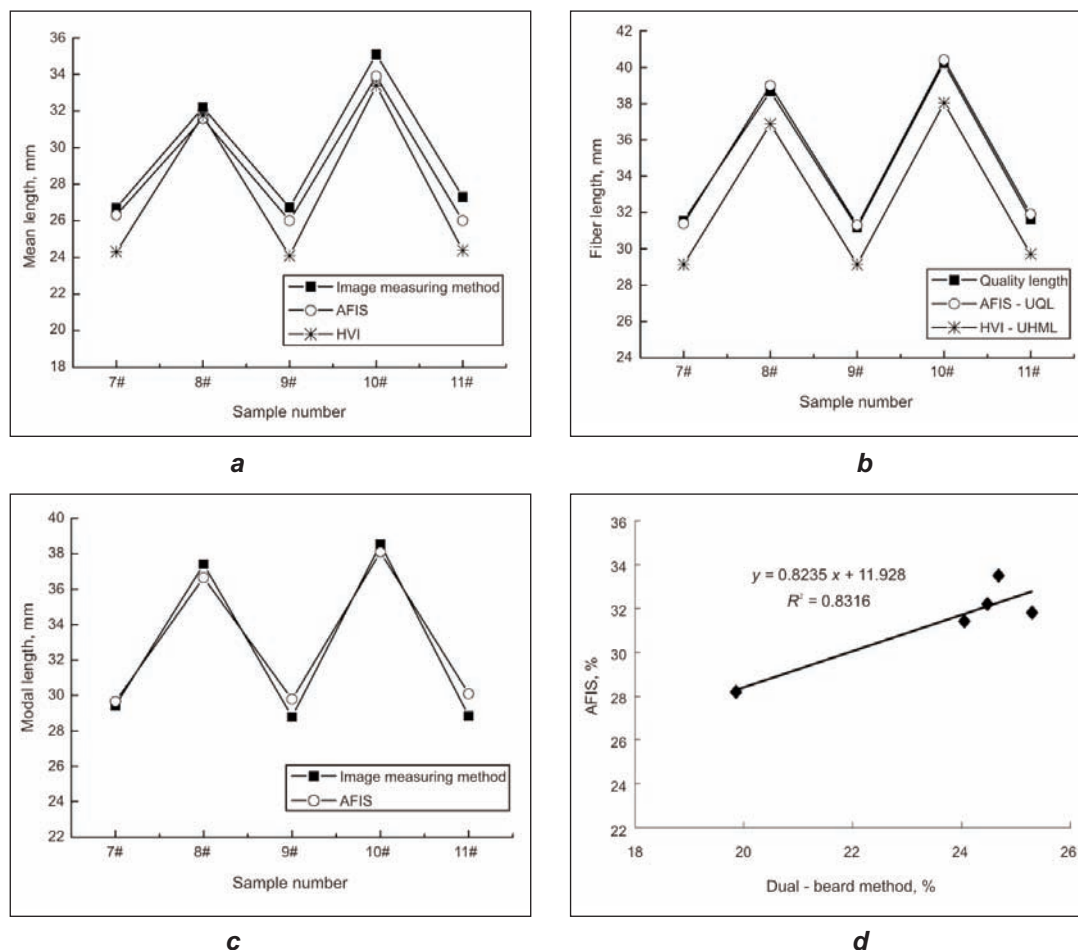
Fig. 6. Data comparisons with image measuring method, AFIS and HVI

CONCLUSIONS

We present a new method for fiber length measurement, namely Image measuring method which involved sampling, obtaining image, extracting fibrogram and calculating fiber length. This new method has two outstanding advantages: it can scan the beard from the holding line to produce the entire fibrogram and can produce two test results by one time using a dual-beard sample. A lot of experiments were performed to examine the new method. Compared to single fiber measurement method, the biases of Image measuring method were small and not significant, so it had high trueness. Then, repeata-bility of image measuring method was in the same level with AFIS and HVI. At last, Image measuring method was compared to AFIS and HVI. The results showed Image measuring method agrees well with AFIS and HVI. Therefore, it can be concluded that Image measuring method has good accuracy, repeata-bility and can be applied to measure fiber length distributions.

BIBLIOGRAPHY

[1] Mogahzy, Y. E., Broughton, R. *A statistical approach for determining the technological value of cotton using HVI fiber properties.* In: Textile Research Journal, 1990, vol. 60, pp. 495–500

[2] Krowicki, R. S., Hinojosa, O., Thibodeaux, D. P. et al. *An AFIS parameter for correcting mass measures on the Spinlab HVI.* In: Textile Research Journal, 1996, vol. 66, pp. 70–72

[3] Zeidaman, M., Sawhney, P. S. *Influence of fiber length distribution on strength efficiency of fibers in yarn.* In: Textile Research Journal, 2002, vol. 72, pp. 216–220

[4] ASTM, Standard D 1447-07. *Standard test method for length and length distribution of cotton fibers (Array method).* Annual Book of ASTM Standards, 2006, vol. 07.01, pp. 334–339

[5] Stewart, James Mc D., Oosterhuis, Derrick M., Heitholt, James J. et al. *Physiology of cotton.* London: Springer, 2010, p. 233

[6] Zeidman, M. I., Batra, S. K. *Determining short fiber content in cotton.* Part I: Some Theoretical Fundamentals. In: Textile Research Journal, 1991, vol. 61, pp. 21–30

[7] Balasubramanian, N. *Influence of cotton quality.* In: The Indian Textile Journal, 1995, pp. 48–51

[8] Nair, A. U., Nachane, R. P., Patwardhan, B. A. *Comparative study of different test methods used for the measurement of physical properties of cotton.* In: Indian Journal of Fiber & Textile Research, 2009, vol. 34, pp. 352–358

[9] Ikiz, Y., Rust, J., Jasper, W. *Fiber length measurement by image processing.* In: Textile Research Journal, 2001, vol. 71, pp. 905–910

[10] Cui, X., Calamari, T. A., Robert, K. et al. *An Investigation of cotton fiber lengths measured by HVI and AFIS.* In: Tenth EFS Research Forum Proceedings, 1997, pp. 115–124

[11] Fischer, H., Rettig, D., Harig. H. *Image processing for measuring the length distribution of reclaimed fibres.* In: Melliand Textilberichte/International Textile Reports, 1999, vol. 80, pp. 94–96

[12] Weilin Xu, Bugao Xu, Wenbin Li, Weigang Cui. *Snippet counting for cotton length distribution measurement using image analysis.* In: Textile Research Journal, 2008, vol. 78, pp. 336–341

[13] Fumei Wang, Hongyan Wu. *A rapid and low-cost method for fiber-length measurement.* China Patent: 201210106711.8

Authors:

HONGYAN WU
FUMEI WANG
College of Textiles
Donghua University
Shanghai 201620, China
e-mail: hongye419@gmail.com; e-mail: wfumei@dhu.edu.cn

DOCUMENTARE

Noi tehnologii

EMULSIE POLIURETANICĂ PENTRU FINISAREA MATERIALELOR TEXTILE

Finisarea textilelor destinate articolelor de îmbrăcăminte sport și echipamentelor de lucru este o condiție-cheie pentru conferirea unor proprietăți funcționale, cum ar fi rezistența la condiții meteo nefavorabile. Cu toate acestea, utilizarea unor agenți de impregnare obișnuiți, cum sunt cei pe bază de compuși perfluorurați este controversată.

Eliberarea acestor substanțe în mediul înconjurător este considerată foarte dăunătoare, deoarece ele se acumulează și devin un pericol pentru mediu și pentru sănătatea oamenilor. În plus, îmbrăcămintea tratată cu unii agenți de impregnare se recomandă să fie spălată doar în anumite condiții, deoarece rezistența la abraziune este destul de mică, ceea ce are un impact negativ asupra funcționalității articolelor de îmbrăcăminte.

Noul produs de finisare a textilelor, *Purtex*, oferă o alternativă unică în acest domeniu. Produsele Purtex, de finisare a textilelor, sunt rezultatul unui proiect de dezvoltare interdisciplinar al companiei *Freudenberg Group*, din Weinheim, Germania. Experiența dobândită în domeniul industriei textile a fost îmbinată cu cercetările în domeniul prelucrării polimerilor și tehnologiei de suprafață, pentru a dezvolta o soluție complet nouă de finisare funcțională a textilelor.

Emulsia poliuretanică Purtex nu conține solvenți și îmbină compatibilitatea față de mediu cu o foarte bună capacitate de spălare și cu proprietățile de impermeabilizare durabilă și de rezistență la abraziune, dar și cu confortul ridicat și tușeul plăcut.

Textilele finisate cu Purtex își păstrează proprietățile funcționale pe întreaga lor durată de viață. Purtex nu conține substanțe considerate a avea efecte dăunătoare asupra sănătății umane sau mediului și, de asmenea, nu conține fluorocarburi, compuși organici ai staniului, ftalați, izocianați, metale grele, etoxilați de alchilfenol și formaldehidă.

Produsul poate fi aplicat pe materialele țesute sau tricotate, în timpul procesului de finisare, prin procedeele industriale obișnuite și își păstrează proprietățile funcționale pe toată durata de viață a articolelor textile realizate.

Sursa: www.freudenberg.de

Yarn quality measurement by digital blackboard system

JIHONG LIU
BO ZHU

HONGXIA JIANG
RURU PAN
WEIDONG GAO

REZUMAT – ABSTRACT

Aprecierea calității firelor folosind un sistem digital cu plăci negre

Placa neagră este un instrument tradițional folosit pentru determinarea neuniformității firelor textile. Deoarece posibilitățile de evaluare a calității firelor erau limitate, s-au făcut eforturi mari pentru înlocuirea plăcilor negre tradiționale și dezvoltarea unui sistem digital cu plăci negre, care să poată fi cuplat la aparatul cu sistem capacitiv de determinare a neuniformității firelor textile. Aspectul firului este reconstruit pe baza rezultatelor măsurătorilor diametrelor firelor, folosind un model matematic de dreptunghiuri și un model de iluminare a firului, precum și un software îmbunătățit. Platforma poate fi utilizată pentru o operare ulterioară, în funcție de necesitățile practice, de exemplu: redimensionarea lățimii și înălțimii, alegerea unei fețe unice sau a ambelor fețe, modificarea culorii plăcii, ajustarea dimensiunii etc. Rezultatele experimentale arată că sistemul are o configurație flexibilă și este ușor de manipulat.

Cuvinte-cheie: placă neagră, calitatea firului, aparat capacitiv, testarea uniformității

Yarn quality measurement by digital blackboard system

Yarn blackboard is a traditional tool of approaching to unevenness characterization of yarn. Since the initial use of the capacitive apparatus in industry, much effort has been put into completely replacing of traditional yarn blackboard. Unfortunately, such development efforts have not succeeded since traditional yarn blackboard can express the alignment effect of yarn, and further significant improvement cannot be expected. This has prompted many groups to develop digital yarn blackboard for replacing of traditional yarn blackboard. In the research a digital blackboard system is developed for measuring yarn quality combining with the measurement result through capacitive apparatus in the research. The appearance of yarn is reconstructed based on the diameter data of yarn using a mathematical model of rectangles and illumination model of yarn. Furthermore, the software is improved. The platform can be used for further operation according to the practical demand: the width and the height can be resized; single or double-face is optional; the color of blackboard can be edited; the magnification or minification can be adjusted freely and so on. The experimental results showed that the system is flexible for configuration and convenient for operating.

Key-words: blackboard, yarn quality, capacitive tester, unevenness characterization

In the textile industry quality control of yarn is an important part of production. Quality improvement can increase competitiveness as well as reducing costs. Consequently, there are many methods for monitoring of quality characteristics [1–6]. Blackboard is a traditional tool of approaching the unevenness characterization of yarn. In the tool, operators must wind the yarn on the blackboard at first. After that the operators analyze quality of yarn by inspecting several blackboards. It is labor-intensive and time-consuming, which makes quality analysis become the bottleneck in the textile production.

With the development of computer technology, lots of methods based on computer graphics have been proposed since last century to analyze quality of yarn. Su et al. [7] studied evaluation method of the unevenness of the stretch-broken tow in the break draft zone of a two drafting three pairs of rollers with double apron draft system using oxidized filament tow. Some new apparatuses were developed to analyze the quality of yarns in different semi-finished products [8]. For getting different properties of yarns, researchers did many works in data mining through acquiring data by Uster apparatus. Liu et al. [9] presented an automatic method for characterizing the parameters of ring slub yarn by analyzing the 2D image using cluster analyses with an amended similarity-based clustering method. Militký et al. [10] proposed that the complex analysis of mass variation curve from Uster apparatus enables a deeper investigation of many phenomena connected with yarn unevenness and related problems. For providing precise higher measurement, automatic systems for determination of mass characteristics of textile yarn were developed based on 1 mm parallel capacitive sensors, working online or offline. This new approach allows direct measurement of yarn mass in the 1 mm range (increasing the resolution by eight times) [11]. Hakan et al. [12] simulated the appearance of woven fabric defects due to yarn faults by a method developed which was based on photographs taken from yarns along with their lengths. For getting different properties of yarns, researchers did many works in data mining through acquiring data by Uster apparatus. The yarn inspection system in Uster Tester 5-C80018 provides the functions of simulation of yarn boards,

woven and knitted fabric. This is a kind of algorithm from yarn to boards or fabric by the measurement data [13], [14].

Here defined the simulation of yarn boards as digital yarn blackboard. Digital yarn blackboard includes mainly two key technologies:

- **Simulation of yarn appearance.** Sriprateep et al. [15] demonstrated the CAD model of fiber and yarn with Nurbs solid. The geometry of yarn structures is modeled through the proposed approach by using the SolidWork CAD software package. The graphical results of fiber migration observed from the experimental results with different twist factors. A number of researches have been carried out to simulate woven fabric appearance from yarn images generated from given yarn structural parameters including count or diameter, together with fabric structural parameters including weave and thread sets [16–24]. Most of these yarn models are of uniform and complex cross sections. The speed of display from the model is slow. The CAD model has also been developed for apparel. Tom et al. [25] investigated the requirements for a CAD interface to facilitate the successful education of fashion and textile students in the area of yarn design and production. Kang et al. [26] have developed a CAD system for the 3D circular braided preform was following the modeling sequences and applied to the parametric study of the preforms. Using the developed CAD system, the relationships between processing variables and geometric parameters have been established. Chen et al. [27] presented the work and progress made in the mathematical modeling of woven structures and in establishing CAD/CAM tools for 3D woven architectures based on the use of the conventional weaving technology. Liao et al. [28] attempted the geometric modeling of woven and braided fabric structures in three dimensions using a computer aided geometric design (CAGD) technique. Some traditional 2D fabric models are extended into 3D models and demonstrated in 3D form. Özdemir et al. [29] have presented a method to simulate fabric surface appearance from achieved yarn properties. The simulation of woven fabric surface appearance depends on yarn and fabric cross sectional geometry as well as on yarn measurements and yarn image recordings.

- **Construction of digital blackboard.** Image processing has also been used in textile analyses recently [30]. Zhou et al. [31] introduced a digital processing of yarn blackboard on the basis of computer image processing and proved the yarn diameter measured by image processing method. Although a number of approaches for yarn quality determination exist, the methods using digital blackboard and analysis algorithms are still under development. Several capacitive sensors-based approaches dedicated to yarn quality assessment have already been proposed. However, these methods use data from capacitive sensors approaches,
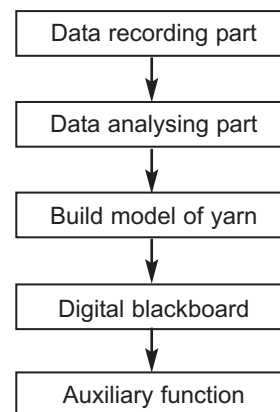
Fig. 1. Flowchart of digital blackboard system

which often lack model of yarn and characteristic as they simulate no more than yarn outline of manual blackboard. This study presents mathematical modeling of yarn and establishes a graphic system of digital blackboard based on the data for capacitive sensor.

EXPERIMENTAL SYSTEM OF DIGITAL BLACKBOARD

A flowchart of digital blackboard system is shown in figure 1. As data recording part, the data of yarn fineness each 4 mm are dynamically recorded using capacitive evenness tester. In the data analyzing part, the data of yarn fineness are converted into the data of yarn diameter according to linear relationship between the data of yarn diameter and AD conversion result of signal of capacitor plates. After that, a model of yarn is built. At last, yarn is wound virtually around a digital blackboard to simulate the appearance of physical blackboard including nep, thick, thin and details, etc. As auxiliary function, the system provides adjusting parameters of digital yarn blackboard, and so on.

Drawing process of digital yarn blackboard is as follows: First draw a color back area according to the size of the blackboard. In general, the color of back area is black. Then according to the data of yarn diameter arrange yarns on the digital yarn blackboard in columns with a certain interval to simulate the action of reeling yarn on a physical yarn blackboard. The means set length's data is skipped after arranging one column of yarn for one side of double face. An experimental system is set up for verifying the function of digital yarn blackboard. The software of Delphi (version: 7.0) was used as the tool to develop the experimental system, and the system of the computer used in the experiment was P8600 3.00 GHz and 2G DDRIII memory. Figure 2 shows an example of digital yarn blackboard with interface of software.

RESULTS AND DISCUSSIONS

Translating data from capacitive measurements

The result characterizes a given yarn's linear mass and the average diameter is deduced from the result,
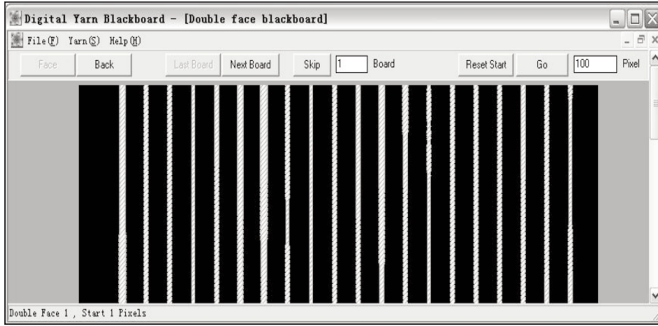
Fig. 2. Example of digital yarn blackboard
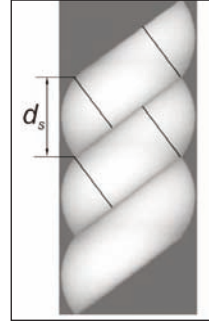
Fig. 3. Yarn model
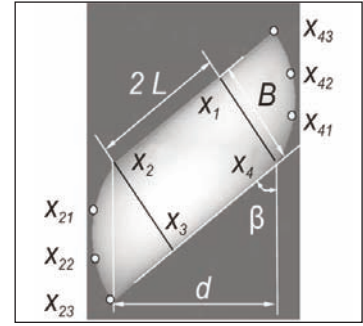
Fig. 4. Rectangle in yarn model

following the industry standard of expressing linear mass N_t, g/km. There is proportional relationship between the result of capacitive measurements U and the linear mass N_t is given in equation (1).

$$N_t = k_1 U \qquad (1)$$

If assumed that the yarn has a cylindrical shape, the yarn diameter is proportional to the square root of its linear mass. The expected relation between diameter d and linear mass density N_t is given in equation (2).

$$d = k_2 \sqrt{N_t} \qquad (2)$$

Therefore, the relation between d and U is:

$$d = k_2 \sqrt{k_1 U} = k \sqrt{U} \qquad (3)$$

where:
k_1, k_2, k are coefficient changing according to the test environment and kind of yarn;
k is equal to the ratio of d and the average square root of U.

Improved yarn model

A set of rectangles with round border is put in parallel column to simulate twist on the surface of cylinder of single yarn as shown figure 3. According the parameter of yarn and figure 4, we can get the equations for single rectangle as following equations (4), (5) and (6).

$$d_s = \frac{100}{T_t} \qquad (4)$$

$$B = d_s \sin \beta \qquad (5)$$

$$d_s = \frac{d - B \cos \beta}{\sin \beta} \qquad (6)$$

where:
d_s is the distance of two twists;
T_t – twist of yarn (t/10 cm);
β – twist angle. Twist angle is calculated by equation (7).

$$\beta = \arctan \left(\frac{T_t}{892} \sqrt{\frac{N_t}{\delta}} \right) \qquad (7)$$

where:
δ is volume weight of yarn.

The volume weight of yarn varies with the type, property and twist of yarn. To simplify the calculation, volume weight of yarn is assumed to be 0.85 g/cm^3 for cotton yarn, 0.78 g/cm^3 for worsted yarn, 0.92 g/cm^3 for silk yarn, 0.75 g/cm^3 for hemp yarn, respectively in the program. The four vertex coordinates of rectangle are calculated by equations (8).

$$\begin{cases} x_2 = x_1 - 2L \sin \beta \\ y_2 = y_1 - 2L \cos \beta \\ x_3 = x_2 + B \cos \beta \\ y_3 = y_2 - B \sin \beta \\ x_4 = x_1 + B \cos \beta \\ y_4 = y_1 - B \sin \beta \end{cases} \qquad (8)$$

To increase simulation effect, two corners of rectangle are drawn to produce visual coarse feel of yarn edge. An arc is drawn from vertex x_4 to x_1 along with key point x_{41}, x_{42} and x_{43}. The coordinates of the key points is given by equations (9).

$$\begin{cases} x_{21} = x_2 - B \cos \beta / 3 \\ y_{21} = y_2 - d_s / 3 \\ x_{22} = x_2 - B \cos \beta / 3 \\ y_{22} = y_2 - 2 d_s / 3 \\ x_{23} = x_2 \\ y_{23} = y_2 - d_s \end{cases} \qquad (9)$$

Another arc is drawn from vertex x_2 to x_3 along with key point x_{21}, x_{22} and x_{23}. The coordinates of the key points is given by equations (10).

$$\begin{cases} x_{41} = x_4 + B \cos \beta / 3 \\ y_{41} = y_4 + d_s / 3 \\ x_{42} = x_4 + B \cos \beta / 3 \\ y_{42} = y_4 + 2 d_s / 3 \\ x_{43} = x_4 \\ y_{43} = y_4 + d_s \end{cases} \qquad (10)$$

In face twist is difference according to difference diameter. The slope angle also changes; however, there is lesser change since the yarn is very thin. Therefore, the change of slope angle is omitted in the system.

DIAMETER OF NORMAL YARN							
Ne, s	80	60	50	40	30	21	10
N_t, tex	7.3	9.7	11.7	14.5	19.5	27.8	58.3
D, mm	0.11	0.12	0.13	0.15	0.17	0.20	0.30

Table 1

MAGNIFICATION OF NORMAL YARN							
Ne, s	80	60	50	40	30	21	10
X	14	12	11	10	9	7	5

Table 2

Fig. 5. Illumination of one point on the surface of yarn

Fig. 6. Effect of simulation for twisted yarn

Pixel number for parameters

The screen of display is comprised of many points called as pixel. According to resolution and size of screen, one pixel has different size. Therefore, the system calculates the height and width of pixel, respectively. In general, the size of pixel is about 0.3 – 0.4 mm, whilst, the diameter of normal yarn is 0.1 – 0.3 mm as listed in table 1 (e.g. *d* = 0.85). When we want to simulate the information of yarn, we must set 4 dots for one yarn at least, which express the curve of reflecting rays. It is very important to select appropriate magnification according to the count of yarn. We advise the minimum magnification for different yarns (table 2) on condition of resolution of screen: 1 024 × 768, ratio of width and height: 4:3 and size of screen: 19 inch (width × height: 15.2 × 11.4). Therefore, in simulation the parameters of yarn must be magnified *X* times, after that the number of pixel can be calculated.

Illumination model of yarn

Under visible light irradiation, the reflection, refractive, transmission, absorption diffraction, interference and so on will be produced by the surface of yarn. To simulate yarns on digital yarn blackboard, the reproduction of realistic intensity profile or illumination model of yarn is the primary task. In fact, a digital yarn blackboard is the intensity profile of a yarn, be it grey or color shades, depends also on position of viewpoint, power and the number of light sources present in the environment. For simple model, there is ambient light and reflection [32].

Diffused reflection model. According to Lambert Cosine Law a yarn can be assumed as a cylinder with constant section to simplify the model as shown in figure 5. To simplify illumination model, diffused reflection is considered only. According to Lambert Cosine Law, diffused reflection is due to the presence of one or more external light sources and represents the direct light being shattered on the yarn surface from the light source(s). The center point *a* is the brightest place when a ray of light perpendicularly irradiate on the surface of yarn. The brightness gradually becomes darker from the center point to both sides points *c*.
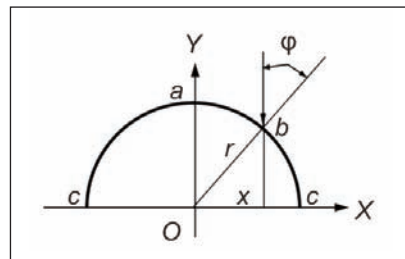
Assuming a single point light source is emanating light energy uniformly in all directions; the diffused reflection is dependent on the incident angle φ between surface normal at the yarn point *b* and the direction of light source. The corresponding illumination for monochromatic light due to this external point light source is given by equations (11) and (12).

$$\cos \varphi = \sqrt{1 - \left(\frac{x}{r}\right)^2} \qquad (11)$$

$$I_d = k_d\, I_p \cos \varphi, \quad 0 \le \varphi \le \frac{\pi}{2} \qquad (12)$$

where:
I_p is the intensity of the point light source.
The degree of the light source diffusion is given by the weight factor k_d = [0, 1] that controls the extent of incident light diffused, depending on the surface property. It is lower for duller surface such as yarn. Diffused reflection I_d has only relation with the cosine value of the light source intensity.
Effect of Yarn Light shining process could be performed to the whole yarn for brightness of the yarn after twisted. The simulation effect of twisted yarn is shown in figure 6.

Development of auxiliary functions

This research demonstrates the feasibility of simulating yarn blackboard. Comparing with physical yarn blackboard, the system has particular properties displaying the data of yarn in different model. The system includes two auxiliary functions: selecting single or double face of the blackboard, adjusting freely the start point.
Selecting view *A* continuous yarn is arranged on the digital yarn blackboard alternating face and back view according to reeling process of yarn blackboard. At most half of the yarn comes into view omitting the thickness of yarn blackboard: face view or back view. Neither view shows all part of yarn since both views skip half of the yarn. The system provides simultaneously face views as shown in figure 7 *a* and back views as shown in figure 7 *b*. We can find the yarn continues from the face view to back view and vice
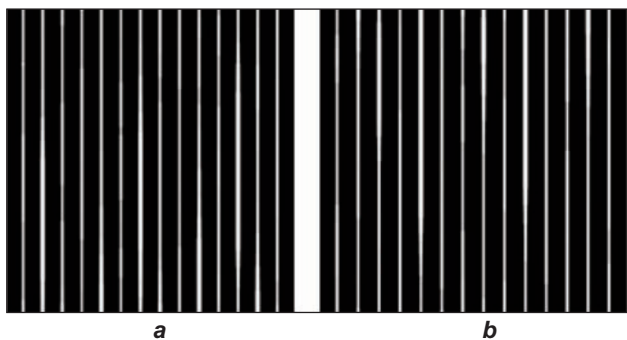
Fig. 7. Face and back views:
a – face view; *b* – back view
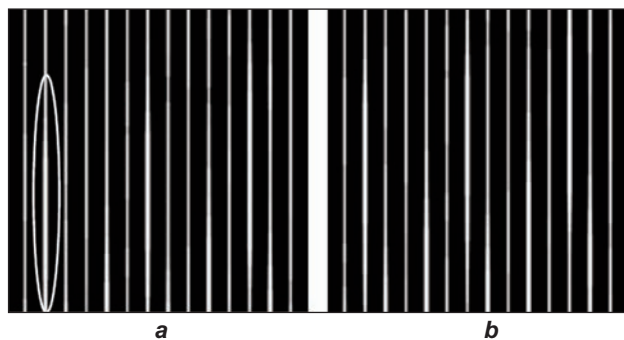
Fig. 8. Result of adjusting the start point:
a – start point 1st pixel; *b* – start point 200th pixel
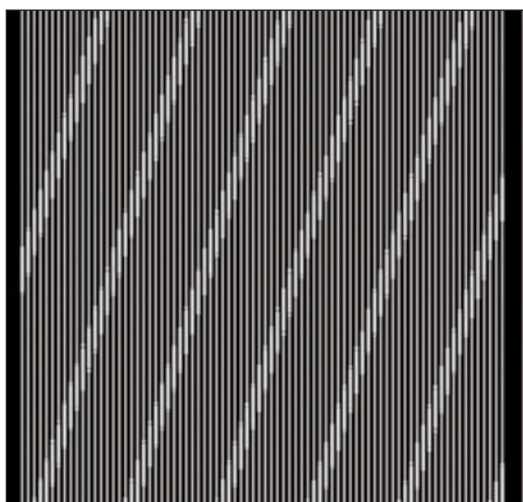
Fig. 9. Typical digital blackboard with periodic defects
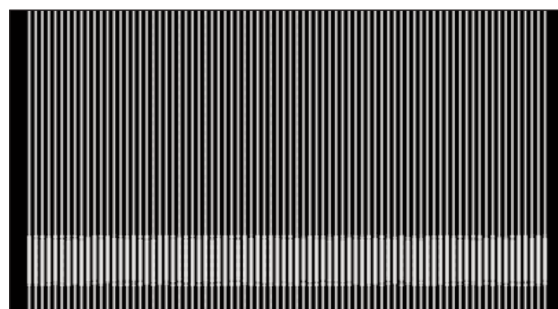
Fig. 10. Typical digital blackboard with 188 mm height

versa. The system also provides single face in which the yarn is continuously arranged on the face view of the digital yarn blackboard.

Adjusting the start point A_s long as the yarns are wound on the physical yarn blackboard, the yarns cannot be re-wound. Comparing with physical yarn blackboard the digital yarn blackboard uses the data of diameter to simulate appearance of yarn; therefore, the yarns can be re-wound on the digital blackboard adopting different start point since the data can be used repeatedly. It can reduce the processing of winding yarn on yarn blackboard. Figure 8 *a* shows an example of digital yarn blackboard. Assumed the start point in figure 8*a* is 1st pixel, figure 8*b* shows an example of digital yarn blackboard in which the start point is 200th pixel. From figure 8*b*, we find that all part of one defect on the second line move to display on the face view of the digital yarn blackboard. We can view the appearance of other defect easy using same method.

Detecting defect of yarn

The periodic defect is a kind of typical example defect. When there are periodic defects on the yarn, a typical digital blackboard is shown in figure 9. From the figure periodic defects can be found. The size of defect is calculated as 28 mm and the distance between two defects is calculated as 160 mm. If we

adjust the height of blackboard to be the cycle of periodic defect, meanwhile we adjust the start point; the periodic can be deduced as shown in figure 10.

CONCLUSIONS

This has prompted many groups to develop digital yarn blackboard for replacing of traditional yarn blackboard. In the research a digital blackboard system is developed for measuring yarn quality combining with the measurement result through capacitive apparatus in the research. The appearance of yarn is reconstructed based on the diameter data of yarn using a mathematical model of rectangles and illumination model of yarn.

Furthermore, the software is improved. The platform can be used for further operation according to the practical demand: the width and the height can be resized; single or double-face is optional; the color of blackboard can be edited; the magnification or minification can be adjusted freely and so on. The experimental results showed that the system is flexible for configuration and convenient for operating. Because the use of winding blackboard is avoided in the research, the system will find widespread use in industry.

BIBLIOGRAPHY

[1] Carvalho, V., Soares, F., Vasconcelos, R., Belsley, M., Goncalves, N. *Yarn hairiness determination using image processing techniques*. Emerging Technologies & Factory Automation (ETFA), 2011 IEEE 16th Conference on, pp. 1–4

[2] Fabijanska, A., Kuzanski, M., Sankowski, D., Jackowska-Strumitto, L. *Application of image processing and analysis in selected industrial computer vision systems.* Perspective Technologies and Methods in MEMS Design. MEM-TECH International Conference, 2008, pp. 27–31

[3] Zhang, X., Gao, W., Liu, J. *Automatic recognition of yarn count in fabric based on digital image processing*. Image and Signal Processing, 2008. CISP '08 Congress, 3, pp. 100–103

[4] Fabijanska, A. *A survey of thresholding algorithms on yarn images.* Perspective Technologies and Methods in MEMS Design (MEMSTECH). Proceedings of 6th International Conference, 2010, pp. 23–26

[5] Kuzariski, M. *The algorithms of the yarn shape detection and calculation of the protruding fibres length.* Perspective Technologies and Methods in MEMS Design. MEMSTECH International Conference 2008, pp. 98–100

[6] Kuzahski, M., Jackowska-Strumillo, L. *Yarn hairiness determination the algorithms of computer measurement methods.* Perspective Technologies and Methods in MEMS Design. MEMSTECH International Conference 2007, pp. 155–158

[7] Su, C., Lai, P. *Evaluating the unevenness of stretch-broken tow in tow-to-yarn direct spinning.* In: Fibers and Polymers, 2010, vol. 11, issue 4, pp. 648–653

[8] Slater, K. *Yarn Evenness*. In: Textile Progress, 1986, vol. 14, issue 3, 4, pp. 1–95

[9] Liu, J., Xie, Z., Gao, W., Jiang, H. *Automatic determination of slub yarn geometrical parameters based on an amended similarity-based clustering method.* In: Textile Research Journal, 2012, vol. 80, issue 11, pp. 1 075–1 082

[10] Militký, J., Ibrahim, S. *Complex characterization of yarn unevenness*. Studies in Computational Intelligence, 2007, vol. 55, pp. 57–73

[11] Vítor, C., Monteiro, L., Soares, F., Vasconcelos, R. *Yarn evenness parameters evaluation: A new approach*. In: Textile Research Journal, 2008, vol. 78, issue 2, pp. 119–127

[12] Hakan, Ö., Güngör, B. *Computer simulation of woven fabric defects based on faulty yarn photographs*. ISCIS 2006, LNCS, pp. 325–333

[13] Zellweger Uster Ltd. *Application report measurement of slub yarns with the Uster®tester 5*, 2009; http://www.uster.com/UI/textile-Fancy-Yarn-Profile-2-3034.aspx

[14] Zellweger Uster Ltd. *Uster Tester 5-C800 technical data*, 2005

[15] Sriprateep, K., Bohz, E. *A new computer geometric modeling approach of yarn structures for the conventional ring spinning process*. In: The Journal of The Textile Institute, 2009, vol. 100, issue 3, pp. 223–236

[16] Liao, T., Adanur, S. *A novel approach to three-dimensional modeling of interlaced fabric structures*. In: Textile Research Journal, 1998, vol. 68, issue 11, pp. 841–847

[17] Lin, H., Newton, A. *Computer representation of woven fabrics by using B-splines*. In: The Journal of the Textile Institute, 1999, vol. 90, issue 1, pp. 59–62

[18] Jiang, Y. Chen, X. *The structural design of software for simulation ftand analysis of woven fabric by geometry model*. Textile Institute Conference, Donghua University Press, Shanghai, 2004, pp. 1 298–1 301

[19] Zhong, H., Xu, Y., Guo, B., Shum, H. *Realistic and efficient rendering of free-form knitwear*. In: Journal of Visualization and Computer Animation, 2001, vol. 12, issue 1, pp. 13–22

[20] Lomov, S., Verpoest, I. *Model of shear of woven fabric and parametric description of shear resistance of glass woven reinforcements*. In: Composite Science Technology, 2006, vol. 66, pp. 919–933

[21] Sherburn, M. *Geometric and mechanical modeling of textiles*. PhD Thesis, The University of Nottingham, 2007

[22] Kayacan, O., Kurbak, A. *Basic studies for modeling complex weft knitted fabric structures.* Part IV. *Geometrical modeling of miss stitches*. In: Textile Research Journal, 2008, vol. 78, issue 8, pp. 659–663

[23] Aileni, R. M., Ciocoiu, M., Fărîmă, D. *Modeling and 3D simulation of the garment product*. In: Industria Textilă, 2011, vol. 62, issue 3, pp. 141–45

[24] Olaru, S., Niculescu, C., Mocenco, A., Săliştean, A., Teodorescu, M. *Shape categories for the Romanian female population and specific clothing recommendations*. In: Industria Textilă, 2011, vol. 62, issue 3, pp. 141–45

[25] Tom, C., Sergei, G., Weih-Her, H. *Yarn CAD simulation for fashion and textile design education*. In: International Journal of Fashion Design, Technology and Education, 2008, vol. 1, issue 1, pp. 13–21

[26] Kang, T., Kim, S., Jung, K. *Analysis of geometrical parameters using a CAD system for a 3-D braided preform*. In: Textile Research Journal, 2008, vol. 78, issue 10, pp. 922–935

[27] Chen, X. *Mathematical modeling of 3D woven fabrics for CAD/CAM software*. In: Textile Research Journal, 2011, vol. 81, pp. 42–50

[28] Liao, T., Adanur, S. *A novel approach to three-dimensional modeling of interlaced fabric structures*. In: Textile Research Journal, 1998, vol. 68, pp. 841–847

[29] Özdemir, H., Baser, G. *Computer simulation of woven fabric appearances based on digital video camera recordings of moving yarns*. In: Textile Research Journal, 2008, vol. 78, pp. 148–157

[30] Semnani, D., Sheikhzadeh, M., Hadjianfar, M., Reyhani, Z. *Study of structural parameters of weft knitted fabrics on luster and gloss via image processing*. In: Industria Textilă, 2012, vol. 63, issue 1, pp. 42–47

[31] Zhou, X., Cheng, L. *Digital image processing method of yarn black board*. In: Journal of Textile Research, 2008, vol. 29, issue 8, pp. 30–34

[32] Mukherjee, D. P., Jana, D. *Computer graphics algorithms and Implementations*. PHI Learning Private Limited, New Delhi, 2011

Authors:

Chief of works dr. eng. JIHONG LIU
Conf. dr. eng. BO ZHU
Conf. dr. eng. HONGXIA JIANG
Conf. dr. eng. RURU PAN
Conf. dr. eng. WEIDONG GAO
Jiangnan University
1800 LiHu Road, Wuxi, 214122 China
e-mail: liujihongtex@hotmail.com; jianghongxiatex@hotmail.com

DOCUMENTARE

Noi tehnologii

CONFORT SPORIT CU SALTEAUA iSURO

Salteaua iSURO, din bobiţe de polistiren şi structuri tricotate din urzeală 3D, tip sandwich, conturate spaţial, optimizează confortul somnului. Alegerea saltelei potrivite poate avea un impact pozitiv asupra calităţii somnului şi, prin urmare, asupra regenerării corpului. Ideal este ca stratul de bază să diminueze presiunea, să susţină coloana şi să ofere libertate de mişcare, cerinţe pe care salteaua iSURO AG le satisface într-un mod inovator. Prin combinarea sferelor de polistiren cu structuri tip sandwich şi spumă, saltelele devin mai uşoare, mai ferme şi mai maleabile decât vechile tipuri de saltele construite convenţional.

Iniţial, salteaua iSURO a fost proiectată pentru a fi utilizată în sectorul medical, construcţia sa specială permiţându-i adaptarea la anatomia corpului omenesc. Miezul construcţiei stratului de bază flexibil este stratul iSU, din aşa-numitele sfere iSURO. Sferele realizate din polistiren, la aceeaşi dimensiune – cât gămălia unui ac, se pot mişca liber în interiorul stratului iSU, ceea ce înseamnă că ele se pot adapta la orice poziţie a corpului, oferind un suport ferm. Prin adăugarea unui amestec fibros, umplutura devine pufoasă. Stratul fibros este inserat în material prin coasere, creând un model ondulat, datorită matlasării pe diagonală. Segmentele previn uzura în centrul saltelei, iar husa este largă şi elastică, permiţând utilizatorului să se aşeze confortabil, fără a simţi puncte de presiune. Materialul tricotat din urzeală, cu o structură tip sandwich, este aşezat pe partea de jos a stratului iSURO. Acest material cu pori deschişi permite circulaţia aerului, menţinând tot timpul un climat echilibrat. Construcţia stratificată, alcătuită dintr-un strat iSU şi un material 3D tricotat din urzeală, este încorporată într-un strat de spumă, pentru a crea un suport ferm.

Utilizatorii acestor saltele confirmă faptul că iSURO conferă o senzaţie de confort şi de cald, garantează un somn relaxant şi ajută la reducerea durerii în regiunea spatelui şi gâtului. Daniela Happel, dezvoltator de produs la iSURO sublinia faptul că "*copiilor le place în special senzaţia că se află într-un cuib, datorită suprafeţei uşor vălurite, create de sfere*". Substratul ferm, dar maleabil, atenuează starea de agitaţie, iar sferele iSURO flexibile permit mişcări independente ale încheieturilor. Suprafaţa flexibilă permite persoanei care doarme să găsească imediat o altă poziţie, iar presiunea să fie redistribuită. Pentru a asigura menţinerea caracteristicilor funcţionale ale saltelei, aceasta trebuie scuturată în mod regulat, iar sferele trebuie împinse către centru.

Institutul pentru sport şi cercetare interdisciplinară a somnului (ISIS) a testat eficienţa saltelelor iSURO. Specialiştii din Münster au efectuat, timp de şase săptămâni, testări pe 32 de bărbaţi şi femei, care au implicat interviuri şi completarea unor formulare, pentru a studia calitatea somnului. Testările au fost efectuate folosind o saltea iSURO şi o saltea cu arcuri. Toate datele culese au arătat că substratul cu umplutură de sfere a îmbunătăţit calitatea somnului. Aproximativ 87,5% din persoanele testate au afirmat că au avut un somn mult mai odihnitor decât atunci când au dormit pe vechile saltele cu arcuri. Numai 12,5% din subiecţii testaţi au afirmat că au dormit mai bine pe salteaua cu arcuri.

În concluzie, se poate afirma că efectele pozitive ale sistemului inovator iSURO constau în aceea că 62,5% din subiecţii testaţi au adormit mai repede, 50% din ei au avut mai puţine întreruperi ale somnului, iar 37,5% au dormit mai profund şi s-au răsucit mai puţin în timpul somnului. Studiul a arătat, de asemenea, că alte valori măsurate în mod obiectiv, cum ar fi variaţia ritmului cardiac, s-au îmbunătăţit semnificativ.

Kettenwirk Textilinformationen Praxis, martie 2013, p. 21

Warp knitted fabrics behaviour under dynamic testing

MIRELA BLAGA

NECULAI-EUGEN SEGHEDIN
ANA RAMONA CIOBANU

REZUMAT – ABSTRACT

Comportarea tricoturilor din urzeală la testarea dinamică

În lucrare se propune o metodă indirectă de determinare a rigidităţii tricoturilor din urzeală, prin analiza comportării dinamice a acestora. Perfomanţele dinamice ale acestor tricoturi au fost evaluate prin determinarea frecvenţelor proprii de vibraţie, obţinute în urma excitării prin şoc a unui ansamblu elastic, compus dintr-o masă metalică şi tricotul ataşat acesteia. Cercetările au avut în vedere determinarea rigidităţilor relative ale diverselor probe de material. Aceste rigidităţi au fost apreciate prin intermediul frecvenţelor naturale ale sistemelor elastice masă metalică - tricot, cunoscută fiind relaţia directă dintre rigiditate și frecvenţa naturală. Frecvenţele naturale au fost determinate prin aplicarea Transformatei Fourier Rapidă, în acest scop utilizându-se instrumentul virtual Spectrum Analyzer, din mediul LabView. Testele au fost efectuate asupra unor tricoturi produse de firmele Karl Mayer și Liba, fiind proiectate ca suport pentru structurile laminate. S-au analizat efectele structurii, ale tipului de fire și ale finisării asupra comportării dinamice a tricoturilor din urzeală.

Cuvinte-cheie: tricoturi din urzeală, vibraţii, comportare dinamică, textile tehnice

Warp knitted fabrics behaviour under dynamic testing

This paper aims at presenting the preliminary results of the research concerning warp knitted fabrics behavior under dynamic stress. The dynamic performances of knitted fabrics have been evaluated through the recorded frequencies caused by one impact hammer. Fast Fourier Transformation-FFT has been applied and the Spectrum Analyzer application from the LabView software was employed to determine the natural frequencies of the system. The tests were carried out on fabrics produced by Karl Mayer and Liba companies, for basic coatings and laminating, geotextiles, and reinforced composites. The effects of structure, yarn type and finishing treatment on the dynamic performance of knitted fabrics were evaluated.

Key-words: warp knitted fabrics, vibrations, dynamic behaviour and technical textiles

Warp knitting is by far the most versatile fabric production system in textiles. Warp knitted fabrics can be produced elastic or stable, with an open or closed structure. The flexibility of warp knitting techniques makes them attractive both to the designer and to the manufacturer of technical textiles, where knitted products can meet the requirements of a large range of applications: medical, protective, reinforced composites, industrial uses [1]. Their continuously spreading use in technical applications increases the research interest related to them, either concerning their complex structure [2], [3], or regarding their mechanical properties.

Textile materials and products made of these materials are exposed to varied load regimes [4]. The load regimes act in two different stages: during their technological processes and during their use. The deformation properties are different in the two cases. During knitting stage, both yarns and fabrics are loaded cyclically, at a relative high frequency, therefore a special vibration testing device has been developed, for textile materials of different kind, during cyclical stress at a high frequency. A vibration sensor was used as exciter, generating cyclical elongation of the textiles. The range of attainable frequencies at the maximum elongation of textiles was determined by the vibration system [5].

Nowadays the warp knitted structures produced by high performance fibers made from glass or carbon are used for composites reinforcement. The tensile behaviors of the CWKF (co-woven-knitted fabric) composite under the quasi-static and high strain rate tension were compared and analyzed in the frequency domain using the Fast Fourier Transform (FFT) method. The results show that the tension behavior, amplitude spectrum and phase spectrum of the CWKF composite are strain rate sensitive. The CWKF composite can absorb higher energy in a specific frequency range [6].

MATERIALS AND METHOD

Materials under testing

Knitting techniques and machinery are extensively used for the production of textile products for garments and industrial use. Warp knitting is the most suitable technique for the production of DOS (Directionally Oriented Structures) fabrics, with non crimped inserted yarns, used for composite materials production. The use of warp knitted fabrics in technical applications usually involves the use of yarns made of high performance fibres such as aramids, glass and carbon, which are more complex due to

their high stiffness, low extension at break and high flexural rigidity [11].

The investigations were carried out on DOS warp knits with parallel non-crimped yarns, as being representative for technical applications, such as: agricultural, road constructions, slope stabilization, roofing, bank reinforcement. These products may be manufactured in a way featuring optimum characteristics in line with the final purpose, on warp knitting machines with specific devices. The fabrics were produced on Karl Mayer and Liba machines, as commercial samples, provided with the purpose of demonstrating the technical facilities of warp knitting machines. The samples were coded and grouped according to their end use, the machine where it has been produced, yarn type inserted into the structure and raw material used. The technical features of the selected fabrics are presented in tables 1–4.

Testing method and equipment

In order to make a complete characterization of the mechanical behavior of warp knitted fabrics, free vibration method was employed [7]. An elastic system out of the position of stable equilibrium, then released, produces free vibrations. In the presence of friction forces, mechanical energy is dissipated, and the vibration is damped by a certain number of cycles. Free vibration frequencies depend on the mass, stiffness and damping of the system. They are independent of the initial conditions of the motion or of the system external forces. Therefore, their frequency or frequencies are called natural frequency of vibrations. For a given system, they have constant values well defined [8].

The dynamic behavior of knitted fabrics has been studied by analyzing the frequencies that characterize the motion of one attached mass. Metal mass attached to the textile material acts like a seismic mass, to the testing directions. Frequencies can be measured using an accelerometer attached to this mass.

Periodic signals can be written as a countable sum of sinusoidal components whose amplitudes and phases can be easily calculated from these signals, which are Fourier series. Fourier transform generalizes the signal decomposition into a sum of sinusoids and non-periodic signals [8]. Fast Fourier transform (Fast Fourier Transformation) allows an easy calculation of the frequency spectrum of a sequence of data.

There are several formulas for calculating the Fourier transform, which differ by the magnitude of the result, scaling or frequency sign. One of the most commonly used formulas is:

$$F(\xi) = \int_{-\infty}^{\infty} f(x)\, e^{-2\pi i x \xi}\, dx \qquad (1)$$

Under certain conditions the Fourier transform can completely recover the original function by applying the inverse Fourier transform:

$$f(x) = \int_{-\infty}^{\infty} F(\xi)\, e^{2\pi i x \xi}\, d\xi \qquad (2)$$

Table 1

			Threading		Chain link		Structural parameters			
							L, mm/rack		M, g/m²	Courses/ 10 cm
Code	Machine	Yarns	GB 1 front	GB 2 back	GB 1	GB 2	GB 1	GB 2		
C_1	RS3 EMS E 18	A – dtex 80 f 24 PES HT B – dtex 1 100 f 200 PES HT C – dtex 1 100 f 200 HT PES	full A Weft: full C	full B	1–0/ 1–2	0–0/ 0–0	2 490	636	184	76
C_2	RS3 EMS E 18	A – dtex 76 f 24 PES B – dtex 550 f 96 PES HT C – dtex 550 f 96 PES HT	full A Weft: full C	full B	1–0/ 1–2	0–0/ 0–0	2 430	695	97	71
C_3	RS3 EMS E 18	A – dtex 80 f 24 PES HT B – dtex 1 100 f 200 PES HT C – dtex 1 100 f 200 HT PES	full A Weft: full C	full B	1–0/ 1–2	0–0/ 0–0	2 550	680	173	72
C_4	RS3 MSU-N E 24	A – dtex 100 f 30 PES B – dtex 1 100 f 200 PES C – dtex 1100 f 200 PES	full A Weft: full C	full B	1–0/ 1–2	0–0/ 0–0	2 540	485	265	100

KARL MAYER – BASIC FABRICS FOR COATING (C) – UNIAXIAL TYPE

Table 2

			Threading		Chain link		Structural parameters			
							L, mm/rack		M,	Courses/
Code	Machine	Yarns	GB 1 front	GB 2 back	GB 1	GB 2	GB 1	GB 2	g/m²	10 cm
L_1	RS3 MSU E 9	A – dtex 80 f 24 PES HT B – dtex 1 100 f 200 PES HT	full A Weft: full B	full B	1–0/ 1–2	1–1/ 0–0	3 460	695	135	35
L_2	RSP3 MSU – V E 18	A – dtex 80 f 24 PES HT B – dtex 1 100 f 200 PES HT C – dtex 1 100 f 200 PES HT D – fleece PES 30 g/m²	full A Weft: full C	full B	1–0/ 1–2	0–0/ 0–0	2 620	695	210	70
L_3	RSP3 MSU – V E 9	A – dtex 80 f 24 PES HT B – dtex 1 100 f 200 PES HT C – fleece PES 30 g/m²	full A Weft: 1B 1 out	full B	1–0/ 1–2	0–0/ 0–0	2 550	680	102	72
L_4	RS3 EMS E 18	A – dtex 80 f 24 PES HT B – dtex 550 f 96 PES HT C – dtex 550 f 96 PES HT	1A 1 out Weft: full C	1 out 1B	1–0/ 2–3	1–1/ 0–0	4 800	1 300	48	71

Table title: **KARL MAYER – BASIC FABRICS FOR LAMINATED (L) – UNIAXIAL TYPE**

Table 3

Table title: **LIBA – GEOTEXTILES (G) – BIAXIAL TYPE**

			Threading			Chain link			Structural parameters		
									Cell size,	M,	Courses/
Code	Machine	Yarns	GB 1	GB 2	FB 3	GB 1	GB 2	FB 3	mm × mm	g/m²	10 cm
G_1	COPCENTRA HS 2-ST E6	A – PES 167 dtex f 34 B – glass 2 400 tex	1A 2 out Weft: 1B 4 out	1A 2 out	1B 2 out	1–2/ 1–0	1–0/ 1–2	0–0/ 0–0	12 × 12	500	42
G_2	COPCENTRA HS 2-ST E6	A – PES 167 dtex f 34 B – glass 2 400 tex	1A 2 out Weft: 2B 4 out	1A 2 out	1B 2 out	1–2/ 1–0	1–0/ 1–2	0–0/ 0–0	12 × 15	624	40
G_3	COPCENTRA HS 2-ST E6	A – PES 167 dtex f 34 B – glass 2 400 tex	2A 4 out Weft: 2B 6 out	2A 4 out	2B 4 out	1–2/ 1–0	1–0/ 1–2	0–0/ 0–0	25 × 25	530	32
G_4	COPCENTRA HS 2-ST E12	A – PES 167 dtex f 32 B – PES 1 100 dtex f 200	3A 14 out Weft: 4B × 6 8 out	3A 14 out	3B × 8 14 out	1–0/ 1–2	1–2/ 1–0	0–0/ 0–0	30 × 30	400	28
G_5	COPCENTRA HS 1-ST E5	A – PES 167 dtex f 32 B – PES 1 100 dtex f 210	Full A Weft: 1B 1 out		Full B	1–0/ 0–1		0–0/ 1–1	5 × 5	115	40

Table 4

			Threading		Number of multiaxial threads			Structural parameters			
								Chain link		*M*,	*Courses/*
Code	Machine	Yarns	*GB 1*	*GB 2*	+45°	90°	−45°	*GB 1*	*GB 2*	g/m²	10 cm
G_6	COP Multiaxial E6	A − PES 76 dtex f 24 +45° glas 68 tex 90° glas 68 tex −45° glas 68 tex	Full A	-	48	72	48	1-0/ 1-2	-	689	64
G_7	COP Multiaxial CNC E5	A − PES 50 dtex f 24 +45° carbon 800 tex −45° carbon 800 tex	empty	Full B	10	-	10	-	1-0/ 0-1	275	38
G_8	COPCENTR Multiaxial CNC E5	A − PES 76 dtex f 24 +35° glas 600 tex 90° glas 600 tex −45° glas 600 tex	empty	Full A	48	30	48	-	1-0/ 1-0	1 106	30

Table title: LIBA – GEOTEXTILES (*G*) – MULTIAXIAL TYPE

From the conceptual argument ξ is a frequency, whereas *x* is a dimension (temporal or spatial). Fourier transform of the function *f* can be noted symbolically:

$$F = \mathcal{F}\{f\} \qquad (3)$$

This capacity for reorganization of the Fourier transform of frequency information (temporal, spatial or otherwise) is very useful in signal processing of various types, to understanding the properties of many physical systems, to solve equations in other scientific fields theoretical and applied. During vibration, mechanical energy dissipates by friction or other resistance. In the presence of damping, free vibration amplitude decreases over time and to maintain constant amplitude of vibration outside forces should be applied. In general, energy dissipation is called damping. It is produced by internal friction in materials, the friction between the components of one structure, the fluid-structure interactions, radiation and motion in electric or magnetic fields. Structural or hysteretic damping is described by a damping force in phase with velocity, but proportional to the displacement [8]. In case of knitted fabrics, energy dissipation is determined by relative friction between the yarns and the specific internal friction yarn structure. The friction depends on the nature of yarn, knitting technology, finishing chemical treatments etc.

Dynamic performance of knitted fabrics has been studied by testing the dynamic behaviour of one metallic piece, 135 g weight, 30 × 70 × 30 mm dimensions, fixed through an adhesive, directly on their surface. Also, the textile material is fixed on one heavy plate, with an adhesive. This way, the relative movements between the piece-knitted fabric-plate has been avoided. This method allows the measure-ment of the vibrations of the metallic piece, by using an impact hammer employed as an exciter. The vibrations were produced and measured on three directions: wale wise (fig. 1*a*), course wise (fig. 1*b*) and perpendicular on the fabric surface (fig. 1*c*). The equipment used as an exciter consists of an impact hammer Piezotronics and vibrations were measured with an accelerometer PCB B52 Piezotronics. The signal is processed with a data acquisition card 6023 National Instruments. In order to determine the natural frequencies of the system, the Fast Fourier Transformation-FFT has been applied and the Spectrum Analyzer application from the Lab View 8.2 software [9] has been employed (fig. 2).

The recorded frequencies obtained by using the employed software are displayed in figures 3 – 6 for one sample from each group of fabrics. For all knitted specimens, the tests were conducted similarly and three experimental values for each sample have been recorded. The average values were calculated and displayed in table 5, to facilitate the discussions and general conclusions.

RESULTS AND DISCUSSIONS

Testing direction

The comparative analysis of fabric's behavior from each group of fabrics has been depicted in figures 7 *a, b, c, d*. The differences between samples within the same group are small, considering the relative less variations of their structural parameters. However, some observations can be made, about the direction along which the vibrations were measured. For the $C_1 − C_4$ group, fabrics natural frequencies
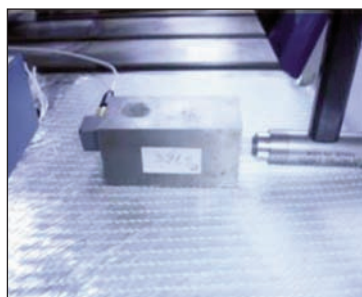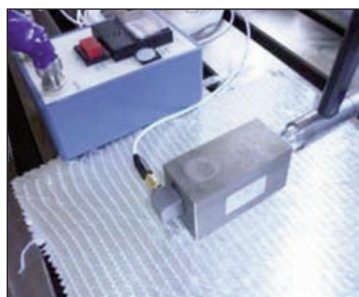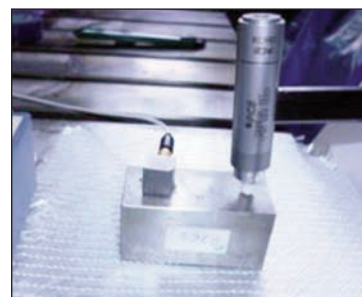
a   b   c

Fig. 1. Direction of producing and measuring the vibrations:
a – walewise; *b* – coursewise; *c* – perpendicular
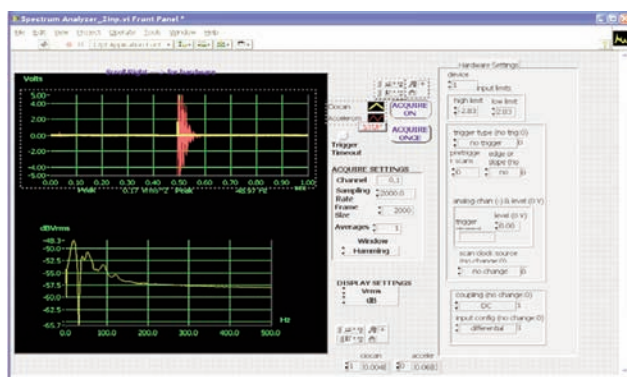
Fig. 2. Spectrum analyzer application

reveal a comparable level of the values on wale and course direction 65–85 Hz, the differences being associated with the machine gauge and fabric square

mass, mostly noticeable for sample C_4, 94–98 Hz. In case of $L_1 – L_4$, fabric L_4 has a sensible increased value of the frequencies, comparing to the other three. This can be explained by its different threading, yarn fineness and consumption. For the group $G_1 – G_5$, the results are comparable, sample G_4 presents the lowest values of the determined frequencies, the differences being justified by the higher machine gauge and cell dimensions. The multiaxial fabrics $G_6 – G_8$, have responded similarly to the dinamic testing, fabric G_6 has the highest values from the group, the machine higher gauge being resposible for this, together with yarn fineness. On the perpendicular direction, the natural frequencies are placed in a higher range of values for all fabrics, fact that can be explained by the increased system rigidity, created by the assembly attached mass – knitted
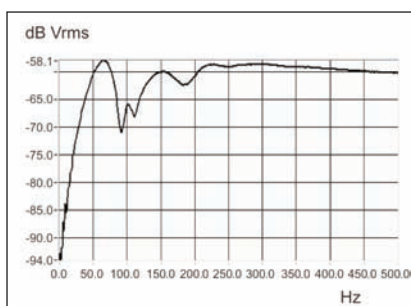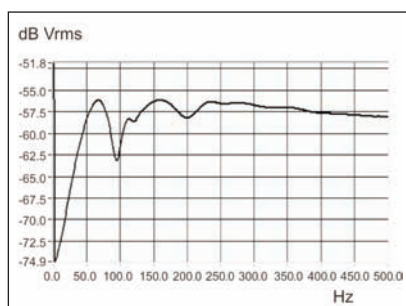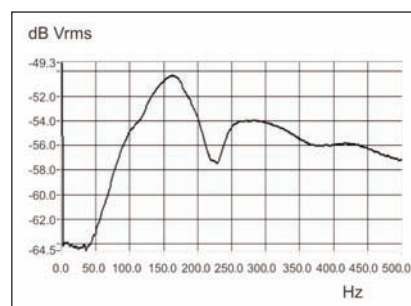
a   b   c

Fig. 3. Natural frequencies of the knitted fabric on various directions – sample C_1:
a – walewise; *b* – coursewise; *c* – perpendicular
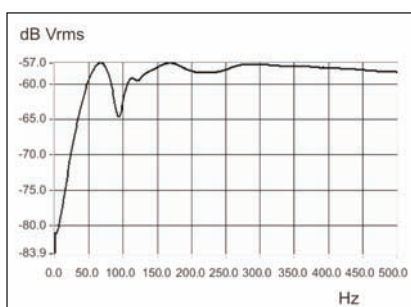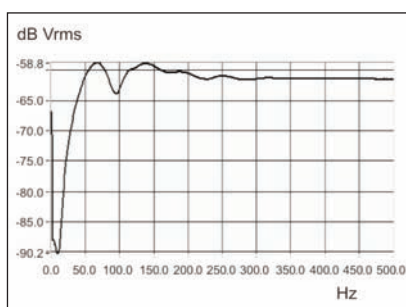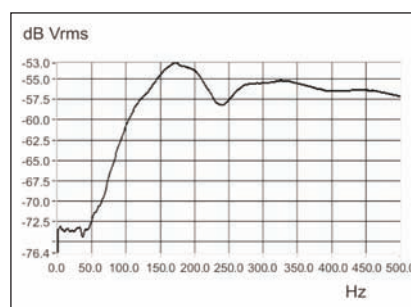
a   b   c

Fig. 4. Natural frequencies of the knitted fabric on various directions – sample L_1:
a – walewise; *b* – coursewise; *c* – perpendicular
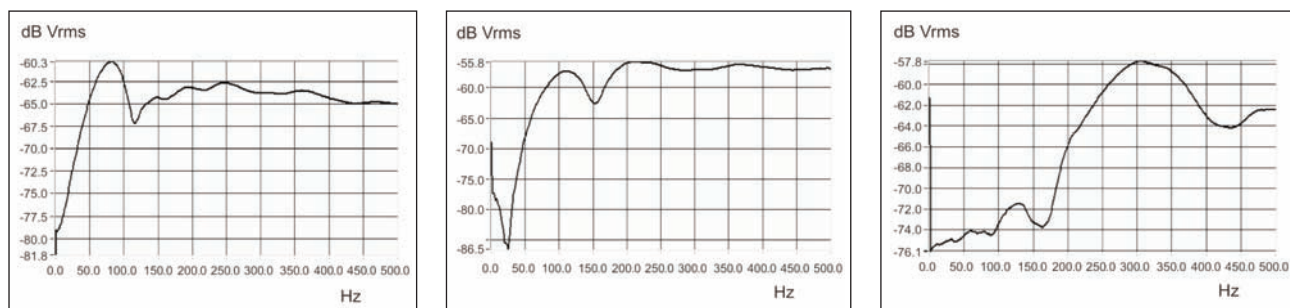
Fig. 5. Natural frequencies of the knitted fabric on various directions – sample G_1:
a – walewise; *b* – coursewise; *c* – perpendicular
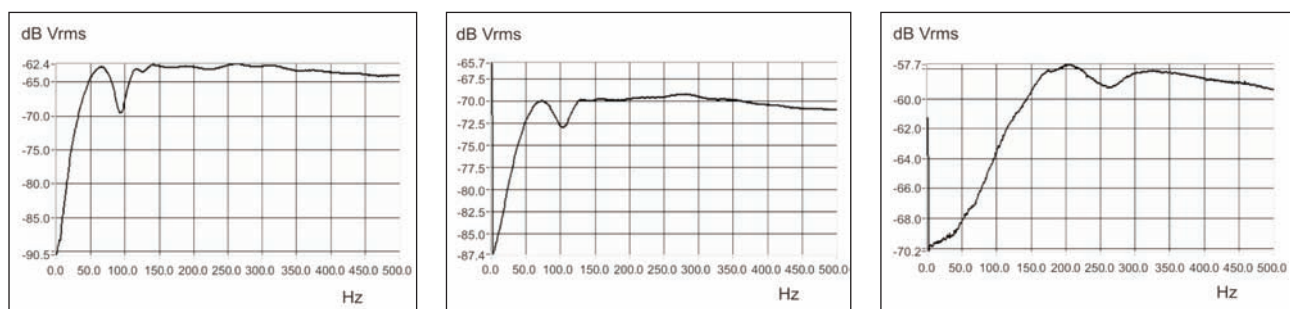
Fig. 6. Natural frequencies of the knitted fabric on various directions – sample G_6:
a – walewise; *b* – coursewise; *c* – perpendicular
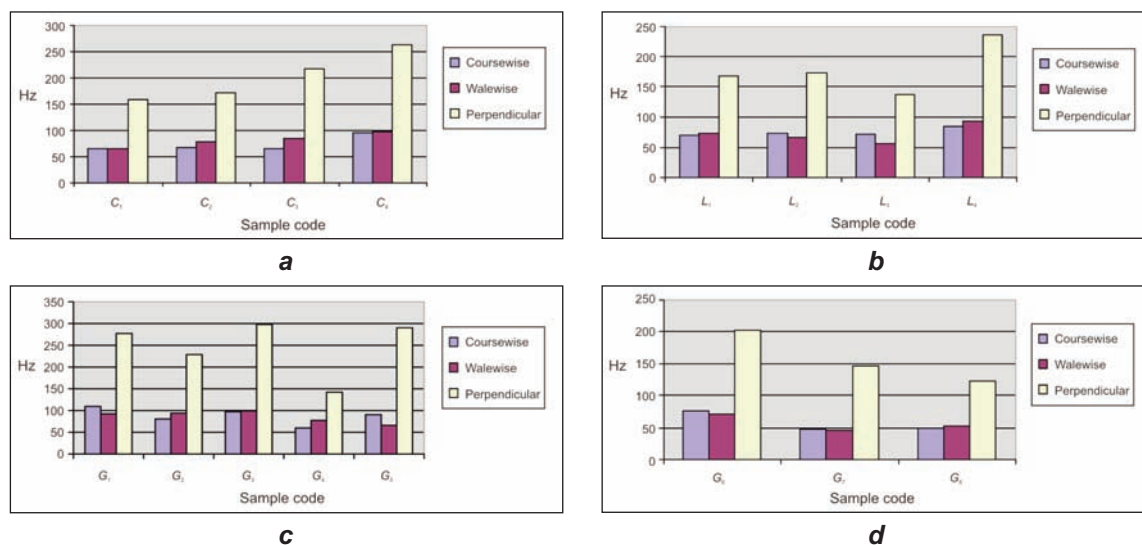
Fig. 7. Natural frequencies of the knitted fabrics in relation with testing direction:
a – fabrics $C_1 - C_4$; *b* – fabrics $L_1 - L_4$; *c* – fabrics $G_1 - G_5$; *d* – fabrics $G_6 - G_8$

fabric. Another explanation can be connected to the fabric thickness and its cross section, the number of contact points between yarns.

Yarn consumption

For the group $L_1 - L_4$, samples with weft parallel yarns, the results can be interpreted from the figure 7*b*. L_2 and L_3 contain a fleece layer, leading to a heavier structure, but with lower yarn consumption. The structural parameters have close values for these two fabrics, from course density to yarn consumptions

for both bars. L_3 is the single sample, having partial threading for weft in-laid yarns, and the lowest yarn consumption. This structural arrangement provides a softer structure, which is reflected in the lowest values of natural frequencies, as can be observed in figure 7*b*. One preliminary conclusion can be drawn: structures with lower yarn run-in [mm/rack] indicate lower values of natural frequencies, and consequently lower fabric rigidity. This theory is confirmed by the sample L_4, which has been manufactured with the highest yarn consumption and also has registered

Table 5

Sample code	Type	Values of natural frequencies, Hz		
		Coursewise	Walewise	Perpendicular
C_1	Uniaxial	65.3	65.3	158.0
C_2		66.6	78.0	172.6
C_3		64.6	85.3	216.6
C_4		94.6	98.0	263.3
L_1	Uniaxial	70.6	73.3	168.0
L_2		73.3	66.6	172.6
L_3		71.3	56.6	136.6
L_4		83.3	92.6	236.6
G_1	Biaxial	109.3	92.6	277.3
G_2		80.6	94.0	228.6
G_3		97.3	99.3	298.0
G_4		60.0	77.3	142.0
G_5		90.6	66.0	290.0
G_6	Multiaxial	76.6	70.6	202.0
G_7		47.3	46.0	146.0
G_8		50.0	53.3	122.0

RECORDED VALUES OF NATURAL FREQUENCIES FOR KNITTED SAMPLES

the highest values of the natural frequencies, as visible in table 5. Within the fabrics class $C_1 - C_4$, the C_4 one exhibits increased values of the frequencies, this sample being produced on a higher machine gauge, having the highest square mass and course density. These factors led to this fabric response and to the conclusion that during the end use, will act with a higher rigidity.

Finishing treatment

Performance enhancement finishes were applied to improve the characteristics of the fabrics from the group $G_1 - G_5$, like tensile and resistance. Coating with PVC and grid type structures make them suitable for road foundation. Their response to the vibration testing is presented in figure 7c. This group has demonstrated superior values of natural frequencies, fact that can be attributed to the finishing treatment, coating with PVC, made to functionalize the raw fabrics for geotextiles end use. The increased values of the recorded frequencies in all testing directions, sustain the clear influence of the fabric finishing treatment on its rigidity. During the finishing process, by chemical agent's action, a consolidation process of yarns contacts is taking place. Thus, the yarns friction becomes lower, with consequence in the structure rigidity increasing.

Another cause of the higher values of the frequencies can be the biaxial type of the structure, with yarns inserted in two directions, contributing thus to an increased rigidity.

Yarn fineness

Despite of the low number of samples from the group $G_6 - G_8$, some comments can be made on fabrics behaviour, based on the values of the frequencies shown in figure 7d. Fabrics G_7 and G_8 made of raw materials with close yarns fineness 600–800 tex have similar values of the frequencies, compared to fabric G_6 produced with yarns of 68 tex, which shows an almost double value of the natural frequencies. One can conclude that raw material fineness influences significantly the fabric behaviour. Fabric G_7 perform differently, comparing to the other two, having the lowest values of the frequencies and this can be attributed to the carbon yarns, used as diagonal yarns. Fabrics G_6 and G_8 having glass yarns inserted under diagonal directions, behave slightly different, fact that leads to the conclusion that the nature of yarns must be taken into account, when such tests and analysis are carried out.

CONCLUSIONS

The presented study is intended to be a preliminary research on knitted fabrics behavior under dynamic stress. Vibration analysis deals with testing the material against random vibrations, shock and impact. Each of these incidences may act under natural vibration frequency to the material which, in turn, may cause resonance and subsequent failure [10].

The tests were carried out on a range of commercial warp knitted fabrics, from the DOS group, with inserted yarns, perfectly straight, giving greater fabric stiffness along the insert direction. These types of knitted

structure are termed non-crimp structures and can be produced in a single stage knitting process. According to the referenced sample of knitted fabric, some preliminary conclusions can be summarized, as follows:

- Research indicated a comparable dinamic behavior on wale and course direction of the fabrics. This similar response can be explained by the grid structures of all samples, well balanced by the presence of the straight yarns, inserted in various directions. The comparable behaviour of the fabrics on the two directions can be attributed to fact that the vibration mechanism does not involve any movement or distribution of the yarn inside the structure.

- The most significant differences of the fabrics natural frequencies were recorded on perpendicular testing direction. This is the direction that knits can be used for shock isolation of the fine mechanic devices, as potential end uses.

- The finishing process, by its chemical agent's action proved a certain influence on the higher natural frequencies values of the tested fabrics. The consolidation process of yarns contacts is taking place, determining a lower yarns friction and thus an increased rigidity of the structure.

Further research will primary taking into account the dynamic testing on the perpendicular fabric direction, correlated with other parameters, such as:

– yarns properties (nature, fineness, bending, rigidity, tensile);
– number of contact points per square unit;
– vibrations amplitude;
– finishing treatment of the knitted fabrics.

The research conducted so far, have been carried out considering that, the fabrics were preloaded on the perpendicular direction, under the action of seismic mass weight. More, the studies will consider various initial pretension values in this direction.

Another future research objective is the study of the energy dissipation way of the vibrating mass, through the ratio between dissipated energy by the yarns bending and yarns friction.

BIBLIOGRAPHY

[1] *Karl Mayer Technical Textiles Guide*. Karl Mayer GmbH, Germany

[2] Renkens, W., Kyosev, Y. *Geometry modelling of warp knitted fabrics with 3D form*. In: Textile Research Journal, 2011, vol. 81, issues 4, pp. 437–443

[3] Kalivretaki, A. et. al. *Finite element modeling of the warp knitted structure*. In: Research Journal of Textile and Apparel, Hong Kong Polytechnic University, 2007, vol. 11, issue 4, pp. 40 – 47, ISSN 1560 – 6074

[4] Morton, W. E., Hearle, J. W. S. *Physical properties of textile fibers*. The Textile Institute Butterworths, Manchester & London, 1962

[5] Tumajer, P. et. al. *Use of the Vibtex vibration system for testing textiles*. In: AUTEX Research Journal, June 2011, vol. 11, issue 2

[6] Pibo, Ma. et al. *Frequency features of co-woven-knitted fabric (CWKF) composite under tension at various strain rates*. Composites: Part A, 2011, vol.42, issue 5, p. 446–452

[7] Seghedin, N. E., Blaga, M., Ciobanu, R. *Weft knitted fabrics behaviour under dynamic testing*. 12th World Textile Conference AUTEX, June 13th to 15th, 2012, Zadar, Croatia, pp. 455–460

[8] Goldman, S. P. E. *Vibration spectrum analysis, a practical approach*. Industrial Press. Inc., 1999

[9] Rades, M. *Vibraţii mecanice*. Printech Publishing House, Bucharest, 2008

[10] Mogahzy, Y. E. El. *Engineering textiles, integrating the design and manufacture of textile products*. Woodhead Publishing Limited, Cambridge England, 2009, ISBN 978-1-84569-048-9

[11] Au, K. F. *Advances in knitting technology*. Woodhead Publishing Limited, Cambridge England, 2011, ISBN 978-1-84569-372-5

Authors:

MIRELA BLAGA

ANA RAMONA CIOBANU

Universitatea Tehnică Ghe. Asachi

Facultatea de Textile-Pielărie şi Management Industrial

Bd. D. Mangeron nr. 53, 700050 Iaşi

e-mail: mirela_blaga@yahoo.com

NECULAI EUGEN SEGHEDIN

Universitatea Tehnică Ghe. Asachi

Facultatea de Construcţii de Maşini şi Management Industrial

Bd. D. Mangeron nr. 43, 700050 Iaşi

SWOT analysis of the efficiency in the production of technological steam for the textile materials finishing

ANCA BUTNARIU   GHEORGHE CONDURACHE

REZUMAT – ABSTRACT

Analiza SWOT a eficienţei producerii aburului tehnologic destinat finisării materialelor textile

În lucrare se analizează eficienţa producerii aburului tehnologic într-o societate comercială care prelucrează articole textile din bumbac şi tip bumbac, utilizând o formă modernă de aplicare a metodei SWOT. S-a plecat de la un studiu de caz asupra acestei societăţi comerciale şi, folosind metoda SWOT modificată, s-a realizat un studiu comparativ între eficienţa circuitului actual de obţinere a agentului termic şi un circuit modernizat, în care este implementată o pompă de căldură, ce poate valorifica energia termică a apelor reziduale. Metoda SWOT aplicată în acest caz a demonstrat clar avantajele economice şi ecologice ale tehnologiei de producere a agentului termic prin utilizarea pompei de căldură.

Cuvinte-cheie: analiză SWOT, eficienţă, materiale textile, finisare

SWOT analysis of the efficiency in the production of technological steam for the textile materials finishing

The paperwork analyses the efficiency of technological vapor production for a textile firm that processes cotton and cotton based products, using a modern way of applying the SWOT method. We have used a study case of a textile firm, in which using the modified SWOT method we have compared the efficiency of the existing circuit of obtaining the heat carrier and a modernized circuit that contains a heat pump that can exploit the thermal energy of the residual waters. The SWOT analysis method that we have implemented clearly gave proof of economic and ecologic advantages of the heat carrier production technology when the heat pump is used.

Key-words: SWOT analysis, efficiency, textile materials, finishing

The SWOT analysis is a research method that indicates the opportunity of the introduction of technological change in the circuit of execution of a certain product. It is considered the first stage of strategic planning of an organization [1], [2].

The SWOT analysis method falls back upon four research directions: strengths, weaknesses, opportunities and threats of the business [3]. The phases of SWOT analysis encompass some stages:

- the identification of strengths, weaknesses, opportunities and threats;
- the analysis of strengths, weaknesses, opportunities and threats;
- the formulation of the strategic alternatives.

The present work submits a SWOT analysis of the production of technological steam in a plant that processes cotton textile products.

EXPERIMENTAL PART

The increasing exigencies of the sustainable development, on account of the reduction of pure water resources, energy resources and not only, represent one of the most important problems for the textile industry firms nowadays.

The SWOT analysis applied in the case of technological steam production in the discussed case, was built on a model that comprehends six strengths, six weaknesses, six opportunities and six threats, and starts from the existing heat carrier production circuit,

indispensable for the manufacturing activity (fig. 1). It continues with a different circuit that improves the thermal potential of the waste waters in the plant (fig. 2).

The identification of weaknesses

The thermal balances performed on the existing circuit of the heat carrier manufacturing presented in the figure 1 showed that the technological steam is obtained on the base of high fuel consumption of methane gas, whose price is continuously increasing. In the same time, the process of production of technological steam is based on the existence of some important emissions of gases with greenhouse effect, as CO_2, CO, NO_x and powders [4] – [6].

Also we can mention that the production of technological steam is supersized and it must be modernized and re-dimensioned to the actual capacities of production.

In these conditions, we could identify the weaknesses and the strengths for the existing variant of obtaining the technological steam (fig. 1).

The weaknesses are:
- over dimensioning of the plant;
- high energy consumption;
- the exploitation of thermal energy of residual waters;
- low yield of the plant;
- high emissions with greenhouse effect and high maintenance costs.
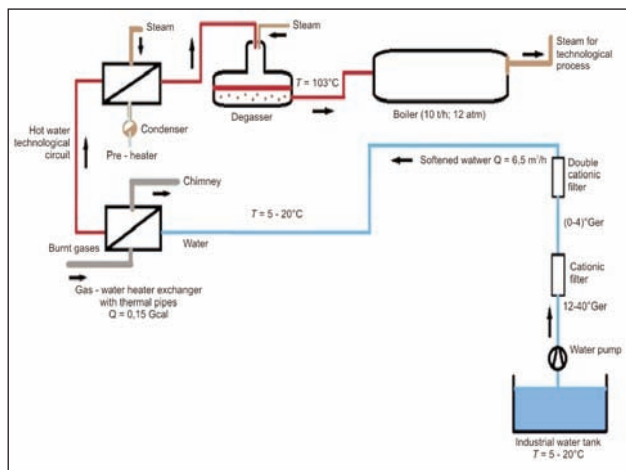
Fig. 1. Existing heat carrier production circuit

According to this scheme, the industrial water used for the production of the steam is pre-heated in a heat changer that uses the burnt gas, the temperature rising to 30ºC. Next, the water is passed through a second heat changer operated by steam, the temperature rising to 84.5ºC. The water is passed through a degasser, its temperature getting to 103ºC, and then enters the steam generator.

The identification of strengths

The study using the SWOT analysis conducted to the nominalization of the following strengths, in the present system of production of technological steam in the company that we have analyzed:

- thermal and energetic efficiency;
- recovery of the thermal energy of burnt gases;
- recovery of the condensed water;
- safety in exploitation;
- invulnerability to weather and flexibility.

The data collected in the introductory analysis that encompasses the weaknesses and the strengths of the system conducted to the conclusion that a technological change of the circuit of steam production is imposed. We proposed an ecological technology with low fuel consumption and consequently with low impact on the environment.

The compliance with this condition could be attained by the acquisition of efficiently energetic equipments, and the present work proposes the utilization of "green" technologies with low effects on the environment, that responds to the increasing demand of consumers for ecological products.

The technological variant proposed by the present work starts from the idea of capitalization of the thermal energy of residual waters in the phase of pre-heating of industrial water used in the process of technological steam production, according to the scheme in the figure 2 [7].

The following weaknesses were identified for this variant of steam production:

- over dimension of the plant;
- high energy consumption;
- vulnerability;
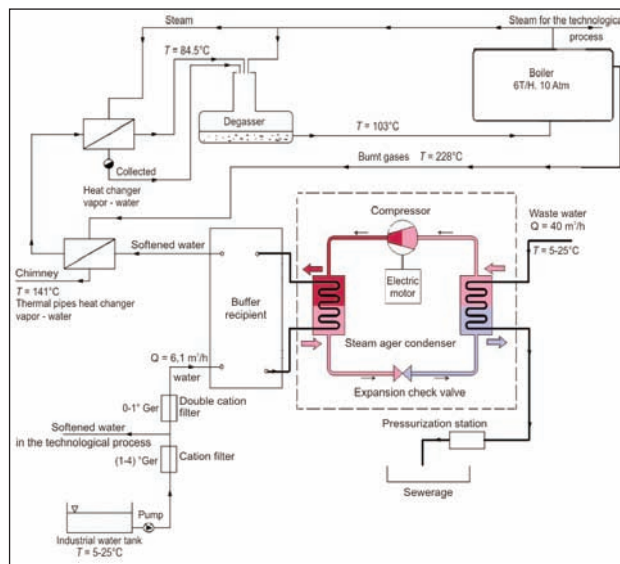
Fig. 2. Optimized heat carrier production circuit

- high maintenance costs;
- low exploitation safety and low flexibility.

In this modified circuit, a heat pump is inserted on the track of the heat carrier, which rises the temperature of the water that charges the steam generator until 60ºC. After the pump, the circuit is identical with the first variant, but the temperatures are higher. In this case, the thermal balances showed a considerable reduction of the demand of steam necessary for the pre-heating and consequently a reduction of fuel demand. That allows a reduction of the gas fumes expelled in the atmosphere [6], [7].

Opportunities for the circuit of steam production

The opportunities identified for the circuit of steam production in the analyzed company are the following:

- attraction of investment funds for the energetic efficiency, an increasing demand of ecological products;
- the development of the business;
- increased market competitiveness by the reduction of costs;
- the promotion of clean technologies and increased business profitability.

We point out that the opportunities and the threats are the same for the both variants. In order to transform the advanced theoretical model of analysis in a specific analysis model we must perform a comparison between the two circuits of technological steam production, respectively the present circuit and the proposed one, that has implemented a heat pump, circuit that exist in the same firm that processes cotton products.

RESULTS AND DISCUSSIONS

Based on the answers of some special questionnaires and on the discussions with a group of experts and specialists we have performed a ranking of the factors found by the SWOT analysis, by assigning weights to every factor, the sum of those for every

Table 1

THE COMPARATIVE ANALYSIS OF STRENGHTS						
Strengths	Initial circuit			Proposed circuit		
	Ki	Ni	ni	Ki	Ni	ni
Thermal energetic efficiency	0.15	2	0.3	0.15	4	0.6
Recovery of thermal energy of burnt gases	0.1	4	0.4	0.1	4	0.4
Safe operations	0.1	3	0.3	0.1	0	0
Low vulnerability	0.05	2	0.1	0.05	0	0
Flexibility	0.1	1	0.1	0.1	0	0
Recovery of the condenser water	0.1	4	0.4	0.1	4	0.4
Low emissions of greenhouse effect gases	0.15	0	0	0.15	5	0.75
High efficiency plant	0.1	0	0	0.1	3	0.3
Recovery of thermal energy of residual waters	0.15	0	0	0.15	5	0.75
Strengths – total	1	-	1.6	1	-	3.2

Table 2

THE COMPARATIVE ANALYSIS OF WEAKNESSES						
Weaknesses	Initial circuit			Proposed circuit		
	Ki	Ni	ni	Ki	Ni	ni
Over dimension of the plant	0.1	4	0.4	0.1	2	0.2
High energy consumption	0.15	4	0.6	0.15	2	0.3
The exploitation of thermal energy of residual waters	0.15	5	0.75	0.15	0	0
Low yield of the plant	0.1	4	0.4	0.1	0	0
High emissions with greenhouse effect	0.15	3	0.45	0.15	0	0
High maintenance costs	0.1	2	0.2	0.1	4	0.4
Vulnerability	0.05	0	0	0.05	2	0.1
Low exploitation safety	0.1	0	0	0.1	1	0.1
Low flexibility	0.1	0	0	0.1	1	0.1
Weaknesses – total	1	-	2.8	1	-	1.2

Table 3

THE COMPARATIVE ANALYSIS OF OPPORTUNITIES						
Opportunities	Initial circuit			Proposed circuit		
	Ki	Ni	ni	Ki	Ni	ni
Attraction of investment funds for the energetic efficiency	0.15	2	0.3	0.15	4	0.6
Increasing demand of ecological products	0.15	2	0.3	0.15	4	0.6
Development of business	0.2	2	0.4	0.2	4	0.8
Increased market competitiveness by the reduction of costs	0.1	2	0.2	0.1	4	0.4
Promotion of clean technologies	0.1	2	0.2	0.1	4	0.4
Increased business profitability	0.25	2	0.5	0.25	4	1
Opportunities – total	1	-	1.9	1	-	3.8

Table 4

THE COMPARATIVE ANALYSIS OF THREATS						
Threats	Initial circuit			Proposed circuit		
	Ki	Ni	ni	Ki	Ni	ni
Degradation of energetic resources	0.1	4	0.4	0.1	2	0.2
Increasing exigencies of the sustainable development	0.15	5	0.75	0.15	2	0.3
Economic recession	0.25	3	0.75	0.25	3	0.75
Increasing prices of energy and fuels	0.15	4	0.6	0.15	2	0.3
Disadvantageous legislation	0.2	4	0.8	0.2	2	0.4
Global warming process	0.15	4	0.6	0.15	3	0.45
Threats – total	1	-	3.9	1	-	2.4

indicator (strengths, weaknesses, opportunities, threats) being 1.

In the tables 1 – 4 we have displayed the data obtained after the ranking of weaknesses and strengths, for both variants and the comparative analysis of opportunities and threats. In these tables K_i is the coefficient of relative importance that values between 0 and 1, and the sum of these coefficients for comparative analysis must equal 1.

The graph representation of the comparative analysis is presented in figure 3.

In order to analyze the level of hierarchy we have used the Likert scale, with notation with five values. Therefore N_i is the grade conferred by the specialists for every factor and has values included between 0 and 5. The value 0 signifies the fact that the respective indicator is not characteristic to that analysis, the
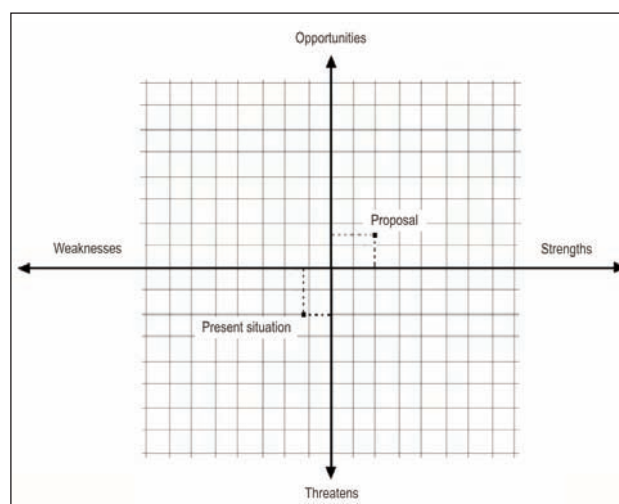
Fig. 3. The graph representation of the comparative analysis

Table 5

STRENGTHS, WEAKNESSES, OPPORTUNITIES AND THREATS		
Analyzed factor	**Present situation**	**Proposal**
Strengths total	1.6	3.2
Weaknesses total	–2.8	–1.2
Opportunities total	1.9	3.8
Threats total	–3.9	–2.4
S – W + OP – TH =	**–3.2**	**3.4**

value 1 – very weak level, and the value 5 – the highest level, the strongest indicator.

The third index used in this analysis, respectively ni – is the weighted value of the factors and it is obtained as a product between Ki and Ni.

Note: The notion of "very weak" or "very strong" has different significance for opportunities and strengths, than for weaknesses and threats. "Very weak" in the first case means bad, "very strong" is good; and vice-versa for the second case.

Table 5 shows the summarized results obtained by the processing of the data for the four indicators.

CONCLUSIONS

- All of the four categories of factors confirm the fact that the proposed solution is superior to that already existent. The strengths and opportunities are superior, the weaknesses and threats are inferior.
- The algebraic sum is, obviously, also favorable (–3.2 for the present solution and 3.4 for the proposed situation).
- An interesting analysis is the grouping on two axes, the horizontal $W – S$ and the vertical $O – T$.
- From a strategic point of view, every quadrant has different significance. Thus, the first quadrant suggests the most favorable situations, that turn into advantage the strengths and the opportunities, the second quadrant signifies the strategies that capitalize the opportunities and diminish the weaknesses, the third quadrant suggests the diminishing of weaknesses and of threats, because they are the strongest, and the fourth quadrant improves the strengths and diminishes the threats.
- We learn that the present technological solution is situated in the third quadrant, for which the weaknesses and threats prevail, while the proposed solution is situated in the first quadrant, where the strengths and opportunities are dominant.
- We also notice that the SWOT analysis is a very suggestive method for analyzing technological circuits and for formulating strategies to increase efficiency and to optimize the economic results of companies.

BIBLIOGRAPHY

[1] David, F. R. *Strategic management.* Fourth Edition, Macmillan Publishing Co., New York, 1997, p. 47

[2] Florescu, M., Visileanu, E. *Analiza statistică şi eficienţa participării României la proiecte europene.* In: Industria Textilă, 2012, vol. 63, issue 3, pp. 137–143

[3] Enache, E. *A Swot analysis on the waste management problem in Romania.* In: Theoretical and applied Economics, 2010, vol. XVII, issue 3, pp. 101 – 108

[4] Tudose, R. Z., Vasiliu, M. *Procese, operaţii şi aparate în industria chimică.* Editura Didactică şi Pedagogică, Bucureşti, 1977, pp. 239–258

[5] Pavlov, C. F., Romankov, P. G., Noskov, A. A. *Procese şi aparate în ingineria chimică. Exerciţii şi probleme.* Editura Tehnică Bucureşti, 1981, pp. 178–211

[6] Berariu, R., Butnaru, R., Condurache, Gh. *Studies on the possibilities of reducing thermal energy consumption in the production of cotton textiles.* In: Proceedings of the 7th International Conference Management of technological changes, 2011, Greece, pp. 345 – 347

[7] Berariu, R. *Studiul posibilităţilor reducerii consumului de energie termică de la finisarea materialelor textile celulozice.* Teză de doctorat, Universitatea Tehnică Ghe. Asachi, Iaşi, 2012

Authors:

ANCA BUTNARIU

GHEORGHE CONDURACHE

Universitatea Tehnică Ghe. Asachi

Facultatea de Textile-Pielărie şi Management Industrial

Bd. D. Mangeron nr. 53, 700050 Iaşi

e-mail: abutnariu@tex.tuiasi.ro

The combination of catalase and cellulase enzyme treatments with reactive dyeing process

ĞASSAN ASKER   ONUR BALCI

REZUMAT – ABSTRACT

Folosirea unor tratamente cu enzime de tipul catalazei şi celulazei în procesul de vopsire cu coloranţi reactivi

Scopul acestui studiu îl constituie studierea avantajelor combinării enzimelor de tip catalază şi celulază în procesul de vopsire cu coloranţi reactivi. În acest scop, au fost efectuate şase experimente diferite, pentru care s-au utilizat patru tipuri de coloranţi reactivi. Rezultatele au arătat că nu există diferenţe importante între procesele bazate pe combinarea de enzime şi procesul de referinţă, în ceea ce priveşte valorile CIELab şi performanţele rezistenţei vopsirii.

Cuvinte-cheie: catalază, celulază, CIELaB, bumbac, rezistenţa vopsirii, colorant reactiv

The combination of catalase and cellulase enzyme treatments with reactive dyeing process

The basic of the study consists of investigating the usage facilities of combining the catalase and cellulase enzymes with reactive dyeing process. For this aim, six different experiment sets were established. The experiments carried out using four different reactive dyes. As results, we found out that there were not any important differences between combined processes and reference one in terms of CIELab values and fastness performances.

Key-words: catalase, cellulase, CIELab, cotton, fastness, reactive dye

The change, development and globalization of the world have brought up new notions and developments in the textile sector. The number of features expected from textile products has increased due to changes in the buyers' expectations and their awareness of quality and environment [1].

Enzyme treatments have become one of the most common wet process techniques in the industry. In general, the enzyme technology has been applied to improve handle, appearance and other surface characteristic of cotton and cotton blends [1], [2].

Catalase is a common enzyme found in nearly all living organisms that are exposed to oxygen. It functions to catalyze the decomposition of hydrogen peroxide (H_2O_2) which is used in the scouring process in textile finishing to the water and the oxygen. The residual hydrogen peroxide on the surface of the textile material must be removed before dyeing. The main aim of the usage of the catalase enzyme in the pretreatment is to remove these kinds of residuals [9]. The catalase has one of the highest turnover numbers of all enzymes; one catalase enzyme can convert 40 million molecules of hydrogen peroxide to water and oxygen each second. The catalase is a tetramer of four polypeptide chains, each over 500 amino acids long. It contains four porphyrin heme (iron-Fe) groups that allow the enzyme to react with the hydrogen peroxide [3] – [7].

The cellulase enzymes used for the bio-polishing and the stone washing processes can be accepted as one of the most common applications. The commercial cellulase may contain mixtures of different cellulases, and the effects on the fabric properties depend on this composition.

There are several benefits resulting from the enzymatic bio-polishing of the cellulosic woven and the knitted fabrics:
- smoother surface;
- more attractive appearance;
- better pilling resistance;
- gentle and soft feel;
- improved drapability;
- the use of environment-friendly technology [8] – [10].

In this experimental study, we studied on the catalase and cellulase enzymes and the determination of the optimum combination conditions of cellulase, catalase enzyme treatments and reactive dyeing. In the literature, some studies are available about combining wet enzymatic processes or usage about cellulase or catalase enzymes in the different area such as using the bleaching effluent again for dyeing [11]. Different from these studies, we combined the processes after bleaching in one bath for different reactive dye. We did not applied catalase enzymes to the bleaching effluent and performed dyeing in this solution. In combined processes, we carried on catalase application with dyeing and cellulase application together. In this study, we established six different processes, and applied eight experiments for each process. As a result, we obtained 48 dyed specimens. After the experiments, we measured CIELab values of all specimens and calculated color differences. In addition, we applied some color fastness tests to the specimens.

MATERIALS AND METHODS

In the study, the single-jersey raw fabrics were knitted on a 30' E 28 fein circular knitting machine in the İSKUR Textile (Kahramanmaraş) and all wet processes were carried on the BİLKUR Textile. The density of the raw fabric is 24 courses/cm and 38 wale/cm. The mass per unit area of the fabric is 121 g/m^2.

The specimen was scoured in the bulk production with discontinue method. The scouring process was applied with wetting agent (0.8 g/L), sequestering agent (1 g/L), 48 Be° caustic soda (2 g/L), H_2O_2 (2 g/L) according to the graphic shown in figure 1. The catalase enzyme application was not applied to the fabric in the bulk production.

The knitted fabric was taken from the machine after scouring. The scouring process was carried on the conventional jet dyeing machine with 1/8 liquor ratio. Four types of reactive dyes used in the study are showed in table 1 and figure 2 as Reactive Yellow 176, Reactive Red 239, Reactive Blue 221 and Reactive Black 5 which are supplied from Denge Kimya (Turkey). The dyebath was prepared with 4% owf (shade) with Na_2SO_4 (70 g/l) and soda (20 g/l), applications were made in the laboratory dyeing machine at 1/8 liquor ratio (M/L). The catalase and cellulase enzyme treatments were carried out in the laboratory dyeing machine, manufactured by the ATAÇ Company (Turkey) which ensured continuous rotation. The whole catalase enzyme treatments were applied with 0.2% owf. The cellulase enzymatic bath was prepared with 1% and 1.6% acid cellulase enzyme supported from Rudolf & Duraner (Turkey) at 1/8 liquor ratio. The graphic of the enzymatic
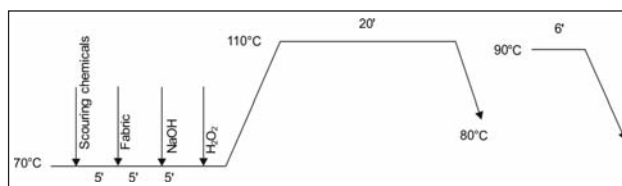
Fig. 1. The graphic of the scouring process

Table 1

EXPERIMENTAL DESIGN (48 EXPERIMENTS)				
Process, P	Specimen code	Reactive dyes	The anchor group of dye	Cellulase concentration, %
No enzyme	-	-	-	0.0
P_1 – reference	N_1	Reactive Black 5	VS	1.0
	N_2			1.6
P_2	N_3	Reactive Blue 221	VS	1.0
P_3	N_4			1.6
P_4	N_5	Reactive Red 239	MCT	1.0
P_5	N_6			1.6
P_6	N_7	Reactive Yellow 176	VS	1.0
	N_8			1.6

Reactive Black 5	Reactive Blue 221
Reactive Red 239	Reactive Yellow 176
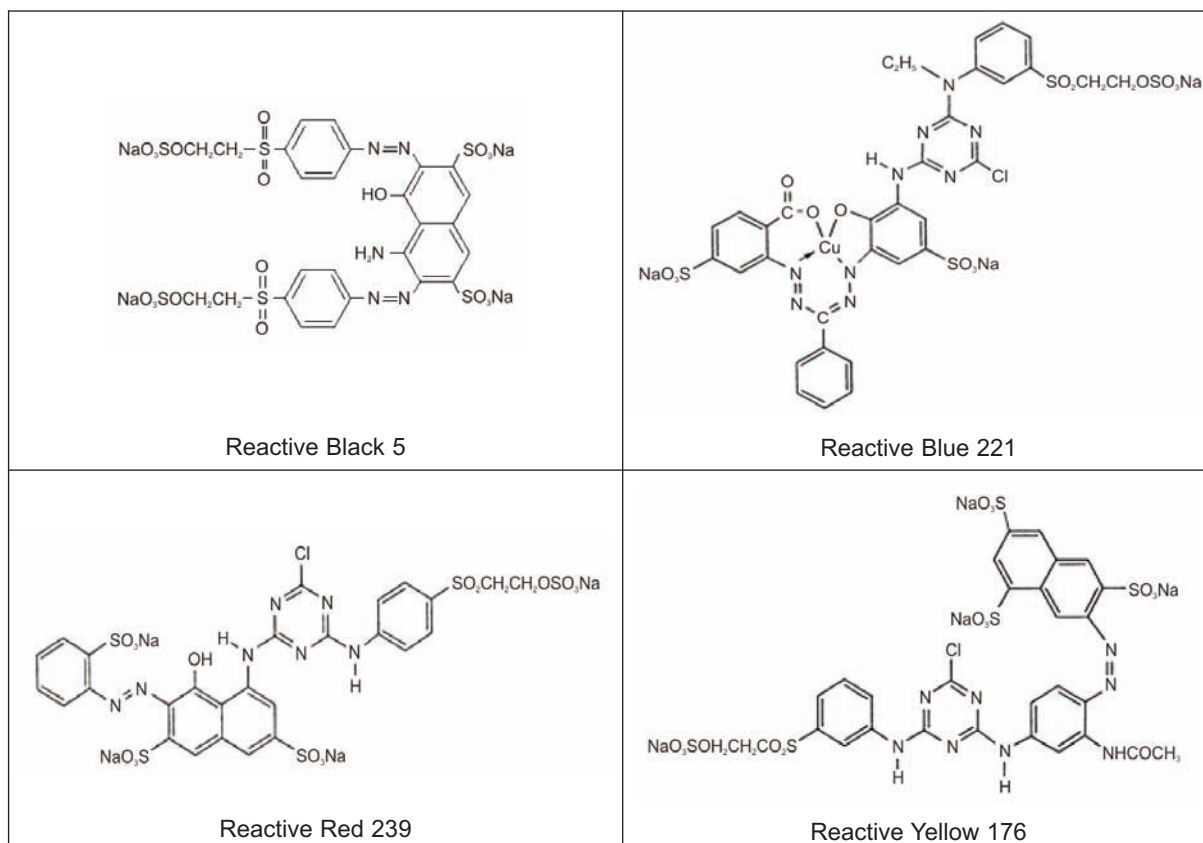
Fig. 2. The chemical structure of reactive dyes used in the study
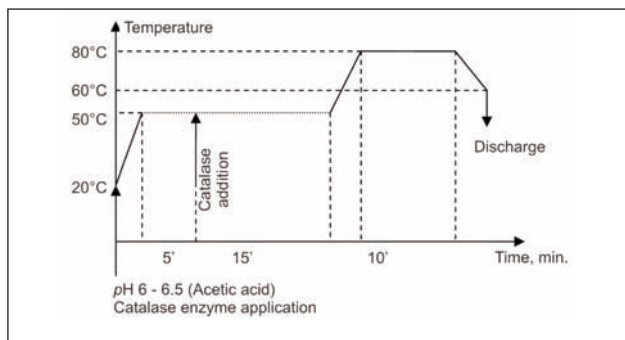
a
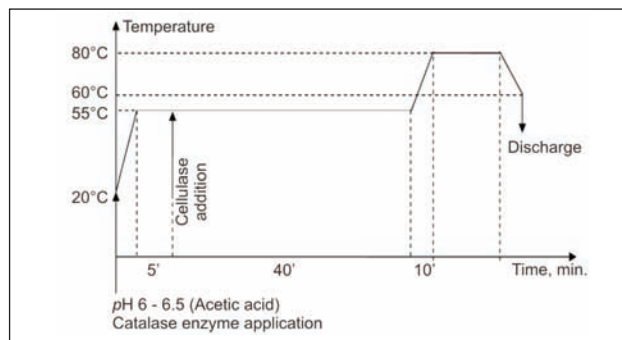
b

Fig. 3. Process P_1 – the graphic of the catalase and cellulase applications:
a – catalase application (*p*H 6 – 6.5); *b* – cellulase application (*p*H 5 – 5.5) + dyeing
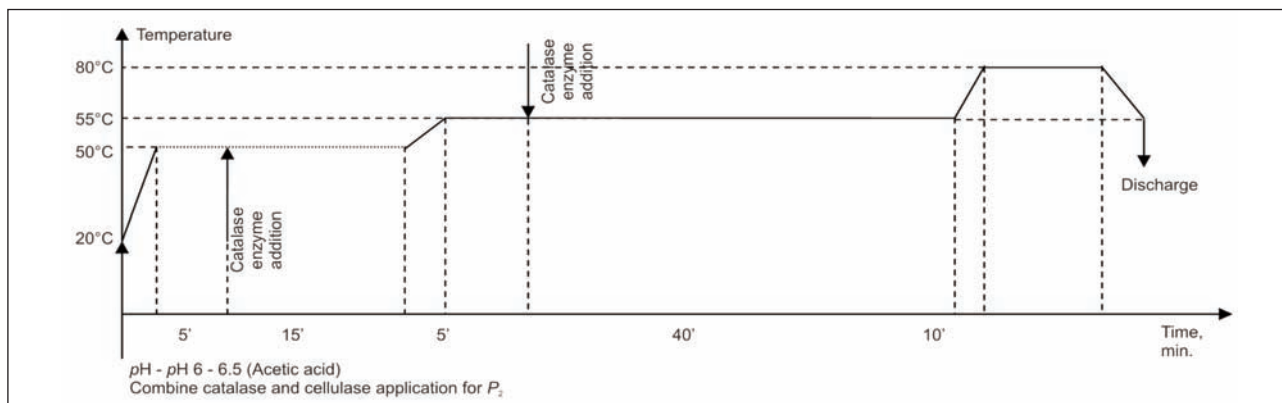
Fig. 4. Process P_2 – the graphic of the combined catalase and cellulase application:
P_2 – catalase and cellulase applications in the same bath – (two steps) – (*p*H 6 – 6.5) + dyeing
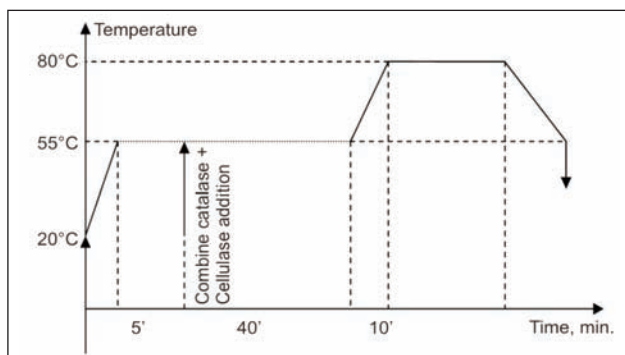
Fig. 5. The combined catalase and cellulase application
(single step) for P_3 and P_4:
P_3 – catalase and cellulase applications in the same
bath – (single step) – (*p*H 6 – 6.5) + dyeing;
P_4 – catalase and cellulase applications in the same
bath – (single step) – (*p*H 5 – 5.5) + dyeing

treatments can be seen in figures 3, 4 and 5 for $P_1 - P_2 - P_3 - P_4$, and the graphic of dyeing process of these specimens is shown in figure 6. The graphic of the process P_5 and process P_6 can be shown in figure 7. These processes can be named as completely combined process in this experimental study. The whole after treatment applied after dyeing was carried on according to the figure 8.

The condition of the processes used in the experimental study and sequence of the applications showed in table 1 and figures 3 – 8 can be summarized as follows:

P_1 – reference - catalase application (*p*H 6 – 6.5) + cellulase application – *p*H 5 – 5.5 + dyeing;

P_2 – catalase and cellulase applications in the same bath – two steps – *p*H 6 – 6.5 + dyeing;
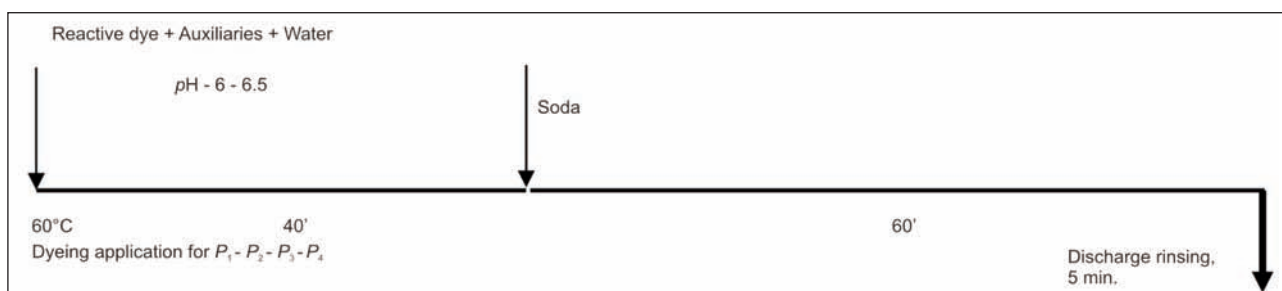
Fig. 6. The dyeing graphic for $P_1 - P_2 - P_3 - P_4$
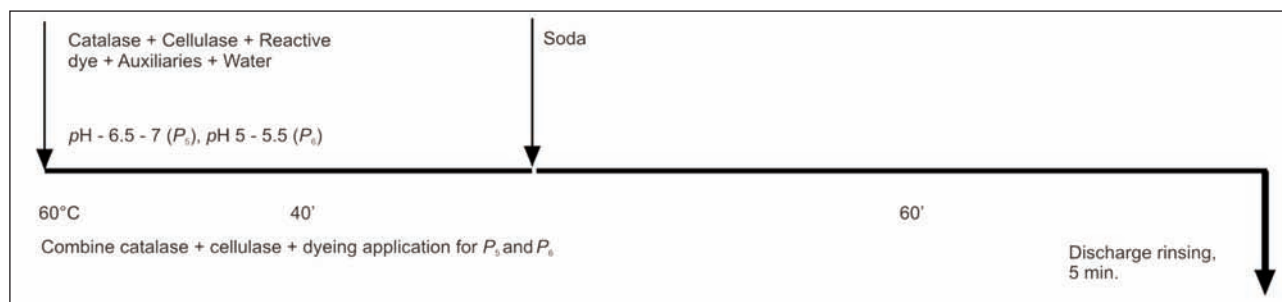
Fig. 7. The graphic of combined process for P_5 and P_6:
P_5 – catalase and cellulase and dyeing applications in the same bath – (single step) – (pH 6 – 6.5);
P_6 – catalase and cellulase and dyeing applications in the same bath – (single step) – (pH 5 – 5.5)
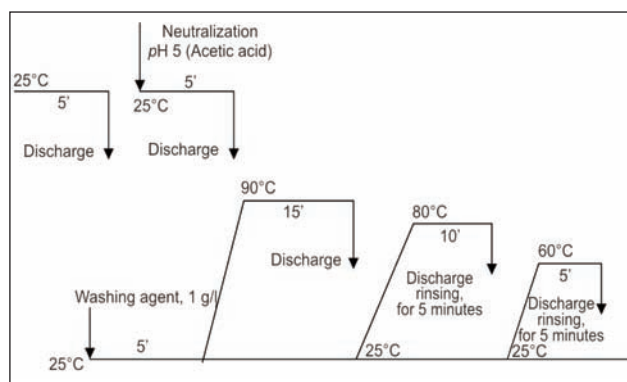
Fig. 8. The graphic of after treatment processes
for all applications

P_3 – catalase and cellulase applications in the same bath – single step – pH 6 – 6.5 + dyeing;
P_4 – catalase and cellulase applications in the same bath – single step – pH 5 – 5.5 + dyeing;
P_5 – catalase and cellulase and dyeing applications in the same bath – single step – pH 6 – 6.5;
P_6 – catalase and cellulase and dyeing applications in the same bath – single step – pH 5 – 5.5.

As it is known, catalase and acid cellulase enzymes having natural protein structures are produced by some organism such as fungal, plants, and catalyze some chemical reactions. These enzymes must be deactivated after the completion of the process into harmless form, and removed from the bath. The enzyme activity can be affected by several molecules. Inhibitors are molecules that decrease enzyme activity; activators are molecules that increase activity. Activity is also affected by temperature, chemical environment (e.g., pH), and the amount of the substrate (for example cotton fibre). Either the increasing of the process temperature above 80°C or fixing the pH above 10 are the best ways in order to deactivate the cellulase and catalase enzymes. In this context, in the study, the deactivation was performed by increasing the temperature above 80°C for $P_1 - P_2 - P_3 - P_4$ processes shown in the graphics. From this view, these approaches can bring extra operation for these processes, and increase the working time and energy consumption. However, in the P_5 and P_6, there were not any deactivation processes, because deactivation of the catalase and cellulase enzymes

could be achieved by increasing the pH of the bath above 10 (approximately 10.5) adding soda after 40 minutes duration.

The whole experimental study was replicated twice. After the experiments, the performances of the specimens were tested with measurement of the color fastness and CIELab values. In addition, we performed pilling and abrasion resistance tests in order to determine the physical properties of samples.

CIELab measurement. The colorimetric measurements were carried out using a DataColor SF 600 Plus spectrophotometer interfaced to a PC. Measurements were taken with the specular component of the light included (SCI) and the UV component excluded, using illuminant D_{65} and 10° standard observer. The samples were folded to ensure opacity and an average of three readings was calculated. We recorded L^*, a^*, b^*, C, $h°$ values of all samples. In addition, CIE "Δ" values between the samples obtained from P_1 (reference samples) and samples processed with $P_2 - P_6$ were calculated according to CIELab formulation (CMC 2:1) by software.

Pilling. The pilling resistance of the fabrics was determined using a Martindale pilling and abrasion tester, according to EN ISO 12945-2. We finished the test at 2 000 revolutions for two samples [12].

Abrasion. The abrasion character of the samples was measured using Martindale pilling and abrasion tester, according to EN ISO 12947-2 (the breakdown of the specimen) [13]. With the help of this analysis, we tried to determine the abrasion resistance performance of the surface of the knitted samples towards external mechanical effects.

Color fastness. In the study, the several fastness performances as color fastness to the washing, color fastness to water, color fastness to perspiration, color fastness to rubbing (wet) were measured according to TS EN ISO 105-CO6 [14], TS EN ISO 105-E01 [15], TS EN ISO 105-E04 [16], TS EN ISO 105-X16 [17], respectively. We recorded only staining result of the samples as fastness results. As a result, in this experimental study, we aimed to obtain new processes having minimum cost accessing the target color and fastness values without causing any change on the pilling and abrasion resistance performance.

Table 2

Parameters		CIELab values					Color differences CMC (2:1)			
Process	*Sample*	*L**	*a**	*b**	*C**	*h°*	*ΔL**	*ΔC**	*ΔH**	*ΔE*
P₁ – reference samples	N_1	17.96	−2.24	−11.87	12.08	259.28	*Ref.* *Other samples*			
	N_2	18.51	−2.31	−12.13	12.35	259.18	$P_1\,N_1\,[P_2\,N_1 - P_3\,N_1 - P_4\,N_1 - P_5\,N_1 - P_6\,N_1]$			
	N_3	29.24	1.57	−29.74	29.78	273.02	$P_1\,N_2\,[P_2\,N_2 - P_3\,N_2 - P_4\,N_2 - P_5\,N_2 - P_6\,N_2]$			
	N_4	28.74	1.55	−29.32	29.41	273.03	$P_1\,N_3\,[P_2\,N_3 - P_3\,N_3 - P_4\,N_3 - P_5\,N_3 - P_6\,N_3]$			
	N_5	38.05	58.30	4.21	58.45	4.14	$P_1\,N_4\,[P_2\,N_4 - P_3\,N_4 - P_4\,N_4 - P_5\,N_4 - P_6\,N_4]$			
	N_6	37.8	57.98	4.126	58.13	4.07	$P_1\,N_5\,[P_2\,N_5 - P_3\,N_5 - P_4\,N_5 - P_5\,N_5 - P_6\,N_5]$			
	N_7	66.14	37.11	76.64	85.15	64.16	$P_1\,N_6\,[P_2\,N_6 - P_3\,N_6 - P_4\,N_6 - P_5\,N_6 - P_6\,N_6]$			
	N_8	66.39	36.80	76.61	84.99	64.34	$P_1\,N_7\,[P_2\,N_7 - P_3\,N_7 - P_4\,N_7 - P_5\,N_7 - P_6\,N_7]$			
							$P_1\,N_8\,[P_2\,N_8 - P_3\,N_8 - P_4\,N_8 - P_5\,N_8 - P_6\,N_8]$			
P₂	N_1	18.60	12.13	−11.93	12.13	259.54	0.576	0.038	0.064	0.581
	N_2	18.07	−2.06	−11.63	11.81	259.92	−0.385	−0.407	0.183	0.589
	N_3	28.88	1.70	−29.82	29.87	273.26	−0.227	0.042	0.104	0.253
	N_4	29.11	1.57	−29.85	29.90	273.01	0.240	0.245	−0.011	0.343
	N_5	37.40	58.28	4.94	58.49	4.85	−0.346	0.015	0.396	0.526
	N_6	37.58	58.43	4.94	58.63	4.83	−0.116	0.185	0.421	0.474
	N_7	66.22	37.21	76.69	85.25	64.11	0.033	0.029	−0.053	0.069
	N_8	66.32	36.76	76.49	84.86	64.32	−0.028	−0.040	−0.018	0.052
P₃	N_1	18.22	−2.30	−11.65	11.88	258.83	0.237	−0.157	−0.111	0.305
	N_2	18.64	−2.32	−11.69	11.92	258.74	0.115	−0.324	−0.109	0.361
	N_3	29.09	1.49	−29.68	29.72	272.89	−0.097	−0.034	−0.061	0.12
	N_4	29.55	1.24	−29.54	29.56	272.41	0.521	0.079	−0.271	0.592
	N_5	38.14	58.98	4.84	59.18	4.69	0.049	0.266	0.308	0.410
	N_6	38.25	59.23	4.85	59.43	4.68	0.244	0.475	0.342	0.634
	N_7	66.74	36.40	76.26	84.51	64.48	0.239	−0.202	0.350	0.469
	N_8	66.67	36.42	76.42	84.66	64.51	0.111	−0.105	0.186	0.241
P₄	N_1	18.48	−2.12	−11.78	11.97	259.82	0.463	−0.086	0.133	0.489
	N_2	18.07	−2.11	−11.79	11.97	259.85	−0.386	−0.282	0.166	0.506
	N_3	28.98	1.67	−29.79	29.83	273.22	−0.222	0.025	0.085	0.239
	N_4	28.98	1.64	−29.77	29.82	273.16	0.156	0.205	0.056	0.264
	N_5	37.62	57.94	4.44	58.11	4.38	−0.228	−0.123	0.134	0.292
	N_6	37.63	57.78	4.27	57.94	4.23	−0.089	−0.069	0.089	0.144
	N_7	66.28	36.74	77.09	85.39	64.51	0.058	0.075	0.388	0.400
	N_8	66.03	37.07	76.52	85.02	64.14	−0.145	0.010	−0.211	0.257
P₅	N_1	17.17	−1.69	−11.35	11.47	261.51	−0.706	−0.469	0.538	1.004
	N_2	17.6	−1.762	−11.36	11.50	261.18	−0.793	−0.643	0.486	1.131
	N_3	27.87	1.86	−29.30	29.36	273.62	−0.867	−0.214	0.259	0.930
	N_4	28.75	1.54	−29.40	29.44	273.00	0.004	0.017	−0.014	0.023
	N_5	36.59	58.02	6.13	58.34	6.03	−0.781	−0.040	1.046	1.306
	N_6	36.62	57.68	6.16	58.18	6.08	−0.634	0.018	1.110	1.278
	N_7	65.29	37.83	77.15	85.93	63.87	−0.340	0.242	−0.315	0.523
	N_8	65.49	38.19	77.42	86.33	63.74	−0.360	0.418	−0.657	0.858
P₆	N_1	17.94	−1.93	−11.55	11.71	260.50	−0.018	−0.289	0.296	0.414
	N_2	17.99	−1.92	−11.66	11.82	260.62	−0.448	−0.401	0.354	0.698
	N_3	29.77	1.22	−29.89	29.92	272.34	0.303	0.066	−0.301	0.433
	N_4	30.17	1.19	−29.90	29.93	272.28	0.914	0.261	−0.333	1.008
	N_5	37.61	58.53	5.28	58.77	5.15	−0.237	0.118	0.566	0.625
	N_6	37.55	58.24	5.05	58.46	4.96	−0.130	0.123	0.493	0.524
	N_7	65.67	37.54	76.88	85.55	63.97	−0.188	0.125	−0.209	0.308
	N_8	66.21	36.96	76.28	84.77	64.15	−0.071	−0.071	−0.211	0.233

RESULTS OBTAINED

Pilling and abrasion resistance

In the pilling test, the Martindale instrument was operated till 2 000 revolutions for all samples (enzyme treated and untreated/1 sample). In order to evaluate the effect of cellulase enzyme on the pilling behavior, we tested both enzyme treated $P_1 - P_6$ and untreated samples (not dyed, only pretreated).

The pilling rate of the untreated samples was 3/4. As it is known, the cellulase enzyme is generally used for biopolishing process in order to improve pilling rate. After the evaluation of these results, it was determined that pilling resistance ratings of the all enzyme treated samples $P_2 - P_6$ were similar to each other, and there was no significant difference between them. According to the qualitative analysis, the rate of the pilling was observed 4/5 for all samples. When the results were investigated in detail for the specimens processed by 1.6% cellulase enzyme, we observed that the forming of the pill on the surface was similar with each experiments; however, the tendency of the fuzzy fiber was less than other applications. In addition, we applied the abrasion resistance test to the specimens in order to display the surface characteristic and mechanical resistance of samples. We accepted the breaking of the two yarns from the surface as criteria. According to the test results, we did not found out any breakage on the fabric surface even after 25 000 revolutions of the test machine.

Thereby, we found out that the new enzyme processes $P_2 - P_6$ did not cause any extra negative difference on the surface of the fabric in terms of the pilling and abrasion resistance performances, when we compared the conventional one P_1.

CIELab values and fastness results

In order to discuss the success of the new developed processes; we should not display change on the CIELab values and fastness results. After the application of the new processes, the CIELab values of the samples should not show differences over the accepted tolerance limits [18].

The whole color measurement values and the calculated color difference values can be seen in table 2. While calculating the color difference values, we accepted the samples produced by process P_1 as reference because it was known as conventional enzymatic application. According to the table 2, it was seen that the CIELab values showed differences after enzymatic applications depending on the process condition and type of the reactive dye.

Beside the experimental study and the results, investigated parameters and statistical contribution of each factor to the total color difference value, ΔE, were discussed using the ANOVA (the analyze of variance). The results were evaluated at 5% significance level by Design-Expert Trial version [19]. The ANOVA results can be seen in table 3. While analyzing of the ANOVA results are being made, we focus on F and p values. F and p values get bigger and less respectively, the significance contribution of the investigated factors on the variance increases. Especially, the p values must be less than 0.05 in order to define the factor as statistically significant. According to the table 3, it was clear that all established models were significant. In addition, the R^2 values of these models were satisfied. These data clearly showed the reliability of our experimental design. It was determined that the A and B main factors had significant effect on the total color difference value, while C had not any significant effect. According to the table 3, the process (factor A) was the most effective factor, and the concentration of the enzyme (factor C) did not have significant effect on the output, individually. However, it can be seen from table 3 that concentration of the enzyme has significant effect depending on the type of the reactive dye. It means that the effect of the factor C on the ΔE output can be seen at the $B \times C$ interaction. Some double interactions also seem as effective factor on the total color difference value. In this respect, $A \times B$ and $B \times C$ are the effective interactions.

For this experimental study, these tolerances were accepted as ±1, ±0.6, ±0.6 and +1 for ΔL^*, Δa^*, Δb^*

Table 3

THE ANOVA RESULTS				
Factors	***F* value**	***p* value**	**Significance**	**Contribution, %**
Model	8.54	0.0003	Significant	-
A process	37.73	< 0.0001	Significant	59.93
B color strength	10.58	0.0014	Significant	13.14
C the concentration of enzyme	3.37	0.0933	Insignificant	-
A × *B*	2.96	0.0412	Significant	14.48
A × *C*	1.59	0.2438	Insignificant	-
B × *C*	3.47	0.0490	Significant	4.32
R value	0.95			
Adjusted *R* value	0.84			

Table 4

Process	Sample	Washing			Perspiration						Water			Rub-bing, wet
		Secon-dary acetate	Cotton	Poly-ester	Secondary acetate		Cotton		Polyester		Secon-dary acetate	Cotton	Poly-ester	
					Ac	Al	Ac	Al	Ac	Al				
$P_1 -$ reference	N_1	4/5	4/5	4/5	4/5	4/5	4	4	4	4	4/5	4/5	4/5	3
	N_2	4/5	4/5	4/5	4/5	4/5	4	3/4	4	4	4/5	4/5	4/5	2/3
	N_3	4/5	3/4	4/5	4/5	4	3	1/2	3/4	3/4	4/5	4	4/5	4
	N_4	4/5	3/4	4/5	4/5	4	2	2	3	3/4	4/5	4	4/5	3/4
	N_5	5	4	4/5	5	5	2	2/3	3	3/4	4/5	3/4	4	3
	N_6	4/5	4	5	5	5	2	2	3	3	4/5	3/4	4	4
	N_7	4/5	4/5	5	5	5	5	5	5	5	4/5	4/5	4/5	4
	N_8	4/5	4/5	4/5	5	5	5	5	5	5	4/5	4/5	4/5	4
P_2	N_1	4/5	4/5	4/5	5	5	4	4	4	4/5	4/5	4	4/5	2/3
	N_2	4/5	4/5	4/5	5	5	4	4	4	4/5	4/5	4	4/5	2/3
	N_3	4/5	3/4	4/5	4/5	5	3	2/3	4	4	4/5	4	4/5	3/4
	N_4	4/5	3/4	4/5	4/5	5	3/4	2/3	4	4	4/5	4	4/5	3/4
	N_5	4/5	4	4/5	5	5	3	3	4	3/4	4/5	3	4	3/4
	N_6	4/5	4	4/5	5	5	2/3	3	4	4	4/5	3	4	3/4
	N_7	4/5	4/5	5	5	5	4/5	5	5	5	4/5	4/5	4/5	4/5
	N_8	4/5	4/5	5	5	5	5	5	5	5	4/5	4/5	4/5	4
P_3	N_1	4/5	4/5	4/5	5	5	4	3/4	5	4/5	4/5	4/5	4/5	2/3
	N_2	4/5	4/5	4/5	5	5	4	4	5	4/5	4/5	4/5	4/5	3
	N_3	4/5	3/4	4/5	5	5	2/3	1/2	4	4	4/5	4	4/5	3/4
	N_4	4/5	3/4	4/5	5	5	2/3	2/3	4	4	4/5	4	4/5	3/4
	N_5	4/5	4	4/5	5	5	2/3	2/3	4	3/4	4	3	3/4	3
	N_6	4/5	4	4/5	5	5	2/3	3	4	4	4	3	4	3
	N_7	4/5	4/5	5	5	5	5	5	5	5	4/5	4/5	5	4
	N_8	4/5	4/5	5	5	5	5	5	5	5	4/5	4/5	5	4
P_4	N_1	4/5	4/5	5	5	5	4	4/5	4	4/5	4/5	4/5	4/5	2
	N_2	4/5	4/5	5	5	5	4	4/5	4	4/5	4/5	4/5	5	2/3
	N_3	5	3/4	4/5	5	5	1/2	1	3/4	3/4	4/5	4	4/5	3/4
	N_4	4/5	3/4	5	5	5	2	2	3/4	4	4/5	4	4/5	3
	N_5	4/5	4	4/5	5	5	3	3/4	3/4	4	4/5	3/4	4	2/3
	N_6	4/5	4	4/5	5	5	3	4	3/4	4/5	4/5	3/4	4	3
	N_7	4/5	5	5	5	5	5	5	5	5	4/5	4/5	5	3/4
	N_8	4/5	5	5	5	5	5	5	5	5	5	4/5	5	3/4
P_5	N_1	4/5	4/5	4/5	5	5	3/4	3/4	3/4	4/5	4/5	4/5	5	2/3
	N_2	4/5	4	4	5	5	3/4	3/4	3/4	4/5	4/5	4/5	5	3
	N_3	4/5	3	4/5	5	5	1	1	3	4	4/5	4	4/5	4
	N_4	4/5	3	5	5	5	1/2	1	3	4	4/5	4	4/5	3/4
	N_5	4/5	4	4/5	4	5	2/3	3	3	3/4	4	3	4	2/3
	N_6	4/5	4/5	4/5	5	5	2/3	3	3/4	3/4	4	3	4	2/3
	N_7	4/5	4/5	5	5	5	5	5	5	5	5	4/5	5	4
	N_8	4/5	4/5	5	5	5	5	5	5	5	4/5	4/5	5	4
P_6	N_1	4/5	4/5	5	4/5	5	4/5	4	4/5	4/5	4/5	4/5	4/5	3
	N_2	4/5	4/5	4/5	5	5	4	5	4/5	5	4/5	4	4/5	2/3
	N_3	4/5	3/4	5	5	5	2/3	2/3	4/5	4/5	4/5	4	4/5	3
	N_4	4/5	4	5	5	5	2/3	2	4/5	4/5	4/5	4	4/5	3/4
	N_5	4/5	4	4/5	5	5	3	3	4	4/5	4/5	3	4	3
	N_6	4/5	4	4/5	5	5	3	3	4	4/5	4	3	4	2/3
	N_7	4/5	4/5	5	5	5	5	5	5	5	5	4	4/5	4
	N_8	4/5	4/5	5	5	5	5	5	5	5	5	4	4/5	4

THE FASTNESS RESULTS OF THE SAMPLES

and ΔE, respectively. According to the table 2, it was found out that while ΔL^*, ΔC^* and ΔH^* values were among the accepted tolerance limits, ΔE values of the samples produced with process P_5 was above the limit value. It was also seen that the samples obtained with process P_4 had the closest CIELab values to the reference process P_1. It was thought that the similarity of the pH condition (pH 5 – 5.5) of the process P_4 and reference process P_1 could be showed the reason of this result. In terms of the production cost, the process P_5 and the process P_6 were seen the most advantageous ones. When we analyzed process P_5 and process P_6, P_5 had negative effect on the CIELab values; however we did not determine similar results for P_6 because the pH value (pH 5 – 5.5) of this process was the most suitable for the acid cellulase enzyme activity. Therefore, it could be said that P_6 was the optimum process in terms of CIELab values. In addition, when the results were analyzed, different color sensibility was determined for the reactive dyes used in the study depending on the interaction between pH values of the process and reactive groups of the dyes.

The fastness results of the whole samples are given in table 4. In this table, we analyzed the stain values on the secondary acetate, cotton and polyester pieces of the multifiber. According to the table 4, the fastness performance of the samples showed differences according to the reactive dye used in the experimental study and new developed enzymatic processes.

When the results of the color fastness to the washing were investigated, the concentration of the enzyme was not seemed as an important factor. When the results of the fastness tests for samples obtained from P_1 were compared with $P_2 – P_6$ we could not find out any crucial difference. We determined similar results for the performance of the color fastness to the washing. We did not recognize important changes after the application of the new enzymatic process for color fastness to the both washing and water.

We determined some changes for the performance of the color fastness to the rubbing. According to the table 4, the performances of the rubbing fastness generally displayed decrease depending on the type of the reactive dye, the enzymatic processes and the concentration of the cellulase enzyme used in the processes. The most decrease was measured for the samples obtained by P_4. The least change on the fastness values was determined for the samples processed by P_2 in which process conditions were approximately same with P_1 in terms of the pH and the temperature. This state showed us the effect of the process pH. While the fastness performance of the processes applied on pH 6.5 – 7 did not show crucial changes, on the contrary, the new established enzymatic processes having pH 5 – 5.5 caused bigger decrease according to the others.

In addition, we found out effect of the type of the reactive dye on the rubbing fastness result. Reactive Black 5, Reactive Blue 221, Reactive Yellow 176 and Reactive Red 239 have VS and MCT reactive group, respectively. In the study, we generally determined the worst rubbing fastness results for the samples N_5 and N_6 dyed using Reactive Red 239 in which reactive group was MCT as different from the other reactive dyes. According to this result, it was possible to mention about the sensitivity of the Reactive Red 239 to the new developed enzymatic processes.

When the results of the color fastness to the perspiration were investigated, first of all, we got satisfactory fastness results for the stain performance on the secondary acetate. In addition, we found out the decrease on the fastness performances for the samples applied by P_4 and P_5 processes.

DISCUSSIONS

In the study, we tried to bring new approach to the cellulase enzymatic treatments of the cellulose based knitted fabric. We established novel wet processes which could decrease the cost of the enzymatic treatment without causing any negative change on the fabric performance.

When the results were investigated from this point of view, the pilling performances and abrasion resistances of the fabrics did not reduce depending on the enzymatic processes and their working conditions. According to these results, we decided to attend experimental study and measured the CIELab values and fastness performances of the all samples. The CIELab values of the new samples did not show crucial differences out of the accepted tolerances when they were compared with the reference ones (P_1 samples) except the samples obtained by P_5 process. In addition, it was found out that the fastness performances displayed similar tendency with the color measurement results.

Therefore, as a conclusion, when we realized whole results, it was clear that P_6 significantly had optimum process conditions in terms of the cost and the quality performances, because all wet processes after the pretreatment as cellulase-catalyze enzymatic applications and reactive dyeing could be combined in single application and bath.

BIBLIOGRAPHY

[1] Özdil, N., Özdoğan, E., Öktem, T. *Effects of enzymatic treament on various spun yarn fabrics.* In: Fibres & Textiles in Eastern Europe, 2003, vol. 43, issue 11–4, pp. 58–61

[2] Yang, C. Q., Zhou, W., Lickfield, G. C., Parachura, K. *Cellulase treatment of durable press finished cotton fabric: effects on fabric strength, abrasion resistance and handle.* In: Textile Research Journal, 2003, vol. 73, issue 12, pp. 1 057–1 062

[3] Chelikani, P., Fita, I., Loewen, P. C. *Diversity of structures and properties among catalases*. In: Cellular and Molecular Life Sciences, 2004, vol. 61, issue 2, pp. 192–208

[4] Maehly, A., Chance, B. *The assay of catalases and peroxidases*. In: Methods of Biochemical Analysis, 1954, issue 1, pp. 357–424

[5] Verenich, S., Arumugam, K., Shim, E., Pourdeyhimi, B. *Treatment of raw cotton fibers with cellulase for nonwoven fabrics*. In: Textile Research Journal, 2008, vol. 78, issue 6, pp. 540–548

[6] Balci, O., Gençer, U. *Cellulase enzyme application for the cotton based woven fabrics.* Part I. *Determination of effect of enzyme on the performance*. In: Industria Textilă, 2013, vol. 64, issue 1, pp. 20–26

[7] Balci, O., Gençer, U. *Cellulase enzyme application for the cotton based woven fabrics.* Part II. *The determining of necessity and cellulase enzyme application sequence in the finishing process*. In: Industria Textilă, 2013, vol. 64, issue 2, pp. 80–88

[8] Rousselle, M. A., Bertoniere, N. R., Howley, P. S., Goynes, W. R. *Effect of whole cellulase on the supramolecular of cotton cellulose*. In: Textile Research Journal, 2002, vol. 72, issue 11, pp. 963–972

[9] Ciechanska, D., Kazimierczak, J. *Enzymatic treatment of fibres from regenerated cellulose*. In: Fibres & Textiles in Eastern Europe, 2006, vol. 55, issue 14–1, pp. 92–95

[10] Tzanov, T., Costa, S., Guebitz, M. G., Paulo, C. A. *Dyeing in catalase-treated bleaching baths*. In: Coloration Technology, 2011, vol. 117, pp. 1–5

[11] Tzanov, T., Costa, S., Guebitz, M. G., Paulo, C. A. *Effect of temperature and bath composition on the dyeing of cotton with catalase-treated bleaching effluents*. In: Coloration Technology, 2001, vol. 117, pp. 166–170

[12] TS EN ISO 12945-2. *Textiles – determination of fabric propensity to surface fuzzing and to pilling*. Part 2: Modified Martindale method (ISO 12945-2:2000), 2002

[13] TS EN ISO 12947-2. *Textiles- Determination of abrasion resistance of fabrics by the Martindale method*. Part 2: Determination of specimen breakdown, 2001

[14] TS EN ISO 105 C06. *Test for colour fastness*. Part C06: Colour fastness to domestic and commercial laundering, 2001

[15] TS EN ISO 105-E04. *Textiles – Tests for colour fastness*. Part E04: Colour fastness to perspiration, 2006

[16] TS EN ISO 105-E01. *Textiles – Tests for colour fastness.* Part E01: Colour fastness to water, 2006

[17] TS EN ISO 105-X16. *Textiles–test for colour fastness.* Part X16: Colour fastness to rubbing-small areas, 2003

[18] Oğulata, R. T., Balcı, O. Effects *of extra washing after treatments on fastness and spectrophometric properties of dyed PET/viscose/elastane fabric*. In: The Journal of Textile Institute, 2007, vol. 98. issue 5, pp. 409-419

[19] Myers, R. H., Montgemery, D. C. *Response surface methodology: Process and product optimization using designed experiments*. Second edition, 2002, pp.17–21, A Wiley-Interscience Publication

Authors:

ĞASSAN ASKER
ONUR BALCI
The Department of Textile Engineering
The University of Kahramanmaraş Sütçü İmam
Avşar Campus
46100 Kahramanmaraş – Turkey

Corresponding author:

ONUR BALCI
e-mail: obalci@ksu.edu.tr; obalci80@hotmail.com

Analysis and improvement of nocturnal enuresis alarm system

INESE PARKOVA   ANDIS UŽĀNS
ALEKSANDRS VALIŠEVSKIS   AUSMA VIĻUMSONE

REZUMAT – ABSTRACT

Analiza și perfecţionarea sistemului de alarmă pentru enurezis nocturn

Enurezisul nocturn este o problemă des întâlnită în întreaga lume, având o prevalenţă foarte ridicată la populaţia preşcolară și o scădere lentă pe parcursul copilăriei. Există câteva tratamente pentru rezolvarea acestei probleme, unul dintre acestea fiind alarma de enurezis, o metodă primară şi eficientă de tratare a enurezisului nocturn la copii. În lucrare sunt prezentate diferite sisteme de alarmă – senzori de umezeală plasaţi pe pat, senzori de umezeală purtabili cu fir, senzori de umezeală purtabili fără fir, precum și avantajele şi dezavantajele acestora. S-au analizat atât modul de funcţionare şi construcţie, cât şi tehnologia de ataşare şi amplasare a unităţilor şi senzorilor de alarmă în obiectele de îmbrăcăminte. În acest studiu sunt prezentate date privitoare la sistemele de alarmă de enurezis, din punct de vedere al confortului şi siguranţei, precum şi recomandări de perfecţionare a proiectării senzorului şi a unităţii de alarmă.

Cuvinte-cheie: enurezis nocturn, sistem de alarmă, confort, fire conductoare

Analysis and improvement of nocturnal enuresis alarm system

Nocturnal enuresis is a common problem throughout the world, it has a very high prevalence in the preschool population and the prevalence slowly falls during childhood. Several therapies exist to solve this problem, one of them being the enuresis alarm, which is a primary and effective nocturnal enuresis treatment method for children. In the paper different alarm systems were summarized: pad-and-bell alarms, wearable wired alarms and wearable wireless alarms, analyzing its advantages and drawbacks. Operation and construction as well as attachment technology and placement in the garment of alarm units and sensors have been explored. This study describes issues related to enuresis alarm systems from the comfort and safety point of view, as well as recommendations for improvement of sensor and alarm unit design.

Key-words: nocturnal enuresis, alarm system, comfort, conductive threads

Bedwetting or nocturnal enuresis is a common problem. Statistical data shows that a significant number of children and teens suffer from nocturnal enuresis. Different approaches towards the treatment of enuresis are being studied – alarm systems are compared to non-treatment and to drug therapies, as well as to combined therapies, analyzing their efficiency and decrease in wetting frequency [1]. The aim of this research is to summarize available nocturnal enuresis alarm systems, to analyze advantages and drawbacks: to compare modules of the systems from the point of view of comfort and efficiency, by analyzing their design, materials and usage convenience. As a result, options for improving the existing alarm systems are proposed, which ensure a more comfortable use of the product.

ENURESIS – DEFINITION OF THE PROBLEM

Nocturnal enuresis or bed-wetting is intermittent incontinence during sleep of children after age of 5 years [2]. This problem affects about 15–20% five year old children and have tendency to decrease by age: it affects 5–10% of seven year olds and about 2% eighteen year olds [3]. Nocturnal enuresis is a condition which is related with psychosocial consequences and may precipitate wide range of behavioral and developmental problems and decreased quality of life. Psychosocial problems have been reported to 40% of affected children. Emotional and behavioral problems [4], social difference and restricted peer relationships are observed.

Causes of enuresis

Nocturnal enuresis can be caused by many factors, it is affected by genetic, physiological and psychological causes. Most often this issue is transmitted genetically. The mode of inheritance is autosomal dominant so if both parents were enuretic as children, the risk for their offspring is 77%, while if only one parent had NE, the risk is about 45% [5].

In paper [6] it is mentioned that the conventional paradigm for bed-wetting presumes three factors: disorder of sleep arousal, nocturnal polyuria and a reduced nocturnal bladder capacity. Upper airway obstruction is another cause of nocturnal enuresis. Behavioral factors predisposing enuresis are excessive fluid intake and inappropriate toilet training. Heterogeneity of enuresis is still topic of research.

Treatment methods

There are several approaches towards the reduction of bed-wetting, for example, reducing the fluid intake during the second half of the day and no liquid intake before going to bed, going to the toilet before going to bed, waking the child at night for repeated

urination and so on. This can reduce the number of bed-wetting, but it does not eliminate the issue completely.

Nocturnal enuresis treatment options include pharmacological and non-pharmacological methods.

Pharmacological methods. Enuresis can be treated with regular drug use, but the effect will only last as long as the drug is used. When it is stopped, the bedwetting often recurs. Besides that, drugs can have adverse effects on child's body – drugs that are commonly used in the treatment of enuresis contain either antidepressants (high doses are harmful) or synthetic hormones, which reduce the amount of urine in the kidneys during sleep (can cause side effects such as headache or abdominal pain or interfere with the proper balance of the body fluids) [6], [7].

Non-pharmacological methods. One of the non-pharmacological methods is the use of a bed-wetting alarm system. In practice this therapy is used both as a monotherapy and in combination with pharmacological methods.

The alarm awakens the child when bed-wetting starts, the child gets out of bed and finishes voiding in the toilet. With time a successful therapy results in a child learning to wake up by himself, when his bladder is full. Child's involvement and a desire to solve the issue are important for this therapy. It is therefore important that the system is convenient, its use does not hinder the child and does not constitute a psychological barrier. Alarm treatment is more effective if strong support is given to child and family and it makes treatment less uncomfortable. Several studies have shown higher results when psychological or educational training is used with alarm therapy.

ANALYSIS OF EXISTING ENURESIS ALARM SYSTEMS

There are several types of enuresis alarm systems available:
- pad-and-bell alarms;
- wearable wired alarms;
- wearable wireless alarms.

Operation and construction of Pad-and-bell alarms

Pad-and-bell alarms are bed-based, with the child sleeping on a pad or mat containing an electrical

Table 1

COMMERCIALLY AVAILABLE PAD-AND-BELL ALARMS			
Type of product	Pad parameters, cm	Material of pad	Material of sensor
Malem bed-mat	54 × 42	plastic	foil
Tunstall enuresis sensor	9.5 × 16 × × 3.5	plastic	foil
Wet call bed-side bed wetting alarm	47 × 62	polyethylene foam	conductive vinyl sheets
Sleep-free digital childcare system	-	breathable and water-resistant material	-

circuit. A bell rings if urine is contacting the electrical circuit. Usually bed-mat is made out of waterproof plastic material, in which conductive (copper, foil etc.) material is embedded in a comb-like manner. It detects wetness by measuring the change in resistance when the sheet is wet [9]. Some of the commercially available examples are summarized in table 1.

The mat is placed between mattress and bed sheet. In order to ensure that humidity gets to the sensor faster, perforated sheet can be used as a top layer. A mat is connected to the alarm unit with a wire and as soon as urine gets on the conductive surface, the alarm unit activates. The vibrating alarm can be placed under the pillow and the sound alarm placed near the bed. Some models allow recording a personalized message or sounding [10]. Examples of mats are shown in figure 1.

In study [9] humidity sensor was used, which consists of conductive threads sewn onto a layer of absorbent paper covered by a thin layer of biodegradable polyethylene. But it is intended for single use only.

Operation and construction of wearable alarm systems

Wearable wired alarms are body-worn alarms where the small sensor is attached to the child's pants and the alarm is worn on the pajamas top. The sensor is located closer to the child's body than it is in a pad-and-bell model, so it can detect bed-wetting quicker. In the wireless version of alarm system a sensor
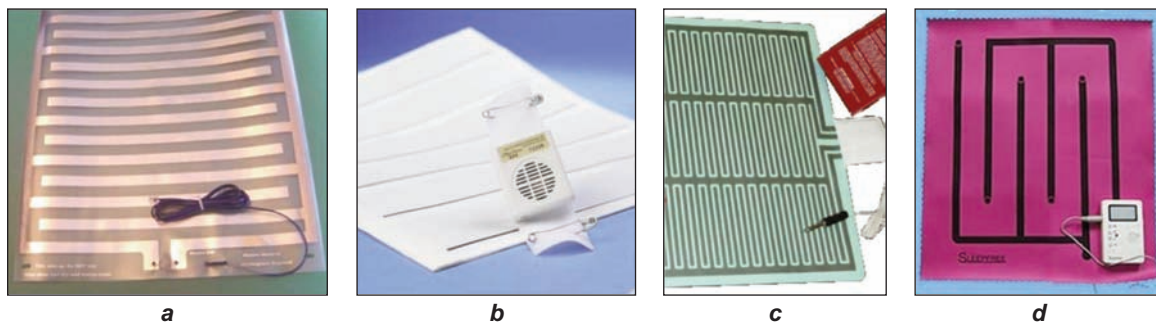

| *a* | *b* | *c* | *d* |

Fig. 1. Commercially available pad-and-bell alarms:
a – Malem; *b* – Wet call bed-side; *c* – Astric dry-bed; *d* – Crazeal sleep free
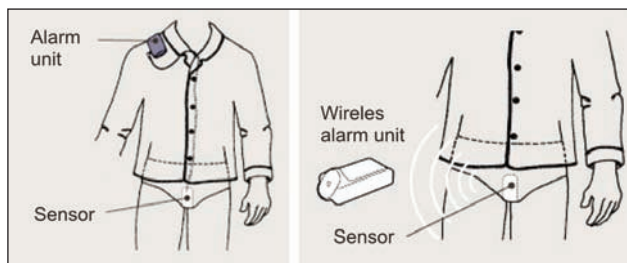
Fig. 2. Operating principle of wired and wireless system

communicates with the alarm by a radio signal. In this case the sensor dimensions are greater, since the sensor system includes a transmitter and a battery. Consequently, the sensor unit shall be completely isolated, which gives it additional stiffness [11].

There are different variants of wearable enuresis alarm systems, but operating principle of all such systems is similar, however they differ in arrangement of elements and in their dimensions, materials, connection technology, sensor and alarm unit communication and signaling type, comfort level etc. Operating principle of wired and wireless systems is shown in figure 2.

Alarm unit placement and attachment

Electronic components of bed-wetting alarm unit are contained in a small plastic box, which is attached to child's pajamas or briefs and signals using an acoustic, light and/or vibrating alarm. In the case of a wireless alarm unit, it can be placed on a table. If the system has a separate vibrating module, it can be placed under the pillow or beneath bed sheet. Alarms equipped with a buzzer are suitable for children who do not respond to an alarm sound or for households in which an alarm disrupts the sleep of others [9]. Some of the commercially available wearable alarm units are summarized in table 2.

Placement of the alarm unit can vary, the module is attached to a collar, a pocket, trousers waistband or elsewhere, depending on the attachment type. Most often it is attached near the ear, so that the acoustic signal could be heard better. There are also alarm units, which use an earphone alarm for privacy and better perception [13], but prolonged use of such headphones can cause discomfort. In some cases, the alarm unit is worn on the wrist like a wrist watch. Alarm unit is attached to the clothing with a magnetic or mechanical clip, Velcro tape, press studs or safety needle. It is important that the child makes some effort in order to deactivate the alarm, so that he wakes up as the result. In this sense, wireless modules are more effective, since the alarm unit can be placed further away from the bed.

Sensor type and design

Sensor of wearable alarm system operates by the same principle as a pad-and-bell alarm: it detects wetness by measuring the change in resistance when the surface is wet [9]. Generally two types of sensors are available: electrodes encased in silicone rubber or in plastic module. Some of the alarm system unit examples are summarized in table 3.

Insertable modular sensors are relatively bulky and uncomfortable to wear, especially the ones with the plastic casing. The silicon-based sensors are flexible, but they also can be felt, especially if the sensor is placed between two closely adjacent briefs. This being the main reason why a child will ultimately refuse to use an alarm [14]. Several examples of sensors are shown in figure 3.

Sensor attachment technology

The way the sensor is attached to the clothing depends on its type. Modular sensors are placed in minipad, pantyliner or into an external crotch pocket. It can also be placed inside a nappy, however nappies have granules, which are designed to absorb liquid and may keep the sensor too dry and fail to trigger. The sensor can be placed between two adjacent briefs. In other cases, sensors are embedded into a magnetic/mechanical or lead-and-clip attachments, which can be attached to any part of clothing. Such attachment is less secure, because the clip can be lost in bed.

Table 2

COMMERCIALLY AVAILABLE WEARABLE ALARM UNITS					
Type of product	Parameters, mm	Case type	Type of attaching	Type of communication	Power supply
DRI sleeper (wired and wireless)	$a - 60 \times 40 \times 15$; $b - 80 \times 40 \times 20$	plastic block	velcro tape	wired wireless	4×1.5 V button cell
Chummie	$65 \times 50 \times 17$	plastic block	snap on clip	wired	2×1.5 V AAA
Malem (wired and wireless)	$a - 49 \times 39 \times 18$; b – transmitter $46 \times 45 \times 22$; receiver $76 \times 74 \times 25$	plastic block (2 blocks for wireless version)	pin/ clip	wired wireless	$a - 3 \times 1.5$ V button cell $b - 2 \times$ AAA $+ 1 \times$ A23
Nite train-r (for boys and for girls)	$64 \times 51 \times 20$	plastic block	pin	wired	1×9V PP3
Wet-stop 3	$60 \times 48 \times 13$	plastic block	magnetic clip	wired	2×1.5 V AAA
Enurad 400	-	clock	-	wireless	A 9V DC adapter

Table 3

ALARM SYSTEM UNITS					
Type of product	**Parameters, mm**	**Material**	**Type of sensor and attaching**	**Communication mode**	**Flexibility**
DRI sleeper (wired and wireless)	*a* – 40 × 20 × 3.5 *b* – -	*a* – electrodes encased in silicone rubber *b* – electrodes in plastic module	insertable module: put in a mini pad or pantyliner	wired wireless	flexible/ not flexible
Chummie	50 × 34 × 3	electrodes encased in silicone rubber	insertable module: put in a mini pad or pantyliner	wired	flexible
Malem (wired and wireless)	*a* – 18 × 2 *b* – 32	*a* – flat gold plated PCB *b* – electrodes in plastic module	*a* – insertable module: put in mini pad or pantyliner *b* – clip-on module: clip-on garment	wired wireless	not flexible
Nite train-r (for boys and for girls)	*a* – 168 × 94 × 3 *b* – 168 × 74 × 3	electrodes encased in foam plastic	inserting module: put between a pair of snug fitting panties	wired	not flexible
Wet-stop 3	-	electrodes in plastic module	clip-on module: clip-on garment	wired	not flexible
Enurad 400	60 × 25 × 7	-	insertable module: put in a mini pad or pantyliner	wireless	-
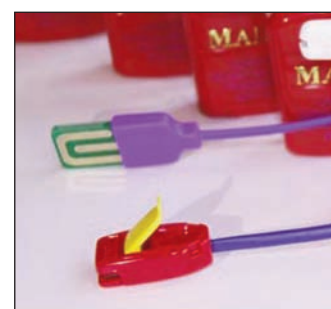
Fig. 3. Alarm system plastic sensors:
a – Chummie; *b* – Enurad; *c* – Nite train-r; *d* – Malem
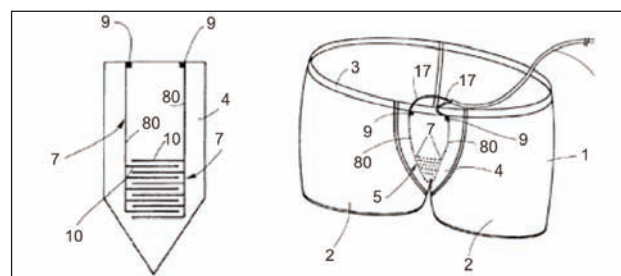
Fig. 4. Textile sensors:
a – Rodger wireless alarm; *b* – pants with conductive threads as the sensor

There is a strong objection to the use of products that have a wired connection attached to the patient since it affects the safety and comfort [10]. Another type of sensor system is micro-wires that are built into underwear and connected to wireless transmitter attached with snaps to waistband of pants [14]. Such approach is used in Rodger wireless alarm (fig. 4). Alarm transmitter uses 3 V button cell, so system remains safe even if the transmitter does get moisture on it. Wires are embedded into briefs using a zigzag stitch. Another solution for improving the enuresis alarm system and making the moisture sensor more suitable for the properties of textile product is described in the patent [11]. It describes briefs with humidity

sensor integrated directly into the textile structure using knitting technique. Conductive threads are used as the sensor material, which are knitted into the crotch area. Sensor is attached to the alarm unit with wires.

REQUIREMENTS FOR COMFORTABLE ENURESIS ALARM SYSTEM

Child's skin is very sensitive and underwear comfort is especially important. This section describes issues related to enuresis alarm systems from the comfort and safety point of view, as well as recommendations for improvement of sensor and alarm unit design.

Comfort options for enuresis alarm system

Factors affecting the comfort of underwear are evaluated from the following aspects:
- sensorial – softness, stiffness, smoothness, roughness, prickliness, dampness, clinginess of the fabrics;
- hygienic – hygroscopicity of underwear fabrics, heat transmission, moisture management;
- motion – fitting, freedom of movements;
- aesthetic – design, quality [12].

During the optimization of enuresis alarm systems, it is necessary to take into account these factors when choosing product materials, design technology and system layout. Below is a description of enuresis alarm system issues from the comfort and safety aspects:

Sensorial. Wires are mostly stiff and inflexible, so that they reduce comfort of the product. Wires in pyjamas can psychologically affect the child, creating a reluctance or a complex towards the product, which may decrease the effectiveness of treatment, because in this case child's willingness to participate in therapy is very important.

Hygienic. Increased perspiration during sleep can lead to false alarms. Moisture management of the intimate apparel is important as it helps to remove excessive wetness. Modified fibres have been applied to sportswear and underwear for perspiration absorbency [12]. Thus, sweat evaporates more quickly and accumulates less on the surface of clothing, which can reduce the likelihood of false bed-wetting alarms. After studying regulations in the area of children's sleepwear safety, it was found that no special restrictions on textile materials, which affect the hygienic properties, are defined. Several regulations were largely based on fire properties of apparel and textiles [13]. Burning characteristics of fibres show that cotton and linen fabrics are least resistant to fire, on the other hand PE, PA, silk and modacrylic fabrics are more secure [14].

Motion. If the elements attached to sleepwear are rigid and inflexible, they reduce the sleeping comfort, especially during movements. The movement also affects the reliable operation of the system – if sleep is restless, insertable or clippable sensor can detach or slip away, connecting wire may break, alarm unit can disconnect.

Aesthetic. Visually the system must be as neutral as possible in order to avoid psychological discomfort or complexes.

Safety. Paper [15] indicates that during the design of a secure children's clothing it is recommended to avoid using long cords that could pose a serious risk of accidents if they get stuck in nearby objects. In the existing enuresis alarm systems cables that connect trousers and pyjamas are located near child's neck, and can pose certain security risks if they get entangled during a troubled sleep [14].

On the other hand, wireless sensors have greater size (because of additional batteries and electronics), which reduces the comfort properties. Perhaps a wireless solution requires constructing a distributed system.

Alarm devices that are attached with a safety needle are dangerous as well, because if they detach accidentally, they may result in a serious injury.

Options for enuresis alarm sensor

It is important to choose an appropriate size of the sensor – if the sensor is too small, then it may not detect the urination, but if it is too large, it may cause discomfort when it is worn [16]. The sensor must be placed in the area, which is mostly exposed to contact with the first drops of urine. Consequently, a solution that ensures greater comfort and detection efficiency is direct sensor integration into briefs crotch area and using conductive material, which is incorporated into the fabric structure. It is possible to integrate conductive contacts or circuits into textile structure, using various non-traditional techniques, such as: printing or laminating of conductive materials, interweaving, knitting, sewing or embroidery with conductive threads. As a result it is possible to obtain a flexible sensor with characteristics of a textile product, which covers the entire area subject to wetting.

When one uses conductive materials suitable for textiles (yarn or coatings), it is necessary to think about their properties – they have to be thin and durable enough and should have good electrical conductivity, as well as they should be resistant to various environmental factors (moisture, friction, bending, tension etc.).

We propose to design sensors with embroidery technique using conductive threads. As was mentioned before, conductive threads are a preferable material for enuresis alarm sensors, since they blend with the textile structure of underwear and bedding sheet, inducing less stress on the treated person.

As was found in a previous study [17], conductive threads behave differently in seams, so before their use in textile circuits it is important to determine the properties of threads. Resistance of conductive seams can be influenced of different variables: type of thread, length of stitch, number of package layers, integration method. Resistance of some samples was affected by tension, for that reason its behavior is influenced by sewing process, which defines strain of thread in fabric.

In order to assess suitability of such threads for the application envisioned, it is necessary to develop a suitable sensor configuration and to test the longevity and stability of the materials used.

Options for enuresis alarm unit

Enuresis alarm systems are placed inside plastic cases – some are bigger and others are smaller, although all are rigid and non-flexible. With the development of smart textiles field, now there are various solutions for flexible electronic circuits, which can be applied to the alarm unit in order to improve the system. Possible ways to improve enuresis alarm system include: development of a flexible or soft alarm module, replacing wires with textile conductive threads, integrating connectors and conductive traces into the textile material. Although certain parts of the system will inevitably remain hard – e.g. a speaker, control electronics etc., it is still possible to add a degree of freedom by placing these elements on a flexible PCB or a circuit printed with conductive ink on a flexible substrate. Further this module can be encapsulated into an elastomer to provide protection without compromising flexibility. Additional protective measures should be applied in this case so that the electronic components do not get damaged by excessive bending. On the other hand, such system is more suitable both for attaching to the garment and to the bed or lining in close proximity to the sleeping person, as it increases comfort and reduces risk of injuries.

CONCLUSIONS

When enuresis alarm system is used in a medical therapy, child's involvement is important, so it is essential that the system is convenient and does not cause the child a psychological discomfort. Existing enuresis alarm systems use wires that connect trousers with pajamas, which can cause a child aversion to therapy. Besides that, cables are located near child's neck and can pose certain security risks if they get entangled during a troubled sleep.

In order to improve the system comfort properties, modular humidity sensor should be replaced with a textile sensor, which is embroidered with conductive threads on fabric. Conductive threads are a preferable material for enuresis alarm sensors, since they blend with the textile structure of underwear and bedding sheet, inducing less stress on the treated person. In order to assess suitability of such threads for the application envisioned, it is necessary to develop a suitable sensor configuration and to test the longevity and stability of the materials used.

Bed-wetting or nocturnal enuresis is a common issue, statistical data show that a significant number of children and youth suffer from nocturnal enuresis. There are different approaches towards the treatment of enuresis – both pharmacological methods and non-pharmacological methods.

Enuresis alarm system is one of the most effective non-pharmacological treatment methods. The alarm awakens the child when bed-wetting starts, the child gets out of bed and finishes voiding in the toilet. With time a successful therapy results in a child learning to wake up by himself, when his bladder is full.

Different enuresis alarm system types have been discussed in the article: pad-and-bell alarms, wearable wired alarms and wearable wireless alarms. Operation and design of all alarm types have been analyzed, describing alarm unit placement and fastening techniques, sensor types and construction. The existing systems were evaluated, highlighting drawbacks and providing requirements for comfortable enuresis alarm system.

BIBLIOGRAPHY

[1] Clinical Guideline Centre: *Nocturnal enuresis – The management of bed-wetting in children and young people.* London, National Clinical Guideline Centre, 2010. Available from www.nice.org.uk accessed: 2012.04.04

[2] Neveus, T., Eggart, P., Evans, J. et al. *Evaluation of and treatment for monosymptomatic enuresis.* A Standardization Document from the International Children's Continence Society. Available from http://i-c-c-s.org/pdfs/standardisation-documents/Monosympt-Enuresis.pdf, accessed 2012-04-06 accessed: 2012.03.04

[3] Neveus, T. *Nocturnal enuresis: theoretic background and practical guidelines.* In: Pediatric Nefrology, 2011, vol. 26, pp. 1207–1214, ISSN 1432-198X

[4] Sempik, J., Ward, H., Darker, J. *Emotional and behavioral difficulties of children and young people at entry into care.* In: Journal of Clinique Children Psych Psychiatry, 2008, vol. 13, no. 2, pp. 221–233, ISSN 1461–7021

[5] Hunskaar, S., Arnold, E. P., Burgio, K., Diokno, A. C., Herzog, A. R., Mallett, V. T. *Epidemiology and natural history of urinary incontinence.* In: International Urogynecology Journal Pelvic Floor Dysfunction, 2000, vol. 11, no. 5, pp. 301–19

[6] Deshpande, A. V., Caldwell, P. H. *Medical management of nocturnal enuresis.* In: Pediatric Drugs, 2012, vol. 14, no. 2, pp. 71–77

[7] *Treating nocturnal enuresis in children.* In: Effective Health Care, 2003, vol. 8, no. 2, ISSN: 0965-0288

[8] Hemani, A., Huang, J., Jayaprakash, G. et al. *Disposable mattress cover that detects when the sheets are wet.* ECE 4884/4007 Senior Design Project, 2007

[9] Thiedke, C. *Nocturnal enuresis.* In: American family physicians, 2003, vol. 67, issue 7, pp. 1 499–1 506

[10] Biswas, J., Wai, A. A. P., Foo, V. S. F. et al. *Design of a smart continence management system based on initial user requirement assessment.* In: Smart homes and health telematics, 2008, vol. 5 120, pp. 62–72, ISBN 978-3-540-69916-3

[11] Jahn, M., Wilhaus, M., Von Riedheim et al. *Knit good with moisture sensor.* Patent US 2011/0132040 A1

[12] Yu, W. *Achieving comfort in intimate apparel, in Improving comfort in clothing.* Woodhead Publishing, Cambridge, 2011, pp. 427–448, ISBN: 978-1-84569-539-2

[13] Horrocks, A. R., Nazaré, S., Kandola, B. *The particular flammability hazards of nightwear.* In: Fire Safety Journal, June 2004, vol. 39, no. 4, pp. 259–276

[14] Jan, S. *Facts about fabric flammability.* North Central Regional Extension Publication 174, 2003

[15] *Quality characterization of apparel.* Edited by Subrata Das, Oxford, Woodhead Publishing, Cambridge, 2009, ISBN 81 908001 3

[16] Page, A. E. *Device and apparatus for detecting moisture.* Patent US 2008/0246620 A1

[17] Parkova, I., Vališevskis, A., Viļumsone, A. et al. *Improvements of smart garment electronic contact system.* In: Advances in Science and Technology, 2012, vol. 80, pp. 90–95

Authors:

INESE PARKOVA
ALEKSANDRS VALIŠEVSKIS
ANDIS UŽĀNS
AUSMA VIĻUMSONE
Riga Technical University
Institute of Textile Material Technologies and Design
14/24 Azenes, LV 1048, Riga, Latvia
e-mail: inese.parkova@rtu.lv

DOCUMENTARE

Confecții textile

FUNCȚIONALITATE SPORITĂ CU *ARNITEL VT*

Prin folosirea membranelor ultrasubțiri *Arnitel VT*, de la **DSM of Sittard** – Olanda, pot fi optimizate proprietățile de impermeabilitate, respirabilitate și confort ale îmbrăcămintei de exterior.

În prezent, se urmărește evitarea utilizării PCM-urilor, care se regăsesc în membranele pe bază de politetrafluoroetilenă (PTFE). Firmele specializate în producerea îmbrăcămintei de exterior caută noi metode de realizare a unor confecții cu performanțe superioare și confort sporit pentru purtător, utilizând materiale și procese cu un impact redus asupra mediului. Cu Arnitel VT, vaporii de umiditate se pot deplasa din interiorul îmbrăcămintei către exteriorul acesteia, iar membrana fiind 100% impermeabilă, spre deosebire de alte produse folosite până în prezent, nu necesită perforări pentru a fi respirabilă. La membranele perforate, capacitatea de ignifugare ar putea fi afectată, atunci când sunt spălate sau când intră în contact cu unele lichide, cum ar fi alcoolul sau combustibilul lichid. Perforațiile reduc, de asemenea, rezistența la rupere a membranei, fapt ce-i alterează și respirabilitatea.

Datorită faptului că Arnitel VT nu este perforat, acesta acționează ca o barieră nu numai în cazul lichidelor, ci și al bacteriilor și virusurilor. Din acest motiv, Arnitel VT este utilizat la fabricarea halatelor chirurgicale cu cel mai ridicat nivel de protecție. Materialul nu conține perfluorocarbon și, prin urmare, este 100% reciclabil.

Unul dintre principalii parteneri ai DSM este **Sympatex Technologies,** din Germania, un furnizor global de materiale funcționale high-tech pentru îmbrăcăminte, încălțăminte, accesorii și aplicații tehnice. Colaborarea dintre DSM și Sympatex a dus la o reducere drastică a amprentei de carbon în procesul de producție a polimerilor, în comparație cu membranele pe bază de PTFE.

Legat de aceasta, Michael Kamm – director general executiv al Sympatex, declara: *"DSM a fost un partener de încredere pentru noi, în dezvoltarea de tehnologii și procese bazate pe principiile responsabilității și sustenabilității ecologice".*

Sursa: www.dsm.com; www.sympatex.com

PLS-based SEM analysis of apparel online buying behavior. The importance of eWOM

GHEORGHE ORZAN
CLAUDIA ICONARU
IOANA CECILIA POPESCU

MIHAI ORZAN
OCTAV IONUȚ MACOVEI

REZUMAT – ABSTRACT

Analiza SEM a comportamentului de cumpărare online a articolelor vestimentare, bazată pe tehnica PLS. Importanța eWOM

Scopul lucrării îl constituie elaborarea și testarea unui model simplu și riguros al comportamentului de cumpărare online a articolelor vestimentare, capabil să explice și să prezică intenția comportamentală. În acest scop, s-a folosit teoria acțiunii motivate (TRA), care confirmă faptul că atitudinea unui individ privitoare la un anumit comportament este determinată de convingerile fundamentale ale acestuia. Pentru a menține simplitatea modelului au fost identificate două convingeri fundamentale, capabile să explice variația în atitudinea consumatorului privitoare la cumpărarea articolelor vestimentare prin intermediul internetului, dar și riscul și beneficiile percepute. Atât atitudinea, cât și influența socială, analizate prin folosirea markerului viral online eWOM, determină intenția consumatorului de a cumpăra online articole vestimentare. Pentru a testa relațiile cauzale dintre variabile, a fost folosită o analiză SEM, bazată pe tehnica PLS, în două faze.

Cuvinte-cheie: comportament, cumpărare online, eWOM, analiză de tip PLS

A PLS-based SEM analysis of apparel online buying behavior: The importance of eWOM

The aim of this paper is to propose and test a simple, yet rigorous model of apparel online buying behavior, capable of explaining and predicting consumers' behavioral intention. We drew on TRA (Theory of Reasoned Actions) framework which postulates that individuals' attitude toward a behavior is determined by their salient beliefs. In order to maintain the simplicity of the model, we have identified two salient beliefs capable of explaining the variance in consumers' attitude towards buying apparel using the Internet: perceived benefits and perceived risk. Both attitude and the social influence, represented in this paper by the influence of eWOM (e-Word-of-Mouth), will determine consumers' intention to buy apparel online. In order to test the causal relationships between variables, we have employed a two phase PLS-based SEM analysis.

Key-words: behavior, online buying, eWOM, PLS analysis

The fashion industry in Romania registered the fastest growth among e-commerce industries in the last year, due to the fact that online consumers are spending higher amounts of money on clothes and shoes, especially on brand products. According to the same source, the average apparel spending rose from an average of 177 lei registered in 2011 to an average of 185 lei. Moreover, transactions over 400 lei (without VAT) increased by 25% compared to last year. The Romanian online apparel market rose to approximately 50 million euro, representing 2,5–3% of the entire Romanian apparel market.

Moreover, the Romanian online apparel market had an ascending trend even in the economic recession period of 2009, entitling the media to affirm that the online apparel market "mocks the recession".

There are numerous players on the Romanian online apparel market which sell significant volumes of clothing and accessories at highly discounted prices: Bon Prix, Kurtmann, Fashion Days and Mini Prix. While price can be perceived as the main benefit of online apparel buying, we are interested in a more holistic approach to analyzing online consumer behavior.

Thus, we integrate both perceived benefits and perceived risks of apparel online buying in a model of online consumers' intention to buy apparel online. We identify perceived benefits and perceived risks when buying online according to a rigorous previous literature empirical evidences. Previous literature review regarding consumers' salient beliefs when buying online is presented in the next section of this paper. Following Fishbein and Ajzen approach to explaining and predicting human behavior [1], we determine consumers attitude based on these salient beliefs as main determinants.

We also pay special attention to the influence of the e-word of mouth on consumers' intention to buy online apparel. The direct and indirect influence of consumers' salient beliefs, attitude and social influence on consumers' intention to buy online apparel are analyzed using a PLS-based SEM analysis.

Our conceptual model and research methodology form the third and forth section of this paper. Data analysis and results of the empirical research is presented in the fifth section.

In the last section of the paper we draw the conclusions and state the managerial implications of this research paper in regards to apparel online market.

ONLINE BUYING: BENEFITS AND RISKS

Previous literature is rich in motivational studies which try to explain why consumers chose to shop online. Authors have identified two types of motivations that drive consumers when engaging in online shopping. First, there is utilitarian motivation or the rationally perceived benefits of using the Internet in the buying process and second, there is the hedonistic motivation, or the pleasure experienced by the consumer when engaged in the online buying experience [2].

An utilitarian consumer will chose to buy online due to various reasons. Perceived convenience has proven to be the top reason of using the Internet to buy goods and services [3]. Convenience is given by the fact that the online consumer can shop from anyplace, home or office, at any given time without being constrained by stores' schedules or clerks' availability [4].

Time can be saved when shopping from home. Consumers will save time by not having to drive to the store, find a parking lot, and wait at check-up. But money can also be saved when choosing to use the Internet for buying goods and services. Perceived lower prices in the online environment is another strong motivation to shop online [3]. Moreover, the Internet offers a great variety of products and goods, easing the process of comparison and selection [5]. There are consumers that chose to shop online because the Internet offers access to products unavailable offline in their immediate proximity [6]. Consumers also mention the lack of sociality as a motivation to shop online. When shopping online there is a smaller chance to be disturbed by shopping partners or noisy sales people [7]. Thus, consumers will choose to buy online if the buying process is faster, easier and also if they obtain a better price [6]. But buying online is not only about benefits. Consumers also report certain types of risks, especially when buying apparel. Especially apparel buyers are skeptical when ordering online due to the fact that sizes may not fit and the product must be returned [8].

The inability of touching, feeling and physically examining the product before buying are considered main obstacles of e-commerce [9]. Thus consumers will wonder whether the product bought online will or will not performed as expected, giving rise to the perceived performance risk [10].

Consumers also perceive financial risk resulting from online fraud. This is the risk associated with the Internet financial data security, namely the fear that the data can be intercepted and willfully manipulated by unauthorized people [11]. Such cases have been revealed and highly promoted by the media, consolidating consumers' negative perceptions about the uncertainty of online payment [12]. Financial risk is one of the main barriers of online buying [9], [3].

Strongly related to the perceived financial risk, there is the perceived privacy risk. In this case, not only that personal data, such as name, address, identification number, can be intercepted but also online vendors can alienate consumers' personal data without their permission [12]. Even though risk can be either real or perceived, the security of both financial and personal data can slow down the adoption of the Internet for buying goods and services [12].

eWOM

Word-of-mouth (WOM) is based on personal recommendations for products or services where the sender is usually known by the consumer, thus, the persuasive nature of WOM is attributed to trust between the sender and the receiver of a message. According to Perju et al., the great influence of WOM lies in the fact that consumers are likely to trust recommendations that come from their community, friends and family, as WOM has greater persuasiveness due to its perceived credibility and trustworthiness [13], [14]. Their research also posits that even though electronic word-of-mouth (eWOM) eliminates the consumer's ability to judge the credibility of the sender and their message, a high amount of users make use of eWOM. Additionally, the quantity of online reviews shows a positive relationship with customers' intention to purchase [15]. Additionally, eWOM is enabled by accessibility and reach at a completely different level than traditional WOM could have ever achieved. eWOM is also more likely to contain references to advertising than traditional WOM, as the Internet allows the sharing of links, pictures, videos and information in general, thus making it easier for consumers to share marketing messages.

The wide dissemination of eWOM communications and the high level of acceptance by consumers suggest that eWOM exerts considerable influence on consumer buying and communication behavior, and, consequently, on the success of products sale in the market [16]. eWOM not only increases marketing messages but also alters consumer information processing [17]. In particular, peer communication through social media, a new form of consumer socialization, has profound impacts on consumer decision making and thus marketing strategies [18].

The socialization process and thus eWOM are facilitated by blogs, instant messaging, and social networking sites, which provide easy and convenient communication tools. For example, new members on social networking sites can be easily socialized into virtual groups in which they may share and find information to help the make consumption-related decisions. Consequently, the multitude of friends or peers acts as a socialization agent, providing vast product information and evaluations and facilitates online education.

Previous literature shows that online advertising effectiveness is related to consumer engagement with a website, as manifested in "finding a basis for conversation and social interaction" [19].

Online reviews on the other hand, can be anonymous or can offer additional personal details of the sender and can thus have an influence on the credibility of the message, which in turn, can induce different attitudes and intentions towards specific products or services.

CONCEPTUAL FRAMEWORK

The best predictor of an individual's behavior as stipulated by Fishbein and Ajzen's Theory of Reasoned Actions (TRA) and subsequent TRA-based studies is a measure of his intention to perform such behavior [1]. Thus, our main objective is to study consumers' behavior when buying apparel online by modeling consumers' stated intentions.

According to TRA framework, individuals' behavioral intention is a function of individuals' attitude and social influence [1]. Thus, we state our first hypothesis:

1. Consumers' attitude towards buying apparel online will directly and positively affect consumers' intention to use the Internet in the apparel buying process.
2. Electronic word of mouth (eWOM) has become an important decision factor for evaluating products as consumers gather information and read reviews of previous consumers before buying online [18]. eWOM has gained importance since there are more and more online discussion forums, reviews web-sites, social network sites of blogs for potential, actual or previous consumers to disseminate information.
3. Many potential Internet shoppers tend to observe the experiences of others who have tried a product before considering whether to purchase it themselves. Contributions on opinion platforms usually include both the verbal account of a consumer's experience with a product and a formalized rating of the product.
4. eWOM can be conceptualized as a form of social influence which, according to TRA, will determine to a great extent individuals' behavioral intention [1]. Thus, we state our second hypothesis:
5. eWOM will directly and positively affect consumers' intention to use the Internet in the apparel buying process.
6. But according to TRA, individuals' attitude towards a behavior is determined by the individuals' salient beliefs [1], which we have identified as being perceived benefits and perceived risk of buying online apparel. Thus, we state our third and forth hypotheses:
7. Perceived benefits of using the Internet in the apparel buying process will directly and positively affect consumers' attitude towards buying online apparel.
8. Perceived risks of using the Internet in the apparel buying process will directly and negatively affect consumers' attitude towards buying online apparel.
9. Based on the TRA framework, our model postulates that perceived benefits and perceived risks are the main determinants of attitude and that attitude together with eWOM will determine consumers' intention to use the Internet for buying online apparel.

METHODOLOGY

In order to test our conceptual framework, we have gathered primary data from 98 consumers that have previously bought apparel online. An invitation to complete the web survey was posted on a Facebook page, Romania's most popular social network. The first part of the questionnaire contained 20 statements, 3 statements for each construct: perceived benefits, perceived risks, attitude, eWOM and intention, measured on a Likert scale from 1 to 7 and the second part of the questionnaire was designed to gather socio-demographic data: gender, age, income and level of education.

Measurements of all five constructs were adapted from previous literature for the specificity of this study. Each construct was constructed as a formative latent variable with three indicators.

"**Intention to use the internet in the apparel buying process**" was constructed following Soderlund and Ohman approach to intentions as wants, expectations and plans [20] ("I want to/I expect to/ I plan to use the Internet in the apparel buying process).

"**The attitude towards apparel online buying**" comprises both the cognitive and the affective component of attitude in a single formative construct according to Fishbein and Ajzen [1] (using the Internet in the apparel online buying process is a good/wise/pleasant idea).

"**eWOM**" was measured as consumers' willingness to rely on information gathered from online discussion forums/blogs/consumers' reviews sites.

"**Perceived benefits**" was constructed as a formative latent variable, measuring apparel online buying benefits identified in previous literature review section - convenience, time savings and price savings (buying apparel online is convenient/saves time/saves money).

"**Perceived risks**" was constructed as a formative latent variable, measuring apparel online buying risks identified in previous literature review section: performance risk, financial risk and privacy risk (apparel bought online may not perform as expected/I can lose money when buying apparel online/I can lose my privacy when buying apparel online).

DATA ANALYSIS AND RESULTS

Data analysis and results section of this paper comprises three main parts: measurements' reliability, measurements' validity and the PLS-based SEM analysis. We have chosen warp PLS 3.0 in order to perform our analysis due to various reasons: Warp PLS can operate with small amount of data, it differentiates between reflective and formative variables and it allows multiple causal relationships between latent variables [21].

Measurements reliability. Measurements' reliability was assessed following Bagozzi and Yi approach by computing Cleibach Alpha, compound consistency and average extracted variance, *AVE* [22].

From table 1 we can notice that the measures posses high internal consistency: all composite reliability coefficients are greater than the critical point of 0.7 [23], varying between 0.898 and 0.930. Moreover, all Cleibach alpha coefficients of all five constructs are greater than 0.7 [24], which yields robust measures in terms of constructs' reliability.

Measurements validity. We have assessed both convergent and discriminant validity of our measurements. Convergent validity measures if indicators of a construct yield similar results among themselves and conclude whether they are supposed to measure the same construct [25]. Convergent validity was performed in warp PLS 3.0 by extracting the factor loadings and cross loadings among indicators.

Table 2 shows that items load according to the construct to which they were designed to. Discriminant validity was asses following Fornell and Larcker's approach of comparing the square roots of *AVE* of each latent variable with every correlation that

implies that latent variable [24]. A good discriminant validity shows that indicators associated with a latent variable are not confused by the respondents with indicators from other *LVs* in regards to their meaning [21].

Table 3 shows that the square roots of *AVE* on the diagonal axis are greater than any of the correlation among LVs, indicating strong divergent validity among constructs.

Table 4 shows the PLS-based SEM analysis run in warp PLS 3.0 and contains the standardized β coefficients, also named path coefficients, and their associated p values.

The PLS-based SEM analysis indicates that all our hypotheses are supported (fig. 1). Perceived benefits and perceived risks are the main predictors of

Fig. 1. PLS-based SEM analysis

Table 1

MEASUREMENTS' RELIABILITY			
Construct	**Composite reliability**	**Cleibach alpha's**	***AVE***
Benefit	0.93	0.930	0.817
Risk	0.902	0.837	0.755
Attitude	0.911	0.853	0.773
eWOM	0.898	0.829	0.746
Intention	0.919	0.868	0.791

Table 2

MEASUREMENTS' CONVERGENT VALIDITY					
	Benefit	**Risk**	**Attitude**	**Intention**	**eWOM**
B1	0.858	−0.099	0.012	0.025	0.011
B2	0.912	0.091	−0.011	−0.047	0.004
B3	0.939	0.002	0	0.023	−0.014
R1	−0.246	0.836	0.11	−0.054	0.082
R2	0.224	0.870	0.047	−0.161	0.008
R3	0.012	0.900	−0.148	0.206	−0.085
AT1	−0.032	−0.009	0.858	0.126	−0.056
AT2	−0.075	0.025	0.903	−0.09	0.091
AT3	0.109	−0.016	0.876	−0.03	−0.038
INT1	−0.07	−0.062	−0.068	0.912	−0.057
INT2	0.105	−0.046	0.056	0.877	0.05
INT3	−0.032	0.11	0.015	0.879	0.009
e1	0.198	0.174	−0.12	0.112	0.816
e2	−0.114	−0.126	−0.018	−0.037	0.887
e3	−0.068	−0.034	0.129	−0.067	0.886

Table 3

MEASUREMENTS' DISCRIMINANT VALIDITY					
	Benefit	**Risk**	**Attitude**	**Intention**	**eWOM**
Benefit	0.904	−0.448	0.548	0.614	0.438
Risk	−0.448	0.869	−0.468	−0.535	−0.209
Attitude	0.548	−0.468	0.879	0.74	0.399
Intention	0.614	−0.535	0.74	0.889	0.408
eWOM	0.438	−0.209	0.399	0.408	0.864

Table 4

PATH COEFFICIENTS AND P VALUES					
	Benefit	**Risk**	**Attitude**	**Intention**	**eWOM**
Benefit	-	-	-	-	-
Risk	-	-	-	-	-
Attitude	0.405 $p < 0.01$	− 0.304 $p < 0.01$	-	-	-
Intention	-	-	0.676 $p < 0.01$	-	0.162 $p = 0.022$
eWOM	-	-	-	-	-

Table 5
MODEL FIT INDICES	
APC = 0.387 ($p < 0.01$)	Good if $p < 0.05$
ARS = 0.472 ($p < 0.01$)	Good if $p < 0.05$
AVIF = 1.239	Good if < 5

consumers' attitude towards buying apparel online, with a standardized β coefficient of 0.405 and −0.304, respectively.

As initially stipulated, perceived risks when buying online have a strong direct negative effect on consumers' attitude towards buying online apparel. However, an even stronger influence on consumers' attitude toward buying online apparel is given by perceived benefits.

As expected, the best predictor of consumers' intention to use the Internet in the online buying process is given by consumers' attitude towards buying apparel online, with a standardized β coefficient of 0.676 at $p < 0.001$.

eWOM has a significant direct effect on consumers' intention to buy apparel online, but not as significant as expected, with a standardized β coefficient of 0.160 at $p < 0.05$.

Consumers rely on eWOM when buying online, but their attitude towards buying apparel online has an obviously greater effect on their stated behavioral intention.

Furthermore, we will test the robustness of the model by analyzing model fit indices and their associated p values.

The warp PLS 3.0 output reports three model fit indices: average path coefficients *APC*, average *R* squared *ARS* and average variance inflation factors, *AVIF*.

Following Kock's approach, the model fit indices indicates show that the model has a good predictive and explanatory capacity if all the assumptions are met (table 5).

CONCLUSIONS AND IMPLICATIONS

Analyzing online consumers' behavior gives researchers and practitioners the opportunity of pruning few high impact determinants. It all comes to lowering risk, increasing the perceived benefits of online buying and offering a highly reputable product at a fair lower price.

By a close examination of the relationship between perceived risks when buying online and consumers' attitude towards using the Internet in the apparel buying process, one can notice that performance risk poses a huge problem for selling online apparel. Consumers may wonder if the colors or the cut will be identically with what they can only see in pictures or video representations of the product, without being able to touch, feel the fabric or try on before purchase. Colors may vary according to the type of screen and colors' fidelity cannot be guaranteed by the online vendors. Another problem when buying apparel online is size, as size varies according to different size charts and measurements.

Lower prices ponder in the decision making process of choosing online buying over traditional buying. Judging by the huge volumes of sales of Romanian discount fashion stores, one can state that lower prices are the main relative advantages of buying online apparel.

The ease of finding and ordering apparel also constitutes a relative advantage of buying online. Consumers can browse in a relative short time among a variety of products without any physically effort. They can easily compare different products and brands, selecting within the shortest time frame the product that best suits current needs and wants.

Also, apparel products should have positive reviews as eWOM is gaining more and more popularity among online consumers. Previous consumers share their experience with products bought online on their personal blogs, social network pages or discussion forums and potential consumers often check others' opinion before purchasing a product.

Without being able to operate with both positive and negative reviews, online vendors' image may be harmed. Marketers should not overlook the power of online opinions and recommendations, particularly the power of spreading negative information.

Marketers should take advantage of consumer participation through active communication to strengthen their relationships. Apparel companies should also allow consumers to not only exchange information about products or services but also engage in "participating and socializing" experiences, across both current and potential consumers [26].

BIBLIOGRAPHY

[1] Fishbein, M., Ajzen, I. *Belief, attitude, intention, and behavior: An introduction to theory and research.* Reading, MA: Addison-Wesley, 1975

[2] Sejin, H., Stoel, L. *Consumer e-shopping acceptance: Antecedents in a technology acceptance model.* In: Journal of Business Research, 2009, vol. 62, pp. 565–571

[3] Saprikis, V., Chouliara, A., Vlachopoulou, M. *Perceptions towards online shopping: Analyzing the Greek University students' attitude.* In: Communications of the IBIMA, 2010, vol. 2010, pp. 1–13

[4] Margherio, L. *The Emerging Digital Economy.* In: U.S. Department of Commerce, Washington, D.C., 1998, available online at http://govinfo.library.unt.edu/ecommerce/EDEreprt.pdf

[5] Gurvinder, S., Chen, Z. *Shopping on the internet–online purchase behavior of New Zealand consumers*. In: Journal of Internet Commerce, 2004, vol. 3, issue 4, pp. 61–77

[6] Croome, R., Lawly, M. *Antecedents of purchase in the online buying process*. In: Journal of Internet Business, 2010, vol. 8, pp. 1–40

[7] Gilly, M. C., Wolfinbarger, M. *A comparison of consumer experiences with online and offline shopping*. In: Consumption Markets & Culture, 2000, vol. 4, issue 2, pp. 187–205

[8] Lim, N. *Consumers' perceived risk: sources versus consequences*. In: Electronic Commerce Research and Applications, 2003, vol. 2, pp. 216–228

[9] Rudolph, T., Rosenbloom, B., Wagner, T. *Barriers to online shopping in Switzerland*. In: Journal of International Consumer Marketing, 2004, vol. 16, issue 3, pp. 55–74

[10] Almousa, M. *Perceived risk in apparel online shopping: A multidimensional perspective*. In: Canadian Social Science, 2011, vol. 7, issue 2, pp. 23–31

[11] Orzan, G., Orzan, M. *Cybermarketing.* Bucharest: Uranus Publihing House, 2007

[12] Jahankhani, H. *The behavior and perception of online consumers: risk, risk perception and trust*, 2009. Available online at http://www.srlst.com/ijist/ijism-Vol7No1/ijism71-79-90.pdf

[13] Popescu, D. I., Popa, I., Cicea, C., Iordănescu, M. *The expansion potential of using sales promotion techniques in the Romanian garments industry.* In: Industria Textilă, 2013, vol. 64, issue 5, pp. 293–300

[14] Perju, A., Iconaru, C., Macovei, O. I. *The impact of E-WOM spread through social networks on the decision making process: a Romanian online community analysis*. 12th WSEAS International Conference on Mathematics and Computers in Business and Economics, Transilvania University of Brasov, Romania, April 11– 13, 2011, WSEAS Press, pp. 66–70, ISBN: 978-960-474-293-6

[15] Chan, Y. Y. Y., Ngai, E. W. T. *Conceptualising electronic word of mouth activity: An input-process-output perspective*. In: Marketing Intelligence & Planning, 2011, vol. 29, issue 5, pp. 488–516

[16] Watts Sussman, S., Schneier Siegal, W. *Informational influence in organizations: An integrated approach to knowledge adoption*. In: Information systems research, 2003, vol.14, pp. 47–65

[17] Casteleyn, J., Mottart, A., Rutten, K. *How to use facebook in your market research.* In: International Journal of Market Research, 2009, vol. 51, issue 4, pp. 439–47

[18] Calder, B. J., Malthouse, E. C., Schaedel, U. *An experimental study of the relationship between online engagement and advertising effectiveness*. In: Journal of Interactive Marketing, 2009, vol. 23, pp. 321–31

[19] Doh, S.-J. M. S., Hwang, J.-S. *How consumers evaluate eWOM (Electronic Word-of-Mouth) messages*. In: Cyber Psychology & Behavior, 2009, vol. 12, issue 2, pp. 193–197

[20] Soderlund, M., Ohman, N. *Intentions are plural: Towards a multidimensional view of intentions in consumer research*. In: European Advances in Consumer Research, 2006, vol. 7, pp. 410–416

[21] Kock, N. *Using Warp PLS in e-collaboration studies: Mediating effects, control and second order variables and algorithm choices*. In: International Journal of e-Collaboration, 2011, vol. 7, issue 3, pp. 1–13

[22] Nunally, J. C. *Psychometric theory*, 2nd edition, 1978, McGraw Hill: New York

[23] Bagozzi, R. P., Yi, Y. *On the evaluation of structural equation models*. In: Journal of the Academy of Marketing Science, 1988, vol. 16, issue 1, pp. 74–94

[24] Fornell, C., Larcker, D. F. *Evaluating structural equation models with unobservable variables and measurement error*. In: Journal of Marketing Research, 1981, vol. 48, pp. 39–50

[25] Jewell D. V. *Guide to evidence-based physical therapist practice*, 2nd edition, 2011, Jones & Bartlett Learning: Ontario

[26] Mersey, R., Davis, E., Malthouse, C., Calder, B. J. *Engagement with online media*. In: Journal of Media Business Studies, 2010, vol. 7, issue 2, pp. 39–56

Authors:

Professor GHEORGHE ORZAN, PhD
Lecturer MIHAI ORZAN, PhD
CLAUDIA ICONARU, PhD
Assist. IOANA CECILIA POPESCU, PhD
The Bucharest University of Economic Studies
6 Romana Street, 010374, Bucharest, Romania
e-mail: orzang@ase.ro

Lecturer OCTAV IONUȚ MACOVEI, PhD
Lumina – The University of South-East Europe
64B Colentina Street
021178 Bucharest, Romania
e-mail: octav.macovei@lumina.org

DOCUMENTARE

Materii prime

BIOSTEEL® – O FIBRĂ DIN MĂTASE DE PĂIANJEN

Păianjenul stăpânește conceptul stabilității. Proteina folosită de păianjeni pentru a forma structura pânzei lor este mai puternică decât oțelul, ceea ce face ca fibrele de mătase să posede o rezistență de trei ori mai decât a celor din Kevlar®49, valori mult mai mari ale alungirii la rupere și flexibilității și o greutate redusă. Datorită caracteristicilor sale, acest produs natural a fost propulsat în avangarda unor cercetări intensive de producere a lui prin procedee tehnologice moderne.

Compania **AMSilk** a reușit, pentru prima oară, să dezvolte o fibră din proteină de mătase de păianjen recombinantă (fig. 1). Acest produs brevetat este cunoscut sub denumirea Biosteel®.

Fig. 1

Principiile procesului de producție au fost elaborate de prof. dr. Thomas Scheibel, de la *Universitatea Bayreuth*. Pentru a produce Biosteel® este nevoie de zahăr, azot și apă, care, mai întâi, sunt tratate cu bacterii, într-un reactor, rezultând un produs sub formă de pulbere. Fibrele obținute din această pulbere, printr-un proces de filare scalabilă, prietenos mediului, au un aspect nedefinit. Volumul produsului rezultat este cu mult mai mare decât al celui obținut doar din proteina de păianjeni. Pe lângă volumul mai mare, noul procedeu oferă și alte avantaje, cum ar fi uniformitatea calității și o bună reproductibilitate sintetică.

Mătasea obținută din fibra Biosteel® are caracteristici similare cu cele ale mătasii tradiționale obținute din insecte și poate fi vopsită. În plus, fibra Biosteel® posedă o mai bună rezistență la rupere decât cea fibrelor din carbon, Kevlar®49 sau poliamidă 6.6. Materialul, de un alb pur, are un tușeu moale, strălucitor și este hidrofob.

Fiind extrem de rezistente, biocompatibile și biodegradabile, fibrele Biosteel® sunt adecvate utilizării în sectorul medical, pentru suturi medicale, pansarea rănilor și implanturi mamare. În contact cu țesuturile, datorită acoperirii foarte fine, mătasea de păianjen acționează cu un scut protector al sistemului imunitar. Alte aplicații se referă la articolele pentru sport,

compozite, filtre, corzi etc. Datorită caracteristicilor excepționale, noile fibre au atras deja atenția specialiștilor din sectorul tricotajelor din urzeală. Aceste fibre inovatoare pot fi combinate cu elastan, în special pentru a da un nou imbold producției de îmbrăcăminte sport și textilelor E-50-gauge superfine, destinate sectorului de lenjerie.

Compania AMSilk a produs deja diferite prototipuri din noua fibră. În următoarea etapă, este prevăzută optimizarea fibrei, precum și producția de materie primă și filarea într-o nouă unitate de producție. În paralel cu dezvoltarea fibrei, se va lucra și la pelicule, filme, rețele, geluri și sfere de mătase.

Kettenwirk Textilinformationen Praxis, martie 2013, pp. 38–39

Calitate

PRIMA ETICHETĂ DE CALITATE PENTRU EFECTUL DE RĂCIRE A FIBRELOR

Fibrele cu proprietăți de reglare a temperaturii, produse de firma **Coolcore,** cu sediul în Portsmouth, S.U.A., sunt primele fibre de acest tip din lume, certificate de Institutul Hohenstein cu eticheta de calitate "Tehnologie inovatoare – putere de răcire".

Cercetătorii de la Institutul Hohenstein au confirmat efectul de răcire a materialelor textile care nu conțin produse chimice și nu se bazează pe stocarea căldurii latente sau pe materiale cu schimbare de fază (PCM-uri), și care utilizează schimbarea de fază solid-lichid, pentru a absorbi și a stoca căldura.

Materialele textile realizate de firma Coolcore utilizează propria transpirație a corpului sau umezeala suplimentară pentru a obține efectul de răcire. Designul sofisticat duce la o evaporare controlată și, prin urmare, efectul "răcirii prin evaporare" este mult mai mare decât în cazul celorlalte materiale.

Acest efect a fost evaluat cu ajutorul testerului WATson de măsurare a pierderii de căldură. Valorile pierderilor de căldură, disipată prin piele, în diferite condiții ambientale – de la căldura tropicală la temperaturi reci, ori viteze mari ale vântului, pot fi cuantificate cu ajutorul acestui dispozitiv.

Testerul WATson de măsurare a pierderilor de căldură se bazează pe principiul plăcii încălzite menținute în stare transpirată (sweating guarded hot-plate), elaborat de Institutul Hohenstein, dar cu unele diferențe tehnice. În cazul acestui principiu, atât structura, cât și măsurătorile realizate în conformitate cu standardele DIN EN 31092 și ISO 11092, presupun un nivel ridicat de consecvență. Pe de altă parte, WATson reacționează cu rapiditate și este sensibil la variațiile de temperatură. Astfel, oamenii de știință de la Institutul Hohenstein pot realiza o evaluare mult mai flexibilă a diferitelor aplicații și a condițiilor climatice asociate. WATson este garantul respectării standardelor de calitate, pe parcursul monitorizării producției.

Smarttextiles and nanotechnology, octombrie 2013, p. 4